



**UCGE Reports  
Number 20244**

Department of Geomatics Engineering

**Levelling Network Analysis for the Definition of a  
Kinematic Vertical Datum in Canada**

(URL: <http://www.geomatics.ucalgary.ca/research/publications/GradTheses.html>)

by

**Balaji Devaraju**

**September 2006**



UNIVERSITY OF CALGARY

Levelling Network Analysis for the Definition of a Kinematic Vertical Datum in Canada

by

Balaji Devaraju

A THESIS

SUBMITTED TO THE FACULTY OF GRADUATE STUDIES  
IN PARTIAL FULFILMENT OF THE REQUIREMENTS FOR THE  
DEGREE OF MASTER OF SCIENCE

DEPARTMENT OF GEOMATICS ENGINEERING

CALGARY, ALBERTA

September, 2006

©Balaji Devaraju

## Abstract

Vertical crustal motion is a prominent process in Canada because of plate tectonic activity and on-going post-glacial rebound. The process is predominant in the eastern (postglacial rebound) and western (plate tectonics) parts of the country; however, the magnitudes range from a few centimetres to a few millimetres. As a consequence, heights measured over time provide information about vertical motion. Since levelling measurements in Canada are being taken for the past 100 years; there is a wealth of deformation information available to constrain vertical motion.

In this research, a part of the Canadian Precise Levelling Network in eastern Canada is analysed, where both postglacial rebound and plate tectonics are active. The aims of this analysis is to find out, if a kinematic vertical datum can be realized, and also, if the levelling dataset can be created as an independent dataset of vertical motion for geophysical studies. The latter objective will extend the knowledge from deformation studies using other geodetic data (Global Positioning System, Very Long Baseline Interferometry, Satellite LASER Ranging, and absolute gravimetry), which provide information only for the past  $\approx 20$  years.

The results from the analysis show that the network has some data gaps, which created excess constraints in addition to minimum constraints that needed to be fixed. This was overcome by using *a priori* information from postglacial rebound models and height values estimated from a static height adjustment by the Geodetic Survey Division, Natural Resources Canada. On further analysis, it was found that the datum realized with the height values as excess constraints fulfilled one of the objectives of this study – defining a kinematic vertical datum. Here, it is called a *workable* kinematic vertical datum to distinguish it from minimum constraint and overconstraint datums.

The results were interpreted with geological data, earthquake data, and postglacial rebound models, which all revealed that the region of the network is seismically active and also had effects of postglacial rebound. However, the major contributor to the vertical crustal motion in the region was found to be the postglacial rebound phenomenon. In addition, there were a few local anomalous patterns identified that correlated well with the tectonic faults in the network.

From all these analyses and interpretations it was concluded that a workable kinematic vertical datum can be defined for Canada even with the data gaps. Further, with the realisation of a kinematic vertical datum, an independent dataset of vertical crustal motion rates was created from the levelling dataset for geophysical studies.

## Preface

The research for this thesis was carried out under the supervision of Drs. Alexander Braun and Nico Sneeuw from September 2003 – July 2006. The funding for this research was provided from the GEOmatics for Informed DEcisions (GEOIDE), Network of Centers of Excellence, projects: ACQ#SID “Development of a Dynamic Seamless Vertical Reference System for Environmental, Climatic, Geodynamical, Oceanographic, Hydrographic and GIS Applications”; and SLM-ASR#36 “Space Gravimetry Contribution to Earth Monitoring”. For this research, the levelling data and the corresponding gravity data was provided by Geodetic Survey Division, Natural Resources of Canada; and the earthquake data was provided by Geological Survey of Canada, Natural Resources of Canada. We thank both the organizations, GEOIDE and Natural Resources of Canada, for providing financial and data support, respectively.

## Acknowledgments

I thank my supervisors Drs. Alexander Braun and Nico Sneeuw for their immaculate patience toward me and unwavering support, both academically and morally. It was a pleasure to work under two contrasting, but rigorous, styles of working: the former being a *liberal* geophysicist, and the latter a *conservative* geodesist. Both of them allowed me the freedom to work at my own pace, which gave me a lot of time to think and apply a variety of methods.

I extend my thanks to Dr. Braun for the long hours of scientific discussions and brainstorming, innumerable number of highly competitive basketball games, and amusing philosophical conversations. Also, I extend my thanks to Dr. Nico Sneeuw for the exciting scientific tussles on the white-board, and also the interesting discussions on history, etymology, culture, and many more. In addition, I thank my defense committee members Drs. Patrick Wu and Matthew Tait for their comments and suggestions for improving the quality of the thesis.

I thank Mr. Marc Verroneau of (Geodetic Survey Division, Natural Resources Canada), for providing the levelling data, and for promptly replying to all my e-mail queries; Dr. Michael Craymer (Geodetic Survey Division, Natural Resources Canada), for providing information on datum conversions; Drs. Kristy Tiampo (University of Western Ontario) and John Adams (Geological Survey of Canada, Natural Resources Canada) for providing the earthquake data; Drs. Georgia Fotopoulos (University of Toronto), and Rossen Grebenitcharsky (Technical University of Delft) for their help and discussions on adjustment theory and levelling networks adjustment; Dr. Michael Sideris (University of Calgary) for his comments during the research group meetings; Dr. AJM Kusters (Rijkswaterstaat, The Netherlands) for providing the Dutch levelling data, their software and its manual; Ms. Azadeh Koohzare (University of New Brunswick) for providing fault line data, and the discussions on data processing of the levelling data; and Westgrid organization for providing high-performance computing facilities.

I thank my colleagues in the gravity research group for their constant support, and for providing a nurturing, competitive, and fun-filled working environment: Wouter, Matthias, Meda, Elena, Chen, Vidya, and Raymond. Furthermore, I would like to thank Elena for the discussions on postglacial rebound and vertical crustal motion estimation as well as Matthias for helping with geoid and gravity anomaly calculations.

I would also like to take this opportunity to express my gratitude to my colleague, dear friend, and house-mate Wouter. He provided me the postglacial rebound models for this research and proof-read some of the chapters. He also motivated and pushed me during the last stages of my research and thesis writing by waking me up early in the morning and keeping a constant eye on my progress. I do not know if he did this for his personal pleasure, but it ended up being positive for me.

I convey my gratitude to the following people, who have taken care of me during my stay in Calgary: Vijay, Valar, Girija, Karthik, Ramki, Suren, Poorani, Gopi, Kumaran, Malarvizhi, Mrs. and Mr. Gnanalingam, Angelo, and Leena. Also, thanks to my soccer teammates, Cecile, Niklas, Jenny, Roxna, Eun-Jeong, and Seunghun, for their moral support.

Finally, I would like to thank my parents and my brother for their constant support, for having faith in me and for all the troubles and hardships they took to send me overseas for my higher studies. Also, I would like to thank my uncles Dr. Muruganandham, and Mr. Nithyanandham, my aunt Mrs. Valli, and my grandparents for their timely help and support, without which my higher studies would never have been possible.

*To my parents Mallika and Devaraju, and  
to my bother Karthikeyan  
for their unceasing love, support, and faith in me.*

# Table of Contents

<b>Abstract</b> .....	<b>ii</b>
<b>Preface</b> .....	<b>iv</b>
<b>Acknowledgments</b> .....	<b>v</b>
<b>Dedication</b> .....	<b>viii</b>
<b>Table of Contents</b> .....	<b>viii</b>
<b>List of Tables</b> .....	<b>xiii</b>
<b>List of Figures</b> .....	<b>xiv</b>
<b>Epigraph</b> .....	<b>xviii</b>
<b>CHAPTER 1: Introduction</b> .....	<b>1</b>
1.1 Time in geodetic reference frames . . . . .	1
1.2 Crustal motion studies and reference frames . . . . .	1
1.3 The Canadian perspective . . . . .	3
1.4 Motivation and objectives . . . . .	3
1.5 Outline of the thesis . . . . .	5
<b>CHAPTER 2: Vertical Datum Definition</b> .....	<b>7</b>
2.1 Gravitation, gravity, and geopotential . . . . .	7
2.2 Height Systems . . . . .	9
2.3 Perspectives in vertical datum definition . . . . .	13
2.3.1 Physical perspective . . . . .	13
2.3.2 Mathematical perspective . . . . .	14
2.3.3 Geodetic perspective . . . . .	15
2.3.4 Perspectives on a good vertical datum . . . . .	15

2.4	Datum constraints and datum matrices . . . . .	16
2.5	Kinematic vertical datum . . . . .	18
2.5.1	Kinematic height model . . . . .	18
2.5.2	Derivation of the Kinematic Vertical Datum Adjustment . . . . .	19
2.6	S-transformation of a kinematic vertical datum . . . . .	24
2.6.1	Height shift . . . . .	24
2.6.2	Velocity and time shifts . . . . .	25
2.6.3	The S-transform . . . . .	26
2.7	Chapter summary . . . . .	29
<b>CHAPTER 3: Levelling Data and Data Processing Methodologies . . . . .</b>		<b>30</b>
3.1	History of the Canadian Precise Levelling Network . . . . .	30
3.2	Levelling dataset of the Canadian Precise Levelling Network . . . . .	33
3.3	Solvability of levelling networks for heights and vertical velocities . . . . .	35
3.3.1	Review of terminology . . . . .	36
3.3.2	Rules for solvability of kinematic levelling networks . . . . .	36
3.3.3	Network with multiple rank deficiency . . . . .	38
3.4	Need for the processing of Canadian Precise Levelling Network data . . . . .	39
3.5	Data Processing of the network . . . . .	41
3.5.1	Finding intersection points . . . . .	45
3.5.2	Removing open lines and loops . . . . .	46
3.5.3	Reduction of levelling observations . . . . .	47
3.6	Network configuration at various stages of data processing . . . . .	49
3.6.1	Equivalence of estimated parameters from networks before and after reduction . . . . .	51
3.6.2	Heights estimated from networks before and after reduction process . . . . .	54
3.7	Relevellings at various stages of processing . . . . .	57
3.8	Chapter summary . . . . .	57
<b>CHAPTER 4: Pre-adjustment Analysis of the Levelling Network . . . . .</b>		<b>60</b>
4.1	Graph theory: A brief overview . . . . .	60

4.1.1	Degree of vertex . . . . .	60
4.1.2	Representations of graphs . . . . .	62
4.2	A detailed excursion through least squares adjustment of a levelling network . .	65
4.3	Statistics of the levelling network . . . . .	72
4.3.1	Number of observations in the releveling lines . . . . .	73
4.3.2	Number of the different epochs of observations at each point in the network . . . . .	73
4.3.3	Time interval between epochs of observation in the releveling lines . . .	75
4.3.4	Length of levelling lines before and after reduction . . . . .	75
4.3.5	Degree of vertices . . . . .	75
4.3.6	Time interval between the first and last observations through each point in the network . . . . .	81
4.4	Trend analysis of the relative velocities from multiple relevelings . . . . .	83
4.5	Chapter summary . . . . .	86

**CHAPTER 5: Realisation of a Kinematic Vertical Datum for the Levelling**

<b>Network</b>	<b>94</b>	
5.1	Subset matrix selection from the kinematic design matrix . . . . .	94
5.2	Methods of applying the constraints in an excess constraints situation . . . . .	95
5.3	Results from adjustment for the realisation of a kinematic vertical datum . . .	96
5.3.1	Fixing the excess constraints with velocities . . . . .	97
5.3.2	Fixing the excess constraints with heights . . . . .	102
5.3.3	Discussion of the results . . . . .	102
5.3.4	Results from adjustment using different weight matrices . . . . .	105
5.4	Least squares error analysis . . . . .	114
5.4.1	Resolution matrices . . . . .	114
5.4.2	Redundancy matrices . . . . .	118
5.5	Statistical testing of the observations . . . . .	125
5.5.1	Baarda's data snooping . . . . .	125
5.5.2	Pope's $\tau$ -test . . . . .	127
5.6	Statistical significance of the estimated parameters . . . . .	128

5.7 Chapter summary . . . . .	131
<b>CHAPTER 6: Geological and Geophysical Interpretation . . . . .</b>	<b>135</b>
6.1 Geological fault lines in the study area . . . . .	135
6.2 Earthquake history in the study area . . . . .	136
6.3 Postglacial rebound phenomenon in the study area . . . . .	140
6.4 Interpretation of results from kinematic vertical datum adjustment . . . . .	142
6.5 Chapter summary . . . . .	147
<b>CHAPTER 7: Concluding Remarks . . . . .</b>	<b>148</b>
7.1 Summary . . . . .	148
7.2 Conclusions . . . . .	150
7.3 Contributions . . . . .	150
7.4 Outlook . . . . .	151
<b>References . . . . .</b>	<b>153</b>

## List of Tables

3.1	Table illustrates the method of storage of the observed data in the GHOST format . . . . .	33
3.2	Table illustrates the method of storage of the station information in the GHOST format . . . . .	35
3.3	Line numbers for the Figure 3.7 . . . . .	43
3.4	Velocity at each height point . . . . .	52
3.5	Height estimates of points . . . . .	54
3.6	Velocity estimates of points . . . . .	55
3.7	Height estimates of points from static adjustment . . . . .	55
3.8	Observations, parameters, and rank defect of the networks before and after reduction; considering them as kinematic levelling networks . . . . .	56
4.1	Edge-node list of the directed graph of Figure 4.1(2). For the undirected graph of Figure 4.1(1), the list will be the same except for the fact that the directions will have no meaning and are interchangeable. . . . .	62
5.1	Table showing the weighting scheme based on the time interval between observations for relevelling lines . . . . .	106
5.2	Table showing the weighting scheme based on the time interval between observations for single levelling lines . . . . .	109
5.3	Statistics summarizing the results in Figures 5.2–5.9. The statistics here show the maximum, minimum, and mean values of all the estimation results: both the parameters and their error estimates. V1, V2, V3, V4, and V5 – velocities excess constraints from models 1, 2, 3, 4, and 5, respectively; H – height excess constraints; Z – zero values for all excess constraints; P – precision of observations used as weights; U – unit weights; Y – time interval between observations as weights . . . . .	113

5.4	Percentage of the significant parameters for the different cases of estimation. The table clearly indicates that the combination of height excess constraints and precision of the observations as weights provide the best results. It also indicates that the precision of the observations as weights provide more statistically significant parameters than any other type of weights. . . . .	130
6.1	Layers and their parameters of the 5 postglacial rebound models used for <i>a priori</i> velocity excess constraints. $R$ – radius from the centre of Earth, $\rho$ – density, $\mu$ – rigidity, $\eta$ – viscosity, UM – upper mantle, LM – lower mantle . . .	142

## List of Figures

1.1	Illustration of the location of the study area . . . . .	5
2.1	The height measurement procedure between two points through levelling measurements. The observed height difference in the field is the value $\Delta H$ . . . . .	9
2.2	A closed circuit of spirit levelling measurements . . . . .	10
2.3	Relationship between geoid undulation and ellipsoidal and orthometric heights	13
2.4	Representation of the kinematic height model as an equation of a line in analytical geometry . . . . .	20
2.5	The height, velocity, and time shifts in a kinematic vertical datum . . . . .	25
3.1	Ideal and scattered kinematic levelling networks . . . . .	36
3.2	Illustration of solvability analysis . . . . .	37
3.3	A network with multiple rank deficiency . . . . .	38
3.4	Relevellings in the network at the section level of the data . . . . .	40
3.5	Illustration of relevelling information at line level and at section level . . . . .	41
3.6	Branching in levelling lines. The different coloured lines show the different branches of a levelling line route. In the first figure the levelling line does not follow a particular route, but forms a network in itself. . . . .	42
3.7	Abnormality in line numbering. Here, all the three colours, red, yellow, and green are observations of the same levelling line but they have been given different line numbers in the dataset. . . . .	44
3.8	An example for the <i>intersection point recognizing</i> algorithm . . . . .	46
3.9	Illustration of the open line and loop in a levelling network . . . . .	47
3.10	Illustration of Reduction process . . . . .	48
3.11	Raw network and network at various stages of data processing . . . . .	52
3.12	Figure shows the excess pseudo-observations after network reduction . . . . .	53
3.13	Simulated examples to show the equivalence of the network estimates before and after reduction. . . . .	53

3.14	Plot of the differences in height estimates from networks after applying the reduction process and after finding the intersection points . . . . .	56
3.15	Histogram of the differences in height estimates from networks after applying the reduction process and after finding the intersection points . . . . .	57
3.16	Relevellings in the network from the raw data and at various stages of data processing . . . . .	58
4.1	Types of graphs . . . . .	61
4.2	Illustration for explaining the kinematic levelling network design matrix . . . .	69
4.3	Histogram of the number of relevellings of the relevelled levelling lines . . . . .	73
4.4	Histogram of the number of years (epochs) in which the observations were observed through each point in the network . . . . .	74
4.5	Histogram of the time interval between the epochs of observation in the relevelled lines . . . . .	74
4.6	Histograms of length of levelling lines before and after reduction . . . . .	76
4.7	Histograms of the degree of vertices of the network points without and with relevellings taken into consideration . . . . .	78
4.8	Spatial plots of the degree of vertices of the network point without and with relevellings taken into consideration. The degree of vertices of the network points without relevellings determine the response of the network to the adjustment. . . . .	79
4.9	Spatial distribution of the degree 2 vertices in the network. The degree 2 vertices are spread out all over the network, and also substantial in quantity. .	80
4.10	Spatial plot of the time difference, $\Delta t$ , between the first and the last observations through each point in the network . . . . .	82
4.11	Histogram of $\Delta t$ between the first and last observations through each point in the network. . . . .	83
4.12	Trend analysis of relative velocities derived from multiple relevellings of a levelling line . . . . .	93
5.1	The 25 datum points fixed for all the adjustments carried out in the research .	97

5.2	Velocities and their errors estimated using velocity excess constraints from model 1 and with weights as the precision of the observed data . . . . .	98
5.3	Velocities estimated from the network with the use of different <i>a priori</i> post-glacial rebound models . . . . .	100
5.4	Velocities estimated from the network by fixing all the constraints with zero and using precision of the observations as weights . . . . .	101
5.5	Velocities and their errors estimated from the network by fixing the excess constraints with heights estimated by Geodetic Survey Division, Natural Resources Canada . . . . .	103
5.6	Velocities and their errors estimated with unit weights for all observations and fixing the excess constraints with velocities from model 1 . . . . .	107
5.7	Velocities and their errors estimated with unit weights for all observations and fixing the excess constraints with heights obtained from static adjustment by Geodetic Survey Division, Natural Resources Canada . . . . .	108
5.8	Velocities and their errors estimated by applying time interval between observations as weights for the observations and fixing the excess constraints with velocities from model 1 . . . . .	110
5.9	Velocities and their errors estimated with time interval between observations as weights for the observations and fixing the excess constraints with heights obtained from static adjustment by Geodetic Survey Division, Natural Resources Canada . . . . .	111
5.10	Resolution matrices of minimum and overconstraint adjustments of the static leveling network in Figure 4.1(2). For the minimum constraints adjustment, point 1 was fixed, and for overconstraints adjustment, point 3 was fixed additionally . . . . .	116
5.11	Diagonal elements of the resolutions matrices of the observations ( $\mathbf{R}_y$ ) and the parameters ( $\mathbf{R}_x$ ) with precision of the observations as weights . . . . .	116
5.12	Diagonal elements of the resolutions matrices of the observations ( $\mathbf{R}_y$ ) and the parameters ( $\mathbf{R}_x$ ) with unit weights for all observations . . . . .	117
5.13	Diagonal elements of the resolutions matrices of the observations ( $\mathbf{R}_y$ ) and the parameters ( $\mathbf{R}_x$ ) with heights as excess constraints . . . . .	118

5.14	Local redundancy values of each of the observations in the network . . . . .	120
5.15	Spatial plot showing observations with a local redundancy value of '0', estimated with the precision of the observations as the weights, and network points with a degree of vertex of '2' . . . . .	122
5.16	Spatial plot showing observations with a local redundancy value of '0', estimated with unit weights for all observations, and network points with a degree of vertex of '2' . . . . .	123
5.17	Spatial plot showing observations with a local redundancy value of '0', estimated with the time interval between observations as the weights, and network points with a degree of vertex of '2' . . . . .	124
5.18	Baarda's data snooping performed on the adjusted residuals that used the precision of observations as the weight values. Figure shows the ratio between the test static of every individual residual and the critical value. Values '> 1' and '< -1' are the erroneous observations . . . . .	126
5.19	$\tau$ -test performed on all adjusted residuals estimated using different weight matrices. Figure shows the ratio between the test static of every individual residual and the critical value. Values '> 1' and '< -1' are the erroneous observations. . . . .	128
5.20	The plots indicate the ratio between the parameter estimates and their error estimates, which is being used as an indicator for statistical significance of the estimated parameters. Statistically significant parameter estimates are plotted as value 1 in the plot and the other statistically insignificant parameter estimates are plotted as value 0. . . . .	129
5.21	The bar graphs show the means values of the error estimates for the points based on the statistic shown in Fig. 4.11. The figures indicate that the time interval between the first and last observations have an impact on the estimated errors of the parameters. . . . .	132
6.1	Different types of faults . . . . .	136
6.2	Geological map of the study area. For the legend refer to Wheeler et al. (1996)	137
6.3	Geological fault lines in the study area . . . . .	138

6.4	Occurrences of earthquakes in the study region with their magnitude and depth. Data courtesy: Dr. John Adams, Geological Survey of Canada, Ottawa. . . . .	139
6.5	Vertical crustal motion rates from postglacial rebound models that were used as <i>a priori</i> information for fixing the velocity excess constraints . . . . .	141
6.6	Illustration of the two regions of focus within the entire network . . . . .	143
6.7	A closer look at the two areas of the network highlighted in Figure 6.6, whose velocity values correlate with the faults . . . . .	145
6.8	Illustration of the areas in the network, whose velocity estimates correlate with the geological rock types of the region . . . . .	146

“How little there was that was fixed, stable, enduring!  
How alive everything was, undergoing transformation  
and longing for change, on the watch for dissolution  
and rebirth!”

– *Childhood of the Magician*

by Hermann Hesse, 1923.

## Chapter 1

### Introduction

This research concerns vertical crustal motion in Canada and the definition of a kinematic vertical datum using levelling data of the last century. In order to exploit this rather long time series, compared to GPS or absolute gravimetry measurements, several geodetic and mathematical methods need to be employed. Among these are graph theory, geodetic network analysis, least squares adjustment and statistical tests. The results of this study will be compared with independent geological and geophysical observations available in the study area. This introduction gives an outline of the background information required to understand the concept and strategies of this research.

#### 1.1 Time in geodetic reference frames

Geodetic reference systems have always reflected the notion that the Earth is static because of the systems' time-invariant three-dimensional positioning conception. This notion has changed as the geodesists have realized that the Earth is dynamic and is changing its shape at a slow rate. In order to incorporate this variations of shape, the time geodetic conception has turned four-dimensional, and geodesists have been deliberating over the possible methodologies and models for this four-dimensional geodesy for a long time now e.g., (Mather, 1973; Vaníček et al., 1987). Mather (1978) went one step further and proposed a four-dimensional reference system for ocean studies thereby establishing the real need. But, all these deliberations have been far and wide, weaning proper attention to the problem of four-dimensional geodesy. In recent times, the attention has been rejuvenated particularly in the development of a vertical reference system that incorporates vertical crustal motions (Kleijer et al., 2001; Marti & Schlatter, 2001).

#### 1.2 Crustal motion studies and reference frames

Crustal motion studies have long been an integral part of geodesy, but confined to small localized areas such as tectonic zones (Mazzotti et al., 2003), earthquake-prone regions (Hearn,

2003), volcanic regions (Dzurisin, 1999), oil and gas fields (Kenselaar & Quadvlieg, 2001), and mines (Wright & Stow, 1999), to name a few. All these studies were traditionally made using terrestrial geodetic measurement techniques and were made from specially designed networks (Xu et al., 2000). But in recent times, space-geodetic methods like the Global Positioning Systems (GPS) (Blewitt, 2000), Synthetic Aperture Radar (SAR) (Bürgmann et al., 2000), Very Long Baseline Interferometry (VLBI) (Campbell, 2000), and Satellite Laser Ranging (SLR) (Tapley et al., 1985) are being used.

The advent of space-geodetic methods brought with it global and homogeneous coverage and hence, global monitoring of the Earth, which prompted the study of global scale crustal motions due to plate tectonics. The result of these studies was the development of a global network of space-geodetic stations that provided the first kinematic global terrestrial reference frame – the International Terrestrial Reference Frame of 1991 (ITRF1991) (Altamimi et al., 2002). Plate tectonic studies and the ITRF have been a real driving force in the development and implementation of modern geodetic reference frames that incorporate plate tectonic crustal motions. Such reference frames have been adopted by New Zealand (New Zealand Geodetic Datum 2000) (Blick, 2003) and Japan (Japanese Geodetic Datum) (Matsumura et al., 2004).

Similarly, the development of a kinematic vertical datum has been made possible by the increased interest in vertical crustal motion due to postglacial rebound, earthquakes, plate tectonics, and oil and gas extraction, among both geodesists and geophysicists. This is valid especially in countries that are experiencing these phenomena: Nordic countries, the Netherlands, Switzerland and Canada. The Nordic countries have a very long history of precise levelling data, some of which date back to 1885 (Mäkinen et al., 2003). The levelling network of the Nordic countries have been relevelled atleast twice and based on the relevelings many land uplift studies have been carried out e.g., (Mäkinen & Saaranen, 1998). Now, the Nordic countries are planning to utilize these precise relevelings to implement a kinematic vertical datum by the turn of the year 2006/2007 (Mäkinen et al., 2003) while the Netherlands (Kleijer et al., 2001) and Switzerland (Marti & Schlatter, 2001) have realized one recently.

### 1.3 The Canadian perspective

Crustal motion studies began in Canada in 1926 when the first crustal motion study was conducted in Québec after the 1925 earthquake. Further, crustal motion studies were carried out close to dams during the period 1959–64 (Gareau, 1986). However, interest turned into the crustal movements due to the postglacial rebound phenomenon in the eastern parts of Canada (Davis & Mitrovica, 1996), centered around Hudson Bay (Mitrovica, 1997), in the prairies (Lambert et al., 1998), and the Great Lakes (Mainville & Craymer, 2005); and the crustal movements due to tectonics along the western coast of Canada especially, the Cascadia subduction zone (Mazzotti et al., 2003). Since the entire Canadian region undergoes some kind of geophysical activity, some attempts were made to produce vertical crustal motion maps of Canada based on the levelling network observations and tide gauge records (Vaníček & Christodulidis, 1974; Vaníček & Nagy, 1981; Sjöberg et al., 1990). But, these attempts used only the releveling observations in combination with the tide gauge records. The work in this direction is still being continued with primary emphasis on postglacial rebound modelling (Koozmare et al., 2005). In addition, in 1991, the *Western Canada Deformation Array* was established to continuously monitor crustal motion due to the tectonics in the Cascadia region (Dragert & Hyndman, 1995). In parallel there are many more geological and geophysical studies that are being carried out with primary regard to postglacial rebound, for example (Peltier, 2002; Wu, 2006).

### 1.4 Motivation and objectives

The Earth is a dynamic planet and in order to completely understand its spatio-temporal dynamics, geodetic, geophysical, and geological data over long time scales and of homogeneous accuracy are essential. Looking at Canada, most of the previous studies have been carried out with GPS observations, and other modern space-geodetic measurement types (absolute and relative gravimetry, SLR, VLBI) all of which cover only the past  $\approx 20$  years. This is a serious handicap for geophysical inversion, which is the aim of using geodetic and geophysical data to constrain Earth parameters. The longer the history of data collection, and the more frequent the observations are repeated, the better the inversion results; however, these are only two of the important aspects of geophysical inversion.

The only geodetic data types that have a longer history to support geophysical inversion studies are traditional triangulation and trilateration data, levelling data, and tide gauge data; all of which have a data history of  $\approx 100$  years. Although, today these measurement types seem obsolete, these historic datasets are very important for geophysical inversion, and especially crustal motion studies. Since the interest of this research is only in vertical crustal motion, only levelling data was considered while tide gauges were kept aside for later cross-validation of the results from the two datasets. Geophysical inversion studies often benefit from different and independent datasets for cross-validation rather than combining them.

In order to retrieve and relate all the different geophysical phenomena from the levelling dataset, it is essential to define a common vertical datum that incorporates the vertical crustal motion. Thus, the objectives of this study are

1. *to determine the feasibility of defining a kinematic vertical datum based only on the levelling network of Canada, and*
2. *to establish the levelling dataset as an independent dataset for vertical crustal motion and geophysical studies.*

The biggest challenge of this study is that the national levelling network will be used for vertical crustal motion determination, although it has not been designed for such studies. In other words, the national levelling networks are designed to provide control for static height measurement and the frequency of measurement for a country of the size of Canada is very sparse. However, the greatest advantage of using historic levelling data for such studies is that they cover the last century as no other land-based geodetic dataset, and that the accuracy of levelling data has not changed a lot during the course of  $\approx 100$  years of measurements. Hence, the levelling observations can be considered homogeneous compared to other types of geodetic data such as GPS, where the improvements in accuracy have been an order or two higher than the first measurements.

The research problem here involves the determination of vertical crustal motion only from the levelling network observation and without any additional *a priori* information from geophysical models. In other words, the vertical crustal motion obtained from the levelling network should be interpretable in itself. If this can be achieved with the levelling network, then the two objectives of this study will be fulfilled, because the feasibility of defining a

kinematic vertical datum depends on whether the data can stand alone in providing the vertical crustal motion information. Thus, it can be seen that the two objectives are intertwined.

For the purpose of this study a small network was chosen from eastern Canada, where repeated observations are taken frequently and also, there are effects of both tectonics and postglacial rebound in this region. The region is depicted in Figure 1.1.

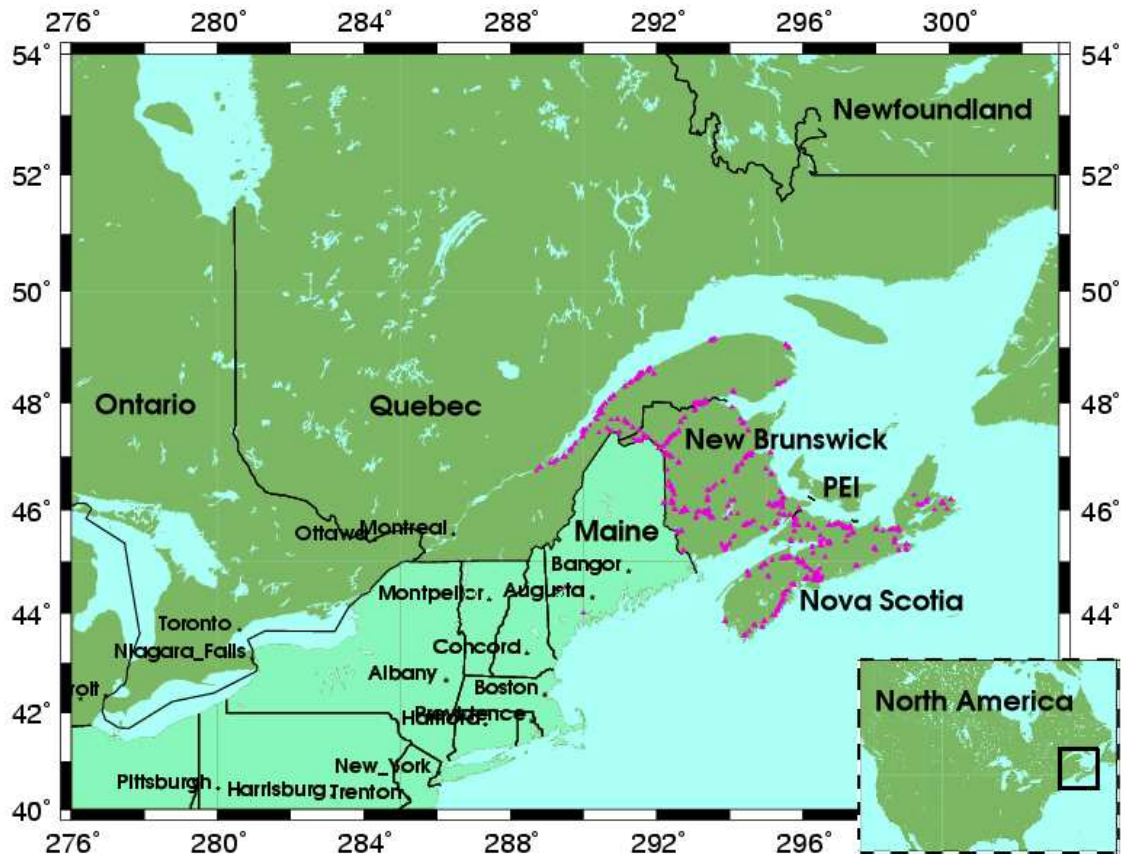


Figure 1.1: Illustration of the location of the study area

## 1.5 Outline of the thesis

The thesis starts with a review of gravitation, gravity, and the geopotential and their relation to the different height systems predominantly used for national levelling networks. Then, the concept of a vertical datum is introduced from three different perspectives, viz., physical, geodetic, and mathematical. The concept is completed with an explanation of datum con-

---

straints. The concept of a vertical datum is then extended to the kinematic vertical datum and the S-transformation of a kinematic vertical datum is derived – chapter 2.

In chapter 3, the history of the levelling dataset of Canada is reviewed for the purpose of evaluating the quality of the data. Then the format of the dataset obtained from the Geodetic Survey Division, Natural Resources Canada, is described and also its implications towards the data processing strategies are discussed. The solvability of levelling networks for vertical crustal motion is explained, and extended into data processing methods. The chapter concludes by illustrating results from the levelling network data processing.

In chapter 4, a review of the rudiments of graph theory is given and it is connected to the levelling network adjustment. Then, the least squares method of adjustment of the levelling networks is explained with examples and is linked with graph theory. In addition, vital statistics of the levelling network are calculated. These statistics characterize the nature of the network and also provide a preliminary idea about the quality of the adjustment process and its results. Also, a trend analysis of relative velocities is carried out for levelling observations that have been re-observed more than once.

In chapter 5, the adjustment results are presented, where adjustment using different types of constraints, and different weighting schemes are illustrated and explained. The results of the adjustments are then analysed from a least squares error analysis point of view, which provides insight into the interpretability of the results. The chapter concludes with performing statistical tests to find outliers in the observations. The adjustment results are geologically and geophysically interpreted in chapter 6, where the nature of estimated vertical crustal motion are discussed. The conclusions of this research and its future scope are discussed in chapter 7.

## Chapter 2

### Vertical Datum Definition

A datum is defined as any numerical or geometrical quantity or set of such quantities which serve as a reference or base for other quantities (Jekeli, 2000). In that sense, a vertical datum is a reference for heights. In this chapter, a brief introduction to the concepts of gravitation, gravity and geopotential will be given in section 2.1; various height systems that exist will be briefly discussed in section 2.2; different perspectives in the datum definition will be discussed in section 2.3; the mathematical model that will be used in the kinematic vertical datum will be discussed in section 2.5; and finally, the *S-transformation* of the kinematic vertical datum is derived in section 2.6.

#### 2.1 Gravitation, gravity, and geopotential

The words gravity and gravitation bring to mind the famous Newton equation of the force of gravitational attraction

$$F_{12} = \frac{Gm_1m_2}{r_{12}^2} \quad , \quad (2.1)$$

where

$F_{12}$  – the force of gravitational attraction between two point masses at 1 and 2 (N).

$G$  – gravitational constant ( $6.672 \cdot 10^{-11} \text{Nm}^2/\text{kg}^2$ ).

$m_1, m_2$  – mass of the point masses (kg).

$r_{12}$  – distance between the two points (m).

From (2.1), the force per unit mass of the mass  $m_2$  can be derived and is given as

$$\begin{aligned} a_2 &= \frac{F_{12}}{m_2} \\ a_2 &= \frac{Gm_1}{r_{12}^2} \quad . \end{aligned} \quad (2.2)$$

When this quantity is considered for a body with respect to the gravitational force of attraction of the Earth, the indices can be removed and equation (2.2) becomes,

$$a = \frac{GM}{r^2} \quad .$$

Since, force is a vector the above equation is written in vector notation,

$$\vec{a} = \frac{GM}{r^3} \vec{r} \quad . \quad (2.3)$$

The quantity  $\vec{a}$  is the gravitational attraction of the mass  $M$ , which is the mass of Earth. The gravitational attraction field of the Earth is a conservative field that means the amount of work done to go from point 1 to 2 is the same regardless of the path taken. Mathematically, this can be expressed as,

$$\text{rot} \vec{a} = \nabla \times \vec{a} = \vec{0}$$

which according to vector analysis is also equivalent to  $\text{rot grad } F$ , where  $F$  is a scalar field. Thus, the gravitational attraction can be written as the gradient of a scalar field and this scalar field is called the gravitational potential field  $V$ . The term  $\vec{a}$  is called the gravitation and the term  $V$  is called the gravitation potential. The gravitation potential of the Earth is given by

$$V = \frac{GM}{r} \quad . \quad (2.4)$$

The above equation can be rewritten with density instead of the mass term,

$$V = G \iiint_{\Omega} \frac{\rho(x, y, z)}{r} dx dy dz \quad , \quad (2.5)$$

where  $\Omega$  represents the volume of the Earth.

Whenever a measurement is done to observe the gravitation of a point the measurement also contains the centrifugal attraction in addition to the gravitation. What is measured is called gravity, the sum of centrifugal and gravitational attraction. Since the gravity has the centrifugal acceleration term, the gravity potential also has the centrifugal potential term.

$$\text{gravity} = \text{gravitational attraction} + \text{centrifugal attraction}$$

$$\vec{g} = \vec{a} + \vec{a}_c \quad (2.6)$$

$$\text{gravity potential} = \text{gravitational potential} + \text{centrifugal potential}$$

$$W = V + V_c \quad (2.7)$$

Since the gravity of the Earth arises from a potential field, the Earth could be visualized as consisting of *equipotential surfaces* of the Earth's gravity potential (refer Figure 2.1), along

which the value of the gravity potential is the same. These equipotential surfaces are also referred to as *level surfaces* Heiskanen & Moritz (2000).

## 2.2 Height Systems

Heights are defined as the perpendicular distances to points of consideration in the vertical direction from a reference surface. Any instrument that is put up on the Earth's surface and levelled with a spirit bubble comes under the influence of the Earth's gravity field and hence, the Earth's gravity potential field. Once the instrument is levelled, i.e. when the spirit bubble is at the center, the instrument is said to lie parallel to the tangent of the equipotential surface (or level surface), of the Earth's gravity potential (geopotential), at that point. The perpendicular line between the center of the instrument and the level surface is called the *direction of plumbline* or *plumbline* in short (Heiskanen & Moritz, 2000). In spirit levelling the height differences measured between two points is in essence the measurement of the height difference between the equipotential surfaces of the geopotential passing through the two points. However, the equipotential surfaces are not parallel to each other and this causes the heights to be non-unique when they are observed using spirit levelling. This is shown in Figure 2.1.

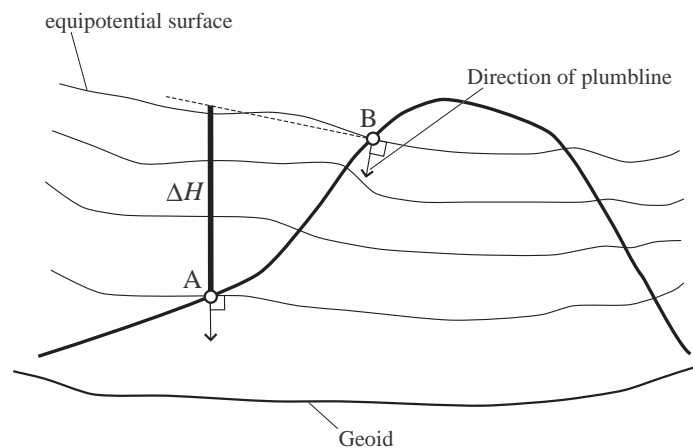


Figure 2.1: The height measurement procedure between two points through levelling measurements. The observed height difference in the field is the value  $\Delta H$ .

The above concept can be easily proved by taking a closed circuit of spirit levelling mea-

surements (Figure 2.2) and then adding them up. By logic of geometry the sum should be zero, because if the starting and ending points of a height measurement are the same then the height difference must be zero. But this will not be the case as there will be a misclosure, which indicates that the equipotential surfaces are not parallel. When the same sum of the circuit is taken with the gravity values, which accounts for this non-parallelity of the equipotential surfaces, for each of those measured points, the misclosure can be expected to zero if the measurements are not affected by observation errors. The other reason being, when the gravity measurements along the measurement lines are combined with the height difference observations the resulting quantity is geopotential. Hence, if the geopotential differences are summed up in a given levelling circuit the sum will be zero. This is also the reason that heights measured based on spirit levelling take one of these equipotential surfaces as their reference (Heiskanen & Moritz, 2000). The gravity values become relevant only for a levelling network whose lines have a distance of few hundred metres and more.

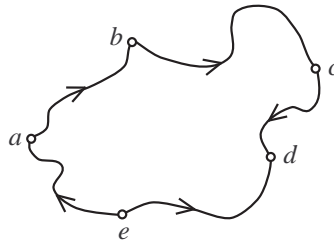


Figure 2.2: A closed circuit of spirit levelling measurements

Other methods of height measurements include triangulation, trilateration, and GPS measurements. The height measurements from these methods are purely geometrical and they are referenced to an ellipsoid; however, vertical deflection corrections need to be made for measurements from triangulation and trilateration. The heights are geometrical in the sense that the ellipsoid, which is the reference surface, is purely geometrical and imaginary when compared to the equipotential surface of the Earth's gravity field. Thus, from the above discussion, the height systems can be broadly classified into *physical* and geometrical height systems based on their reference surfaces (Meyer et al., 2004). Following is a list of the common physical height systems used for national height networks and topographic mapping.

*Orthometric Heights*

$$H_P = \frac{C_P}{\bar{g}} \quad (2.8)$$

*Dynamic Heights*

$$H_P^{\text{dyn}} = \frac{C_P}{\gamma_o} \quad (2.9)$$

*Normal Heights*

$$H_P^n = \frac{C_P}{\bar{\gamma}} \quad (2.10)$$

*Normal Orthometric Heights*

$$H_P^* = \frac{C_P^*}{\bar{\gamma}} \quad (2.11)$$

where

$$\begin{aligned} C_P &= W_0 - W_P \\ &= \int g \, dH \end{aligned} \quad (2.12)$$

is the geopotential number with  $W_0$  representing the geopotential at the reference point and  $W_P$  representing the geopotential at point  $P$ .

$\bar{g}$  is the mean gravity along the plumbline between  $P$  and the geoid.

$\bar{\gamma}$  is the mean normal gravity along the normal plumbline between  $P$  and the quasi-geoid.

$\gamma_o$  is the normal gravity at a chosen latitude, which is usually  $\phi = 45^\circ$  latitude.

$$\begin{aligned} C_P^* &= U_0 - U_P \\ &= \int \gamma \, dH^* \end{aligned} \quad (2.13)$$

is the normal geopotential number with  $U_0$  representing the normal geopotential of the quasi-geoid and  $U_P$  representing the normal geopotential at  $P$ . The physical nature of these heights can be explained in the following manner. In Figure 2.1, if the gravity values are measured at the points A and B, they will represent the gradient of gravity potential at those points as

it is known that gravity is the grad  $W$  (cf. Section 2.1). Taking the mean gradient along this measurement line and integrating that with the measured height difference gives the gravity potential. This is what is done in equations (2.12) and (2.13). The other dimension through which this physical nature of the physical heights can be visualized is the density term in the gravitational potential term (cf. (2.5)). Gravity variations are a consequence of density variations in the Earth. In geophysical prospecting this property of gravity is utilized to locate mineral resources or other density anomalies.

Of the above mentioned height systems the orthometric height system is the most widely used height system because it uses true gravity values, when compared to other height systems. The only problem with the determination of orthometric heights is that the calculation of mean gravity along the plumbline requires the knowledge of the density variations of the crust between the point of consideration and the geoid, which is difficult, if not impossible. This is also one of the reasons that we have other height systems in place. For example, the normal height system was proposed to overcome this difficulty of finding the density variations along the plumbline. In the normal height system, the heights are referred to a surface called *quasigeoid*, which is *an approximation of the geoid due to the use of normal gravity*. However, the quasigeoid is not an equipotential surface, but coincides with the geoid over the oceans (Heiskanen & Moritz, 2000).

Due to the extensive labour and high cost involved in spirit levelling measurements, national height networks are slowly being replaced by GPS/levelling techniques. This technique exploits the simple relationship between ellipsoidal heights, orthometric heights and geoid undulations, which is given as

$$h = H + N \quad , \quad (2.14)$$

where

$h$  – ellipsoidal height,

$H$  – orthometric height, and

$N$  – geoid undulation. (Heiskanen & Moritz, 2000)

The geometric relationship of the three quantities is shown in Figure 2.3

The main drawback of the above method are the accuracies of GPS heights and geoid undulations, which are still at the few centimetres level. A detailed study of this method has

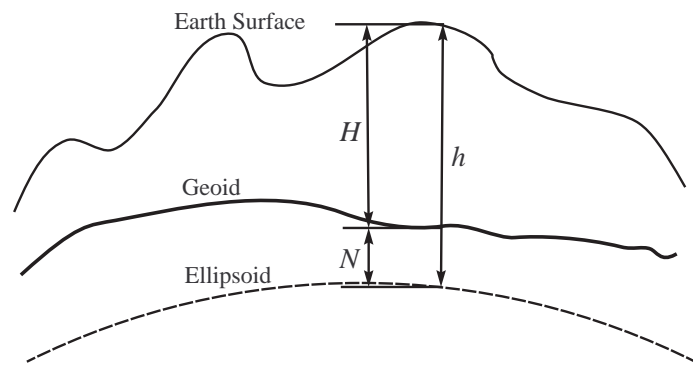


Figure 2.3: Relationship between geoid undulation and ellipsoidal and orthometric heights

been carried out by Fotopoulos (2003). For a detailed discussion of the height systems refer Heiskanen & Moritz (2000); Vaníček & Krakiwsky (1986); Torge (2001); Meyer et al. (2004, 2005).

## 2.3 Perspectives in vertical datum definition

### 2.3.1 Physical perspective

The visualization of a vertical datum can be either physical as always in the case of physical geodesy literature, where the vertical datum is pictured as a physical surface: usually a geoid. The *geoid* is defined as an equipotential surface of the gravity field of the Earth that is closely approximated by the mean sea surface. This definition was first proposed by C.F. Gauß and his Ph.D. student J.B. Listing and hence, the above definition of geoid is called the *Gauß-Listing geoid*. This definition has long been used in geodesy to define a vertical datum. Sometimes, this geoid definition is loosely referred to as the *mean sea level* and the heights above it the heights above mean sea level. So, one of the perspectives of vertical datum definition is a physical surface. Although, a geoid is an imaginary surface physically realized via the mean sea level obtained from mareograph measurements. A complete discussion on this perspective is given in Heck (2002); Jekeli (2000).

### 2.3.2 Mathematical perspective

The above perspective was from physical geodesy, while the other perspective of vertical datum definition comes from geodetic network analysis. The spirit levelling measurements taken in a network form a network similar to the electrical potential circuits (networks). The similarity comes from the fact that levelling network represents the network of geopotential difference measurements. This network is represented by the *design matrix* in the least squares adjustment of the network. The design matrix is referred to as the *edge-node incidence matrix* in *graph theory* (cf. Strang (1986)).

The whole network consists only of measurements of the height differences between the points in the network, while the requirement is absolute heights of points. Determining heights only from height difference measurements is impossible (Casparly, 1988). Thus, a constant needs to be added to the measurements without changing the differences to determine the heights (Strang, 1986). This lack of information appears as a column rank deficiency in the design matrix of the network. This lack of information, and hence, the column rank deficiency, is termed the *datum problem* in geodetic network analysis. The datum definition can now be considered as satisfying this rank deficiency by supplying some relevant information, for example, assuming a constant to be the height of one of the points in the network. This is the mathematical or computational perspective of the datum definition. Since the constant could be any convenient value, and also, the point in the network could be any convenient point the vertical datum definition can be considered arbitrary.

A complementary explanation to the mathematical perspective is given by Strang (1986); Lanczos (1997), which comes from matrix calculus theory. Strang (1986) says that design matrix in a least squares adjustment problem can be considered as a hyperplane having the dimension of the number of parameters being estimated. The singular value decomposition of this matrix tells us how much information the matrix carries in each of those axes of the hyperplane. When there is a rank deficiency the singular values are zero corresponding to the rank deficiency number. Hence, the zero singular values indicate lack of information along those axes. In order to overcome this situation, information has to be supplied to the matrix along those axes (Lanczos, 1997), and this is where the constant comes into play. In geodesy, this constant is termed the *datum constraint*.

### 2.3.3 Geodetic perspective

The two different perspectives might give a feeling that they will be treated separately in the vertical datum definition. Traditionally, the marriage between the two perspectives is made possible by establishing that the equipotential surface passes through a chosen mareograph location, and the mean sea level value at the mareograph station serves as the constant according to the mathematical perspective of datum definition. In essence, datum definition drops down to a geodetic network adjustment problem, where the network appears as the design matrix; the potential differences appear as the vector of observations; and the datum problem appears as the column rank deficiency. The generalized inverse of the design matrix taken by supplying the constant in the column of the mareograph station point provides both the datum definition and estimates the absolute heights of points.

### 2.3.4 Perspectives on a good vertical datum

In keeping with the perspectives of vertical datum definition, it is also imperative to look into the perspectives of good vertical datum definition. Grant & Blick (2001) have come up with a list of items that need to be taken care of in realizing a vertical datum. Following is the list of the items,

- *unified and definitive* – There must be only a single vertical datum for the whole of a country;
- *based on an equipotential surface* – The vertical datum must be based on an equipotential surface such as the geoid because of the fact that height determination is dependent upon the gravity potential of the Earth;
- *consistent with gravimetric geoid models* – The vertical datum should use the gravimetric geoid models so that it facilitates the conversion of ellipsoidal heights obtained from GPS to orthometric heights;
- *zero height close to sea level* – This is a requisite for hydrographic studies, storm water and river system management studies, and land title boundary demarcations along the coastline;

- *applicable to islands* – The vertical datum developed should be applicable to constituent islands of a country across vast stretches of oceans. Countries like New Zealand suffer from separate vertical datums for the constituent islands, which renders the height system followed in one island useless or difficult for transformation in the other islands;
- *consistent with international standards and systems* – Proper reductions of gravity data and height data, which are upto the standards followed globally should be done; and
- *able to support sea level modelling* – The vertical datum should support studies related to sea level changes and hence should avoid using the mean sea level as a reference for the vertical datum.

## 2.4 Datum constraints and datum matrices

The term *datum constraints* was introduced in section 2.3.2. The term *constraints* comes from data analysis, where the datum problem of the levelling network, in the sense of geodetic network analysis, becomes a *constrained least squares problem* (van Loan, 1985). The linear equality constrained least squares problem is given as (van Loan, 1985; Golub & van Loan, 1996),

Solve

$$\mathbf{y} = \mathbf{Ax} + \boldsymbol{\epsilon} \quad (2.15)$$

subject to

$$\mathbf{Bx} = \mathbf{c} \quad (2.16)$$

In the case of geodetic networks, the constraint equation becomes,

$$\mathbf{D}^T \mathbf{x} = \mathbf{c} \quad , \quad (2.17)$$

where

- $\mathbf{y}$  – vector of observations,
- $\mathbf{A}$  – co-efficient or design matrix,
- $\mathbf{x}$  – is the vector of parameters, and
- $\boldsymbol{\epsilon}$  – random errors in the observations,
- $\mathbf{B}$  – condition matrix,
- $\mathbf{D}$  – is the datum matrix,
- $\mathbf{c}$  – is the vector of constants.

The datum matrix indicates which parameters in  $\mathbf{x}$  will be fixed by a constant to estimate the absolute values of the parameters with respect to the constants (an example of a datum matrix is given in section 2.6.3). The solution to the problem in (2.15) subject to the constraint in (2.16) can be obtained by least squares by minimizing the variation function in (2.18) via Lagrange multipliers.

$$\phi(x, \lambda) = \|\mathbf{y} - \mathbf{A}\mathbf{x}\|_2^2 + \lambda(\|\mathbf{D}^T\mathbf{x}\|_2^2 - \mathbf{c}) \quad (2.18)$$

where

- $\phi(x, \lambda)$  – variation function
- $\lambda$  – Lagrange multipliers

Minimizing the equation (2.18) results in

$$\hat{\mathbf{x}} = (\mathbf{A}^T\mathbf{A} + \mathbf{D}\mathbf{D}^T)^{-1}(\mathbf{A}^T\mathbf{y} + \mathbf{D}\mathbf{c}) \quad (2.19)$$

A complete derivation of the solution is provided in Caspary (1988) from the datum matrix point of view and the subject of constrained least squares is covered in detail in Golub & van Loan (1996).

The constraints can be applied to the least squares problem in three different ways: *minimum constraints*, *inner constraints* and *over-constraints*.

- When the number of constants equal the rank deficiency of the design matrix of the geodetic network, then the equality constraints are called minimum constraints. In other words, supplying whatever information that is lacking in the design in the form of constraints is called minimum constraints. This is a case of *linear equality constrained least squares*. Minimum constraints are applied to national geodetic networks of the

primary order and the important characteristic of minimum constraints adjustment is that it preserves the geometry of the network.

- When some conditions on the parameter-side or on the observation-side are applied, instead of supplying constants to the parameters, then such form of constraints are called inner constraints. The least squares adjustment carried out with inner constraints is also referred to as *free network adjustment*. It is predominantly carried out to find erroneous observations. The difference between the conditions applied on the parametric-side here and in the minimum constraints case is that in minimum constraints the constraint values are taken from external sources, but in inner constraints the conditions come from within the parameters.
- When the number of constants supplied to the least squares problem is more than what is required by the rank deficient design matrix, then the equality constraints are called over-constraints. This is again a case of linear equality constrained least squares. This type of constraints are mainly applied to lower order networks in order to fit them to the higher order networks. The over-constraint adjustment strains (distorts) the geometry of the network (Kuang, 1996).

## 2.5 Kinematic vertical datum

Three types of vertical crustal motion can be distinguished, viz., *secular*, *periodic*, and *episodic*. Plate tectonics and post-glacial rebound fall under the realm of secular motions, although post-glacial rebound is not secular over long periods of geological time; the deformation and gravity changes caused by tidal forces are periodic; and vertical deformation due to Earthquakes, and landslides are episodic. It must be noted that eventhough the tidal forces generate deformation that is periodic in nature, permanent tidal deformation also occurs, which is treated as a systematic effect and removed from the observations. The values are calculated based on solid Earth tide models (Gareau, 1986).

### 2.5.1 Kinematic height model

The different types of vertical crustal motion can be incorporated into the vertical datum either *kinematically* – without considering the forces causing the vertical motion, or *dynamically* –

considering the forces causing the vertical motion. Since in this research a kinematic vertical datum is the area of focus, only the kinematic vertical datum will be discussed. Nevertheless, it is essential to analyse the nature of the deformation in the region of concern before attempting the realization of a vertical datum that takes into account the vertical crustal deformation. In Canada, the major sources of vertical deformation are post-glacial rebound and plate tectonics, which are secular in nature. Hence, a secular deformation model will be used for the kinematic vertical datum. The following is the secular (linear) model of the kinematic vertical datum,

$$H_i(t_k) = H_i(t_0) + v_i(t_k - t_0) \quad i \in \{1, n\} \quad , \quad (2.20)$$

where

- $H_i$  – height of the point  $i$
- $v_i$  – vertical velocity of the point  $i$
- $t_k, t_0$  – epochs of observation and the datum respectively.

The reason for assuming a linear model is also that there data are not sufficient to verify if there is any acceleration of heights in the region. This will be discussed in the next chapter. However, Mäkinen & Saaranen (1998) applied an accelerating model for the Finnish levelling network, but were unable to find any significant acceleration.

### 2.5.2 Derivation of the Kinematic Vertical Datum Adjustment

By assuming a linear model for the vertical deformation, every point in the network is parameterized by one height and one velocity. The linear model can be visualized as an equation of a line in analytical geometry (Figure 2.4), which is given by

$$y = f(x) \quad (2.21)$$

$$y = mx + c \quad , \quad (2.22)$$

where

- $y$  – the ordinate,
- $x$  – the abscissa
- $m$  – the slope of the line
- $c$  – the intercept.

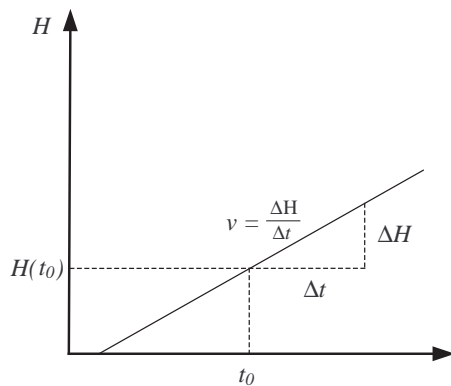


Figure 2.4: Representation of the kinematic height model as an equation of a line in analytical geometry

In the kinematic height model, the height at the datum epoch  $t_0$  is the value  $c$ ; the velocity of the point is the slope of the line  $m$ ; and time and height are the abscissa and the ordinate axes, respectively. Since, only geopotential differences are available to estimate both heights and velocities of the points, only height differences and velocity differences (relative velocities) will be estimable from the observations. However, as mentioned in section 2.3.2, if a constant is supplied, both the height differences and velocity differences can be transformed to absolute (with respect to the constants) heights and velocities.

As mentioned in section 2.3, the datum definition drops down to a geodetic adjustment problem. The adjustment of a kinematic vertical datum is very similar to the adjustment of a vertical datum, because the observations are still the network of geopotential differences. The two major differences that break this similarity are

1. time-tagging of the observations, and
2. addition of velocities and time epoch to the vector of parameters to be estimated.

The time-tagging of observations has implications in that the vertical velocity of height points are discretized within the time-span chosen; and time becomes a datum parameter. The time-span could be a decade, an year, a month, a day or even an hour. This further implies that the discretization makes the heights of the points static within the time-span chosen, or in other words, the movement of the height point within the time-span chosen is assumed insignificant. More often than not the time-span is chosen based on the frequency of observation. The other implication that time becomes a datum parameter comes from the fact that if a  $t_0$  is not prescribed, the reference time epoch will be the beginning of Julian calendar, i.e., 0A.D. The estimated heights will all refer to that year for which there is no information about what the heights were in that period and also, there is no way of validating such heights. So, it is not sensible to keep such a value as a reference epoch. Hence, a time epoch that is within or closer to the observation time period is always chosen as the reference epoch. Time as a datum parameter has been used in a study of the star catalogues based on Hipparcos satellite measurements (Arias et al., 2000). In that study the authors develop an error estimate based on the reference epoch shift.

Realisation of a kinematic vertical datum involves the estimation of heights and the vertical deformation (velocities). As the kinematic vertical datum is as arbitrary as the vertical datum, one height, one velocity and a time epoch all need to be fixed. Thus in the realisation of a kinematic vertical datum three datum parameters need to be fixed, which are height, velocity and time. But the value of time can be chosen as a constant or a deterministic variable in the model (2.20). If the time epoch is chosen as a deterministic variable then the linear model becomes a non-linear model and hence, the model has to be linearized in order to use least squares estimation to estimate the parameters. This linearization is shown in the following derivation of the least squares adjustment equation of the kinematic vertical datum.

The levelling difference observation at a given time  $t_k$  between two points  $i$  and  $j$  is given as

$$H_{ij}(t_k) = H_j(t_k) - H_i(t_k) \quad i, j \in \{1, n\} \quad . \quad (2.23)$$

Substituting equation (2.20) gives

$$H_{ij}(t_k) = H_j(t_0) - H_i(t_0) + (v_j - v_i)(t_k - t_0) \quad . \quad (2.24)$$

Since in (2.20) both  $v_i$  and  $t_0$  are parameters, the equation needs to be linearized. The height at a particular time  $t_k$  can be thought of as a function of height at a chosen time epoch ( $H_i(t_0)$ ), velocity ( $v_i$ ), and time epoch ( $t_0$ ). So, the first derivative of the height of a given point can be written in the following form,

$$dH_i = \frac{\partial H_i}{\partial H} dH + \frac{\partial H_i}{\partial v} dv + \frac{\partial H_i}{\partial t_0} dt_0 \quad (2.25)$$

The linearized form is given as,

$$H_i(t_k) = H_i(t_0) + v_i(t_k - t_0) + dH_i + (t_k - t_0) dv_i - v_i dt_0 \quad (2.26)$$

Making the differentials finite gives,

$$H_i(t_k) = H_i(t_0) + v_i(t_k - t_0) + \Delta H_i + (t_k - t_0) \Delta v_i - v_i \Delta t_0 \quad (2.27)$$

Substituting (2.27) in (2.23) for  $i$  and  $j$  gives

$$\begin{aligned} H_{ij}(t_k) = & H_j(t_0) - H_i(t_0) + (v_j - v_i)(t_k - t_0) + (\Delta H_j - \Delta H_i) + \\ & (\Delta v_j - \Delta v_i)(t_k - t_0) - (v_j - v_i)\Delta t_0 \quad . \end{aligned} \quad (2.28)$$

Simplifying the above equation notation-wise gives the following equations

$$\begin{aligned} H_{ij}(t_k) = & H_{ij}(t_0) + v_{ij}t_{0k} + \\ & (\Delta H_j - \Delta H_i) + (\Delta v_j - \Delta v_i)t_{0k} - v_{ij}\Delta t_0 \end{aligned} \quad (2.29)$$

$$H_{ij}(t_k) - H_{ij}(t_0) - v_{ij}t_{0k} = (\Delta H_j - \Delta H_i) + (\Delta v_j - \Delta v_i)t_{0k} - v_{ij}\Delta t_0 \quad . \quad (2.30)$$

Equation (2.30) if written in matrix notation will be as follows,

$$\begin{bmatrix} H_{12}(t_k) - H_{12}(t_0) - v_{12}t_{0k} \\ \vdots \\ H_{nm} - H_{nm}(t_0) - v_{nm}t_{0k} \end{bmatrix} = \begin{bmatrix} -1 & 1 & \dots & \dots & -t_{0k} & t_{0k} & \dots & \dots & v_{12} \\ \vdots & & & & \ddots & & & & \vdots \\ \dots & -1 & \dots & 1 & \dots & -t_{0k} & \dots & t_{0k} & v_{nm} \end{bmatrix} \begin{bmatrix} \Delta H_1 \\ \Delta H_2 \\ \vdots \\ \Delta H_m \\ \vdots \\ \Delta H_n \\ \Delta v_1 \\ \Delta v_2 \\ \vdots \\ \Delta v_m \\ \vdots \\ \Delta v_n \\ \Delta t_0 \end{bmatrix} \quad (2.31)$$

Thus the above equation represents the linearized observation equation

$$\mathbf{y} = \mathbf{A}\mathbf{x} + \boldsymbol{\epsilon} \quad , \quad (2.32)$$

which when estimated with least squares becomes,

$$\hat{\mathbf{y}} = \mathbf{A}\hat{\mathbf{x}} \quad . \quad (2.33)$$

The  $\mathbf{A}$  matrix (called the design matrix) will have a rank deficiency of two; one for height, and one for velocity. While removing columns for satisfying the rank deficiency two columns of the  $\mathbf{A}$  matrix should be removed: one each for height and velocity. If the datum matrix method is being adopted, then the datum matrix will have a dimension  $((2n) \times 2)$ , which when split up becomes  $(n(\text{heights}) + n(\text{velocities}))$ . Even though there are three datum parameters, only height and velocity need to be fixed while time can be estimated from the observations' time-tagging.

## 2.6 S-transformation of a kinematic vertical datum

The kinematic vertical datum adjustment is obtained from a rank deficient design matrix. This rank deficiency makes the estimated parameters biased estimates because of the information supplied by constants via the columns of the design matrix (Teunissen, 1985). The estimates depend on the choice of the columns along which the information is supplied. By changing the constants and/or the columns, an innumerable number of solutions can be obtained. All these solutions are related to each other by a similarity transformation, which enables the transformation of parameters defined by one set of constants to another set of constants (Strang van Hees, 1982).

S-transformation is a similarity transformation that transforms the stochastic (variance-covariance) information in addition to transforming the co-ordinates. This is an important tool for transforming co-ordinates from one datum to the other along with their stochastic information. The advantage of using a S-transformation is that the whole process of adjustment need not be carried out over and over again for transforming the co-ordinates and their stochastics from one datum to other. The S-transform, which will be derived in the sequel, does the job of transferring the co-ordinates and their stochastic information in one simple step.

After equation (2.32) has been solved for the parameters, the heights, velocities and the time epoch will all be known in one datum that has been fixed. If the datum parameters need to be transformed to other datum parameters, i.e., from  $[H_a, v_a, t_0^a]$  datum to  $[H_b, v_b, t_0^b]$  datum, then there will be a constant shift in height, velocity and time epoch. There are a few things that need to be thought about these shifts in datum parameters as they are not straightforward, atleast in their conception. The shifts in each of height, velocity and time is explained in the following sections.

### 2.6.1 Height shift

In the kinematic vertical datum definition and transformation it is essential to fix the *reference time epoch*. This is because heights are a function of time  $H = f(t)$ , similar to the equation of a line 2.21, as the heights keep changing with time. Estimated heights are referenced with a time epoch to indicate the relevance of the height value in time. Thus, it is obvious that

before definition or transformation of a kinematic vertical datum, the reference time epoch should be fixed. Reviewing (2.20) gives

$$H_i(t_k) = H_i(t_0) + v_i(t_k - t_0) \quad ,$$

where  $t_k$  is the instantaneous time and  $t_0$  is the reference time epoch. From the kinematic adjustment only the height at  $t_0$  is estimated. Hence, in the datum transformation the interest is in transforming the heights at reference epochs and the intention is only to transform them to a new datum.

As mentioned above, it is assumed that  $[H_a, v_a, t_0^a]$  are known and  $[H_b, v_b, t_0^b]$  are required. It is also assumed that the kinematic vertical datum parameters in  $b$  do not have the same epoch as  $a$ . Now, in order to find the shift, the height of the vertical datum parameter in  $a$  has to be moved from time  $t_0^a$  to time  $t_0^b$ .

$$H_i^a(t_0^b) = H_i^a(t_0^a) + v_i^a(t_0^b - t_0^a) \quad (2.34)$$

Thus, the height shift between the two datums is determined as follows,

$$\Delta H_{ab} = H_i^b(t_0^b) - H_i^a(t_0^b) \quad . \quad (2.35)$$

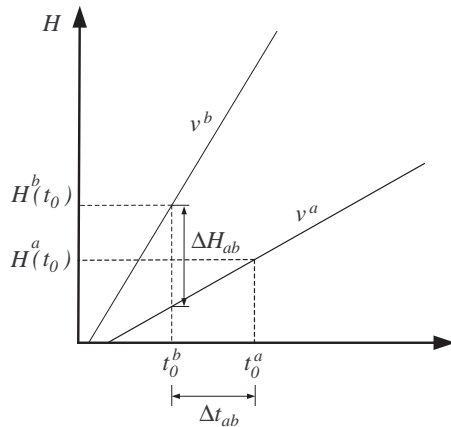


Figure 2.5: The height, velocity, and time shifts in a kinematic vertical datum

### 2.6.2 Velocity and time shifts

The interesting thing about the vertical velocity of a point is that, since the kinematic height model is assumed to be linear, its shift as a datum parameter does not depend on time or

height. Therefore it is straightforward.

$$\Delta v_{ab} = v_i^b - v_i^a \quad (2.36)$$

Similar is the case with time shift and it is again just the difference of the time epochs between which the transformation is done.

$$\Delta t_{ab} = t_0^b - t_0^a \quad (2.37)$$

Both the height and time shifts are illustrated in Figure 2.5.

### 2.6.3 The S-transform

Putting all the above datum shifts together gives

$$\begin{aligned} \Delta H_{ab} &= H_i^b(t_0^b) - H_i^a(t_0^a) - v_i^a(t_0^b - t_0^a) \\ \Delta H_{ab} &= H_i^b(t_0^b) - H_i^a(t_0^a) - v_i^a \Delta t_{ab} \end{aligned} \quad (2.38)$$

$$\Delta v_{ab} = v_i^b - v_i^a \quad (2.39)$$

$$\Delta t_{ab} = t_0^b - t_0^a \quad . \quad (2.40)$$

Rearranging the above equations gives

$$\begin{aligned} H_i^b(t_0^b) - H_i^a(t_0^a) &= \Delta H_{ab} + v_i^a \Delta t_{ab} \\ v_i^b - v_i^a &= \Delta v_{ab} \\ t_0^b - t_0^a &= \Delta t_{ab} \quad . \end{aligned} \quad (2.41)$$

The above equations are the equations of similarity transformation of a kinematic vertical datum. If these equations are written in matrix notation, the following will be obtained:

$$\begin{bmatrix} H_1^b(t_0^b) - H_1^a(t_0^a) \\ \vdots \\ H_n^b(t_0^b) - H_n^a(t_0^a) \\ v_1^b - v_1^a \\ \vdots \\ v_n^b - v_n^a \\ t_0^b - t_0^a \end{bmatrix} = \begin{bmatrix} 1 & 0 & v_1^a \\ \vdots & \vdots & \vdots \\ 1 & 0 & v_n^a \\ 0 & 1 & 0 \\ \vdots & \vdots & \vdots \\ 0 & 1 & 0 \\ 0 & 0 & 1 \end{bmatrix} \begin{bmatrix} \Delta H_{ab} \\ \Delta v_{ab} \\ \Delta t_{ab} \end{bmatrix} \quad . \quad (2.42)$$

Simplifying the notation for the above equation will give

$$\mathbf{X} = \mathbf{TP} \quad . \quad (2.43)$$

Whenever a datum transformation is made, there are some points in the network whose coordinates are known in both the datums between which the transformation is made. Now, we introduce a datum matrix that tells us the points with which we can estimate the shift in the datum parameters.

$$\mathbf{D}_b = \begin{bmatrix} 1 & 0 & 0 \\ \vdots & & \\ \vdots & & \\ 0 & 1 & 0 \\ \vdots & & \\ \vdots & & \\ 0 & 0 & 1 \end{bmatrix} \quad (2.44)$$

and the values of the datum constraints are given by the constraint equation,

$$\mathbf{D}_b^T \mathbf{H}^b = \mathbf{c} \quad . \quad (2.45)$$

Pre-multiplying the transpose of  $\mathbf{D}_b$  with (2.43) gives

$$\mathbf{D}_b^T \mathbf{X} = \mathbf{D}_b^T \mathbf{TP}$$

In the above equation  $\mathbf{D}_b^T \mathbf{T}$  is a regular square that can be uniquely inverted and hence, the above equation becomes,

$$(\mathbf{D}_b^T \mathbf{T})^{-1} \mathbf{D}_b^T \mathbf{X} = \mathbf{P} \quad (2.46)$$

Substituting (2.46) in (2.43) gives,

$$\mathbf{X} = \mathbf{T}(\mathbf{D}_b^T \mathbf{T})^{-1} \mathbf{D}_b^T \mathbf{X} \quad (2.47)$$

Expanding the above equation gives

$$\mathbf{H}^b - \mathbf{H}^a = \mathbf{T}(\mathbf{D}_b^T \mathbf{T})^{-1} \mathbf{D}_b^T (\mathbf{H}^b - \mathbf{H}^a) \quad (2.48)$$

$$\begin{aligned} \mathbf{H}^b - \mathbf{H}^a &= \mathbf{T}(\mathbf{D}_b^T \mathbf{T})^{-1} \mathbf{D}_b^T \mathbf{H}^b \\ &\quad - \mathbf{T}(\mathbf{D}_b^T \mathbf{T})^{-1} \mathbf{D}_b^T \mathbf{H}^a \quad . \end{aligned} \quad (2.49)$$

Based on the constraint condition, the above equation can be written as

$$\begin{aligned} \mathbf{H}^b - \mathbf{H}^a &= \mathbf{T}(\mathbf{D}_b^T \mathbf{T})^{-1} \mathbf{c} \\ &\quad - \mathbf{T}(\mathbf{D}_b^T \mathbf{T})^{-1} \mathbf{D}_b^T \mathbf{H}^a \quad . \end{aligned} \quad (2.50)$$

Post-adding  $\mathbf{H}^a$  to the above equation gives

$$\begin{aligned} \mathbf{H}^b &= \mathbf{T}(\mathbf{D}_b^T \mathbf{T})^{-1} \mathbf{c} \\ &\quad - \mathbf{T}(\mathbf{D}_b^T \mathbf{T})^{-1} \mathbf{D}_b^T \mathbf{H}^a + \mathbf{H}^a \end{aligned} \quad (2.51)$$

$$\begin{aligned} \mathbf{H}^b &= \mathbf{T}(\mathbf{D}_b^T \mathbf{T})^{-1} \mathbf{c} \\ &\quad + (-\mathbf{T}(\mathbf{D}_b^T \mathbf{T})^{-1} \mathbf{D}_b^T + \mathbf{I}) \mathbf{H}^a \quad . \end{aligned}$$

By the commutative law of matrix addition we write the above equation as

$$\begin{aligned} \mathbf{H}^b &= \mathbf{T}(\mathbf{D}_b^T \mathbf{T})^{-1} \mathbf{c} \\ &\quad + (\mathbf{I} - \mathbf{T}(\mathbf{D}_b^T \mathbf{T})^{-1} \mathbf{D}_b^T) \mathbf{H}^a \quad . \end{aligned} \quad (2.52)$$

The variance-covariance matrix of  $\mathbf{H}_b$  based on the *law of propagation of errors* is given as follows,

$$\begin{aligned} \mathbf{Q}_{x_b x_b} &= (\mathbf{T}(\mathbf{D}_b^T \mathbf{T})^{-1}) \mathbf{Q}_{cc} (\mathbf{T}(\mathbf{D}_b^T \mathbf{T})^{-1})^T \\ &\quad + (\mathbf{I} - \mathbf{T}(\mathbf{D}_b^T \mathbf{T})^{-1} \mathbf{D}_b^T) \mathbf{Q}_{x_a x_a} (\mathbf{I} - \mathbf{T}(\mathbf{D}_b^T \mathbf{T})^{-1} \mathbf{D}_b^T)^T \end{aligned} \quad (2.53)$$

The first term on the right hand side of the equation is applicable only if the variance-covariance matrix of the datum constraints are given.

Since, an infinite number of datums are possible by changing the constants and the parameters, it is essential to determine the best of the possible datums. S-transformation facilitates this determination. According to Baarda (1981), to determine the best set of parameters to be fixed to determine the datum, the variances of the datum constraints must be kept to zero. This ensures that the estimates are not corrupted by external accuracies from the constraints,

and the variance-covariance matrix of the estimates obtained is a complete artefact of the datum parameters chosen. Hence, equation (2.53) becomes,

$$\mathbf{Q}_{x_b x_b} = (\mathbf{I} - \mathbf{T}(\mathbf{D}_b^T \mathbf{T})^{-1} \mathbf{D}_b^T) \mathbf{Q}_{x_a x_a} (\mathbf{I} - \mathbf{T}(\mathbf{D}_b^T \mathbf{T})^{-1} \mathbf{D}_b^T)^T, \quad (2.54)$$

where  $(\mathbf{I} - \mathbf{T}(\mathbf{D}_b^T \mathbf{T})^{-1} \mathbf{D}_b^T)$  is the S-transform. The above derivations were carried out based on the derivations by Strang van Hees (1982). Further, a clear mathematical elucidation of the S-transformation concepts is given by Teunissen (1985); Strang van Hees (1982).

## 2.7 Chapter summary

In this chapter the theory behind height systems and vertical datums was reviewed briefly. The perspectives in defining and realizing a vertical datum were also discussed. The idea of applying datum constraints was explained. Then these ideas were extended to the kinematic vertical datum. Some important points on the kinematic vertical datum given in the chapter are as follows:

1. the kinematic vertical datum was shown to be a vertical datum incorporating a mathematical model for vertical motion, which was chosen to be a linear model;
2. time was established as a datum parameter, and also, the reference time epoch was shown to be a determinable from the observations;
3. if time was considered a determinable variable then it was explained that the kinematic height model becomes non-linear and hence, it has to be linearized to perform least squares adjustment; and
4. the S-transformation of a kinematic vertical datum incorporating a linear kinematic height model was derived.

## Chapter 3

# Levelling Data and Data Processing Methodologies

Mathematical techniques and procedures are very well suited and work perfectly for ideal data. When it comes to field data it is never straight-forward to apply these mathematical techniques and procedures. This is due to the fact that field data collection is not carried out under ideal conditions, but the data collection is influenced by environmental, human, and instrumentation factors. In order to bring the field data into a computable form, a certain amount of processing is required. The amount of processing indicates the quality of the data, and further, the amount depends on how detailed the field data collection was carried out. Therefore, this chapter will discuss the nature of the data and the need for data processing thereby reflecting on the data quality available for the study.

In this chapter, first a look at the history of Canadian levelling network and the related height datums is given (section 3.1); then the format of the levelling dataset storage is explained (section 3.2); in the following, the need for the data processing is discussed (section 3.4); and finally, the data processing that was carried out on the data is described in detail (section 3.5).

### 3.1 History of the Canadian Precise Levelling Network

In order to determine the possibility of estimating the rate of change in heights, a thorough study of the history of levelling network is essential. The study of the history is also essential to properly designate accuracies to the various epochs of measurements involved in the adjustment as the measurements might have been taken with different kinds of instruments and also with different standards (Xu et al., 2000). A detailed history of the Canadian levelling network and the various vertical datums adopted so far has been covered by Gareau (1986). Further, Nassar (1977) has also accounted a brief history of the Canadian levelling network and also has given gravity correction formulas to account for the local gravity variations along the levelling lines.

In addition to the above two reports some interesting literature has also been published

by Vaníček & Nagy (1981), wherein they had published the vertical uplift rate map of Canada with the very few relevelings (5046 levelling segments) and the data from tide gauges (47). The map was compiled based on the vertical rates obtained through a method suggested by Vaníček & Christodulidis (1974) for scattered geodetic relevelings. Apart from these reports and articles not much has been written about the Canadian levelling network. The other source of information was the personal communication with Geodetic Survey Division, Natural Resources Canada – with Mr. Marc Véronneau.

The above literature have revealed that very few relevelings have been done in Canada. According to Gareau (1986), these relevelings were made as part of maintenance of the levelling network. Further, some of the relevelings were done close to dams to check if there was any vertical crustal motion around the dam due to the load of the dam. Also, the Trans-Canada levelling line that originally ran along the Trans-Canada railway line was relevelled along the Trans-Canada highway. A discrepancy of 2.2m was found out between the relevelings, which prompted investigations into vertical crustal motion along the Trans-Canada levelling line. This also invoked the authorities responsible for levelling, to design a program for releveling the entire Canadian network every 40 years (Nassar, 1977). Thus, it will take another 11 years to get the first releveling of the entire Canadian network to estimate the velocities. In this context, Hazay (1977) brings out an interesting point that to obtain reliable estimates of vertical crustal motion (mainly due to secular changes) a minimum of three relevelings are required, in which case reliable estimates of the vertical crustal motion can be obtained only in 2057.

In the initial stages of the development of the Canadian levelling network, levelling was conducted with various initial benchmarks, which later became the benchmarks constraining the Canadian vertical datum. The Canadian vertical datum was defined in 1928 and is called the Canadian Geodetic Vertical Datum of 1928 (CGVD28). In addition to this datum, two other datums existed at the time of the definition of CGVD28, viz., Great lakes datum of 1903; and Chaloner datum. Later on there were several readjustments (Gareau, 1986) to incorporate the new levelling lines that were added to the levelling network.

Of the readjustments, the North American Vertical Datum of 1988 (NAVD88) is of particular interest because of the fact that the whole of North American levelling networks, which includes the levelling networks of Canada, United States of America and Mexico, were

adjusted with *Rimouski*, Quebec in Canada as the datum point. NAVD88 was more of a readjustment than a new vertical datum definition, but it was scientific in its adjustment as only one point was chosen as the datum point, and not six as in the case of Canada and also, true gravity values were used in the adjustment. The other interesting thing is that the heights that are in use in the United States of America are based on NAVD88 (Zilkoski et al., 1992).

The heights used at present in Canada are still based on CGVD28, which is defined by constraining six tide gauges, namely, Rouses point, Point au Père, Halifax, Yarmouth (all in the east coast), Vancouver and Prince Rupert (all in the west coast) (Gareau, 1986), but Nassar (1977) refers to only five of them (leaving out Vancouver). Although the datum is called CGVD28 it was officially adopted in the year 1931 (Gareau, 1986). The 1928 adjustment of the levelling network did not involve gravity and in the later adjustments normal gravity values were used to suffice the problem. Currently, observed gravity values are used for the computation of heights (personal communication with Mr. Véronneau).

In addition to the changes in gravity values used, there were also changes in the accuracy standards used for the levelling measurements. Before and during the 1928 adjustment the accuracy standard for precision was kept at  $4\text{ mm}\sqrt{\text{km}}$ . However in 1972, GSD classified the levelling based on the precision involved, according to which there were 6 classes, namely,

- $(0\text{ mm} - 2\text{ mm})\sqrt{K}$
- $(2\text{ mm} - 4\text{ mm})\sqrt{K}$
- $(4\text{ mm} - 5.4\text{ mm})\sqrt{K}$
- $(5.4\text{ mm} - 6.8\text{ mm})\sqrt{K}$
- $(6.8\text{ mm} - 8.5\text{ mm})\sqrt{K}$
- $8.5\text{ mm}\sqrt{K}$ .

where  $K$  – the length of each levelling segment in km (Gareau, 1986). In spite of this levelling precision revision, the precision for all the epochs of levelling measurement can be considered homogeneous compared to the other types of height measurement, for example, GPS. The reason for such a revision of the precision was the transition to better instrumentation. Gareau

(1986) provides a comprehensive list of the different types of the instruments used for the levelling measurements until the NAVD88 readjustment. A weighting scheme considering the different instruments used was proposed for NAVD88 although, there is no record indicating the implementation of such a weighting scheme.

### 3.2 Levelling dataset of the Canadian Precise Levelling Network

The levelling dataset of the Canadian Precise Levelling Network (CPLN) is stored in a format called the GHOST format at three different levels of detail: sections, links, and lines. All field measurements are taken at the section level and then combined to form links. And then, links are amalgamated together to form lines. It is presumed that lines are the basic units at the level of design of the levelling networks, and links are formed based on the number of section measurements carried out in a day. Usually, the levelling lines are tens of kilometres in length while the length of the sections vary from a few hundred metres to a few kilometres depending on the roughness of the terrain. Table 3.1 illustrates the method of storage of the observed data in the GHOST format.

1	2	3	4	5	6	7	8
14	70E7249	001B78780121	78B034	0080019	3.36547	1.9016	.917
14	78B034	001B78780121	70E7245	0080020	-.11187	1.6957	.722
14	70E7245	001B78780121	78B035	0080021	-1.35341	2.4115	1.480

Table 3.1: Table illustrates the method of storage of the observed data in the GHOST format

Column description

1. Code 14 indicates a levelling observation
2. Unique station number (From)
3. Line identification number
4. Unique station number (To)

5. The first three characters indicate the link number and the rest of the characters indicate the section number for the given line
6. Levelling height difference in geopotential numbers(m kGal)
7. Precision of observation (mm kGal)
8. Levelled distance between stations (km)

Columns 3 and 5 in Table 3.1 will be explained in detail as all the other columns are self-explanatory. Essentially, each line of the observed data indicated by code 14 provides information on each observed section. So, if columns 3 and 5 were combined it would provide a unique section identification number. The whole section identification number, for example, section 001B787801210080019 can be split-up in the following manner,

$$001 \mid B \mid 78 \mid 78 \mid 0121 \mid 008 \mid 0019$$

, where 001 indicates the line; B indicates the province; 78 indicates the year the line was first observed; 78 indicates the year the line was observed last; 0121 indicates the project number; 008 indicates the link number within the line; and 0019 indicates the section number within the line. The point that needs to be noted here is that if the section is levelled again in a different year then the last year of observation and the project number will change. Hence, the first 6 characters, viz. 001B78, become the unique line identification number. Further, the last year of observation is an indication of whether the line has a releveilling or not. Thus, the significant that can be exploited are the first 8 characters of the line identification number, or, the unique section identification number.

Column description:

1. Code 4 indicating information about a station
2. Unique station number
3. Latitude (degree minute second)
4. Longitude (degree minute second)
5. Estimated heights in geopotential numbers (mm kGal)

1	2	3	4	5
4	78B054	46 5832.3214	64 0304.4785	54.0130
4	01N161 A	44 1006.5698	61 5104.2318	123.8756
4	79L*0055	47 5428.0000	68 4408.0000	178.5672

Table 3.2: Table illustrates the method of storage of the station information in the GHOST format

The GHOST data format also stores information on the stations in the levelling network as shown in Table 3.2. There are a few important things that need to be noted with respect to the unique station number. The first two characters of the station number indicate the year in which it was installed; the third character, which is an alphabet, indicates the province in which it is installed; and the rest of the characters indicate the station number.

In Table 3.2, three different types of station numbers are shown. The station number shown in the first row indicates a stable and permanent benchmark, which is provided with a marker and a description. The station number in the second row has an alphabet at the end of the end of the station number indicating that the station has been *floatated*. A station is floatated if it has significantly moved with respect to the other surrounding benchmarks; or it has been dislocated by an earthquake, construction, or vandalism. The station number in the third row has an ‘ \* ’ mark in the fourth character, which indicates that the station is a temporary benchmark, and so, it does not have a marker and a description in the field.

### 3.3 Solvability of levelling networks for heights and vertical velocities

In order to understand and justify the need for data processing it is essential to understand how the solution of a kinematic levelling network works to estimate heights and vertical velocities of the points in the network. It will be shown in this section that it is not a straight forward problem of algebra, where the parameters are estimable when the number of equations are more than (overdetermined solution) or equal (unique solution) to the number of parameters, as in the case of a static levelling network.

### 3.3.1 Review of terminology

Levelling is relative and hence, always done between a pair of points. The objective of levelling is to find the heights of the points between which the observations are measured. The group of points that are connected by levellings is called a network. The levelling networks, whose only purpose is to estimate heights of the points in the network, are referred to as *static levelling networks*. When the observations of the levelling network are repeated over time then the repeated observations are referred to as *relevellings*. The levelling networks, whose purpose is to estimate heights and their variations in time (velocities) of the points in the network, are referred to as *kinematic levelling networks*.

When every observation of a static network is observed repeatedly over time then it will be referred to as an *ideal kinematic levelling network*. If instead only a few observations in the static network are observed again then it will be referred to as a *scattered kinematic levelling network*. The following figures give a visual picture of the above.

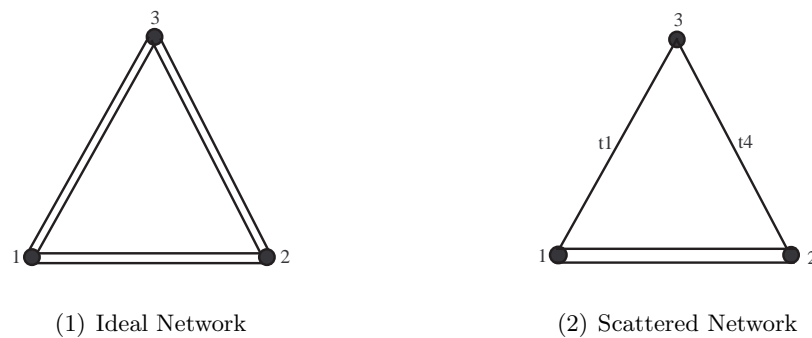


Figure 3.1: Ideal and scattered kinematic levelling networks

### 3.3.2 Rules for solvability of kinematic levelling networks

Consider, the following three figures.

In Figure 3.2(1) the line  $1 - 2$  has been relevelled and hence, there are two observations but four unknowns – height and velocity for  $1$  and  $2$ . In order to find the parameters of one point the parameters of the other point should be fixed, because are only height differences are available to estimate both heights and vertical velocities of the points. Now, consider Figure 3.2(2), which is a triangle and all its sides have been relevelled. In this figure there are six observations and six unknowns. Eventhough there are equal number of observations

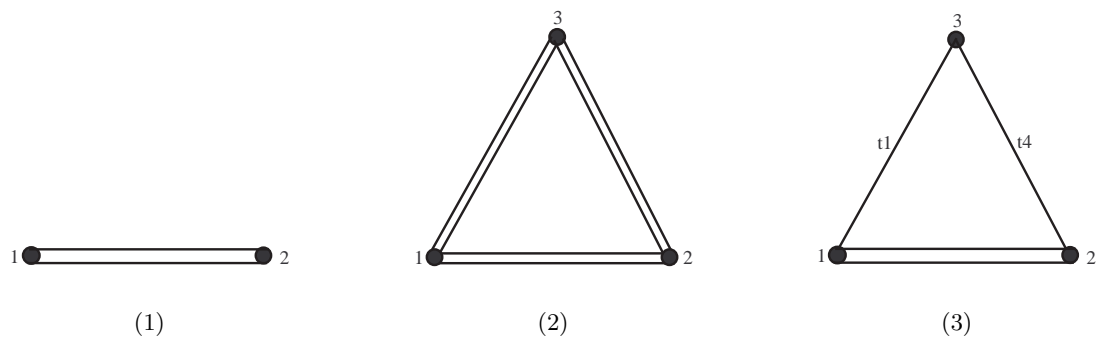


Figure 3.2: Illustration of solvability analysis

and unknowns presenting an unique solution situation, one height and one velocity need to be fixed to have absolute heights and velocities relative to the fixed quantities.

Now, consider Figure 3.2(3), where there is only one relevelling between points 1 and 2 and there are two single levellings to point 3. In this case, there are four observations and six unknowns, but, as in the Figure 3.2(2) there is a rank deficiency of 2 because of the relative measurement process. Since, there is only one relevelling line this case seeks special attention, and so, the solution is explained *step-by-step*. Taking line 1 – 2 into consideration and solving it like Figure 3.2(1). Then there are four known parameters – two fixed and two estimated, which leaves the situation with two observations – 1 – 3 & 3 – 2, and two unknowns – height and vertical velocity of point 3. At this juncture one important thing needs to be considered, which is *Is there velocity information in the given observations?*

Velocity information of a point in a kinematic network is available in two forms.

1. Relevellings
2. Two or more observations to a point from a solvable network observed in atleast two different epochs. For example, in Figure 3.2(3) the solvable network would be the relevelling line 1 – 2. Also, a careful look at the previous statement shows the emphasis on observations at two or more different epochs. This is because, if there is/was deformation in that particular point of concern, then the observations will show a misclosure, which will be significant apart from the errors. Hence, it will contribute to velocity information.

Thus, Figure 3.2(3) presents the latter situation with two observations at different epochs.

Hence, it is possible to determine height and velocity of point 3 with those two observations, inspite of the fact that we do not have relevelings to 3. So, the rank deficiency of Figure 3.2(3) is also 2. This triangle will not be solvable if both the observations – 1 – 3 & 3 – 2, had the same time epoch of observation. The triangle of Figure 3.2(3) can be extended into a huge network with only single levellings by making sure that every point has two connections at different observation epochs.

### 3.3.3 Network with multiple rank deficiency

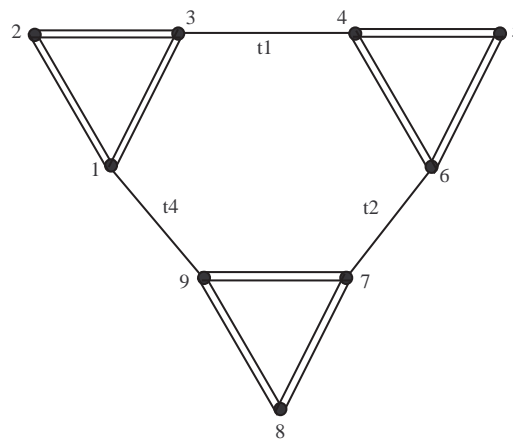


Figure 3.3: A network with multiple rank deficiency

The above concepts are applied to a complex situation shown in Figure 3.3, where we have multiple rank deficiency. The three triangles are solvable in themselves, and if done so will have a rank deficiency of two for each triangle. Since combination of single levellings also have velocity information, the network needs to be analysed for solvability taking the single levellings into consideration. Now, triangle 1 – 2 – 3 has one connection each with the other two triangles. Hence, there is no possibility of transmitting the velocity information to either triangle as two single levelling connections are required to transmit the velocity information. Therefore, triangle 1 – 2 – 3 will have two parameters fixed and either triangle 4 – 5 – 6 or triangle 7 – 8 – 9 will have one parameter fixed. The third triangle need not be fixed for any parameters as it has two connections to this integrated group of triangles. And finally, the network will have a rank deficiency of 3, wherein the excess deficiency is referred to as *excess constraint datum parameter(s)*. One important observation has to be noted here: there are

more equations (21) than the parameters (18) needed to be estimated. Therefore, a solvability check has to be made before attempting a kinematic vertical datum solution.

In the above multiple rank deficiency example, there is a rank deficiency of three, which is one more than for a network whose heights and vertical velocities can be estimated by a minimum constraint datum solution. But this situation is different from the overconstraint datum solution, because in an overconstraint situation there are enough observations to apply a minimum constraint. The purpose of applying an overconstraint is mainly to fit the given observations to a set of known co-ordinates. However, in the case of multiple rank deficiency there is a data gap or lack of observations to perform a minimum constraint adjustment. So, there are constraints in excess of what is ideal and hence, such solutions to multiple rank deficiency problems will be referred to as *excess constraint* solutions. In an excess constraint solution, if the constraints are close to true values then they will provide as good solutions as a minimum constraint solution.

If the rank deficiency is more than 2, a choice can be made in fixing a combination of the height and velocity parameters. For example, in the case of Figure 3.3, where there is a rank deficiency of 3, a choice can be made to fix either two heights and one velocity or, one height and two velocities. It will be advantageous to use the former choice as they are more easily available, while the choice of fixing more than one velocity will make the datum dependent on *a priori* geophysical/geodynamical models. This will be touched upon again in chapter 5 with some results from the levelling network.

### 3.4 Need for the processing of Canadian Precise Levelling Network data

The aim of this research, as stated before, is the definition of a kinematic vertical datum for a levelling network for which the fundamental component is the relevellings in the network. So, the data was analysed for finding out the relevelled lines in the network. The data analysis for relevellings was performed at the section level, because if there are sufficient relevellings in the network at the section level then both heights and velocities can be estimated for all the available benchmarks (points) in the network. If the other levels of the data are chosen, then the velocities of some of the benchmarks have to be estimated by interpolation methods. In Figure 3.4 the relevellings at the section level of the data are shown. The relevellings are

all over the network, but they are completely disconnected, which means that the network is not an ideal kinematic levelling network.

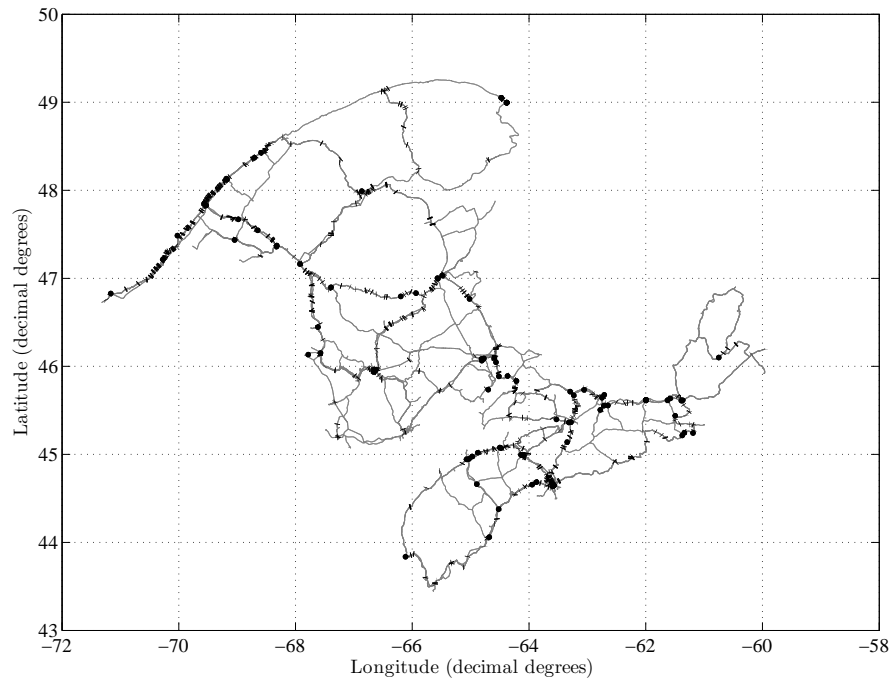


Figure 3.4: Relevellings in the network at the section level of the data

The scattered relevellings were expected of the network, because a review of the history indicated that there were hardly any dedicated relevelling campaigns, and most of the relevellings that are seen are mainly due to the maintenance measurements (cf. section 3.1). So, it was decided to look into the higher level of the data, viz. at the line level of data. To analyse at the level of the links will not make sense, because it is purely used for managerial purposes (cf. section 3.2). In order to understand the implications of using line level of data, consider Figure 3.5. In that figure, if the data is analysed at section level, then no relevellings will be identified, because none of the sections have been revisited neither along the same route, nor in a different route. But, if the same data were analysed at the line level, i.e., lines  $e1$  and  $e2$ , then it will be found out that they are relevellings.

The line level of data was analysed with the year information present in the line identification number (cf. section 3.2). This method, eventhough provided information on which lines

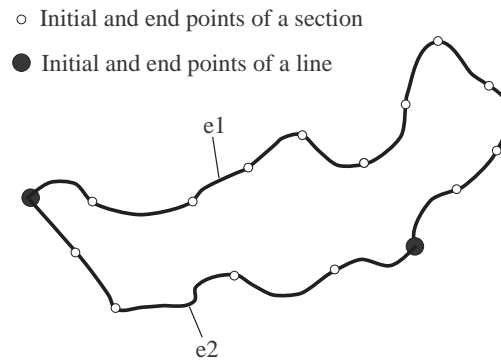


Figure 3.5: Illustration of levelling information at line level and at section level

are relevelled and those not, did not provide the complete solution. This is because of the two major obstacles in the network: *branching*, and *relevelings of the same line having different line identification numbers*. First, the lines with the same line identification number were all segregated together and then they were compared with the other lines with the same unique line identification number (cf. section 3.2). The lines were not continuous (continuous in the sense of Figure 3.5) as they had some sections that were diverging out of the main levelling route of the line. For example, the line showed in Figure 3.6 is a network in itself. So, these kinds of lines cannot be compared at the line level. Also, some relevelings of the same line had different line identification numbers at different epochs. An example of such an inconsistency is shown in Figure 3.7, and the corresponding line numbers in Table 3.3. This made it impossible to rely upon the information in the line identification numbers. So, it was futile to do the processing at both the line and section level and hence, provided motivation and justification to carry out other data processing methods.

### 3.5 Data Processing of the network

Data processing of the network consists of finding the intersection points between the lines; removing loose ends; removing loops; and reduction of the levelling observations based on the time-tagging. This is a crucial step in the whole levelling network analysis as this step tries to manipulate and exploit all the available vertical motion information. In doing so the methods alter the geometry of the network and hence, the methods must be evaluated and validated before they are applied to the field data. In this section and the following section the data

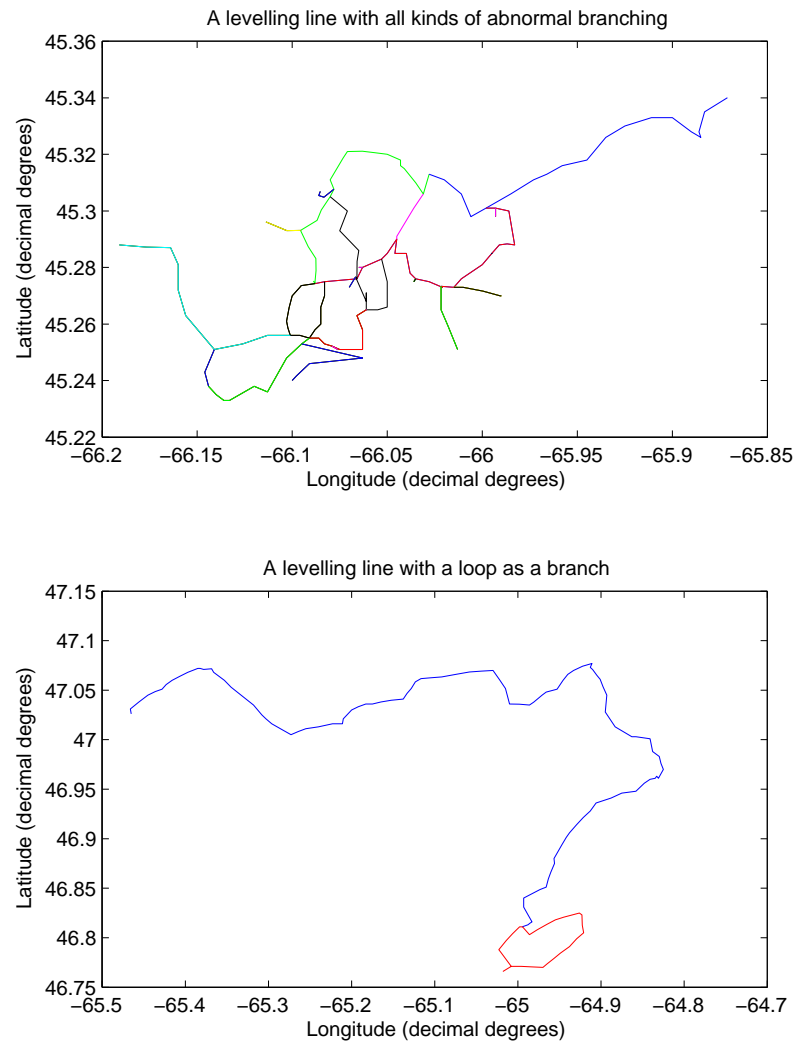


Figure 3.6: Branching in levelling lines. The different coloured lines show the different branches of a levelling line route. In the first figure the levelling line does not follow a particular route, but forms a network in itself.

---

Yellow	Green	Red
056L15250251	085L19190248	255L54540109
		255L54550145
		255L54680101C
		255L54690144C
		255L54700146
		255L54710385A
		255L54710385B
		255L54720386A
		255L54730387B
		255L54740388B
		255L54750097A
		255L54790151B
		255L54790151C
		255L54790151D
		255L54830501A
		255L54830501B
		255L54870548
		255L54960600

---

Table 3.3: Line numbers for the Figure 3.7

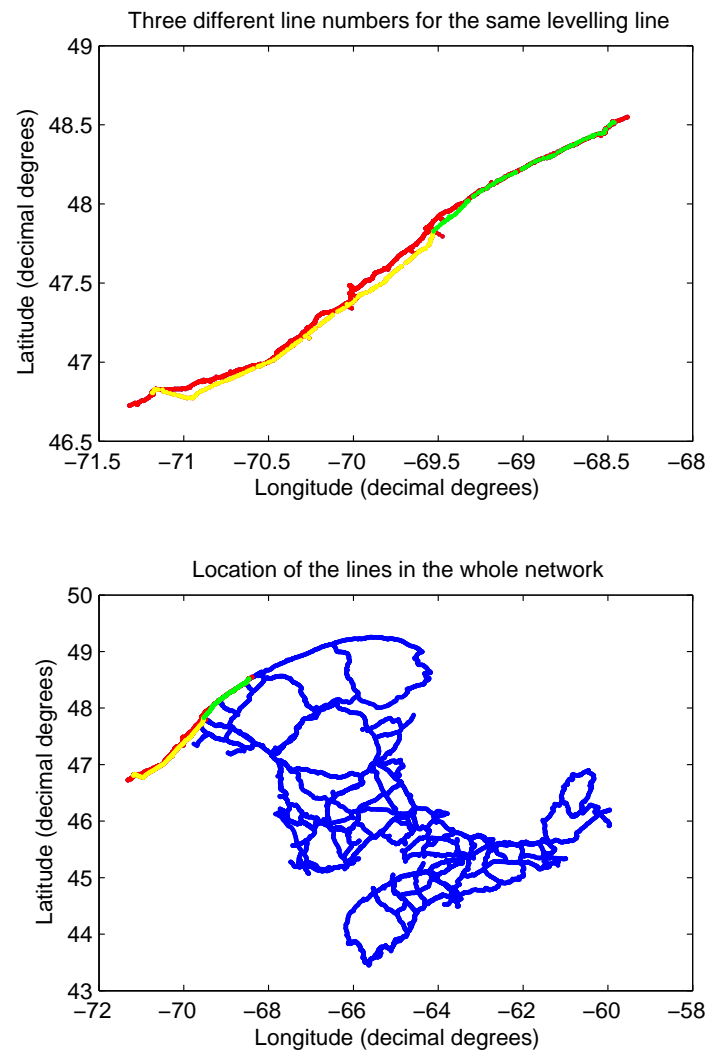


Figure 3.7: Abnormality in line numbering. Here, all the three colours, red, yellow, and green are observations of the same levelling line but they have been given different line numbers in the dataset.

processing methods and their validity will be discussed.

### 3.5.1 Finding intersection points

To explain the process of finding the intersection points in the network, Figure 3.8 is taken as an example. In Figure 3.8(1) lines  $e2$ ,  $e3$  and  $e4$  are relevelings of parts of line  $e1$ , and line  $e5$  is a releveling of line  $e3$  (with the individual numbers denoting the intersection points between the lines). In the Figure 3.8(2), the lines  $e1$  and  $e3$  after the algorithm is applied are depicted.

For every line a matrix is drawn with the column space indicating the points that form the line and the row space indicating the number of connections that the line has with other lines. For example, the matrix for  $e1$  will have 8 points through the column and 3 lines through the row (an  $8 \times 3$  matrix). Then in each column of the matrix the line number is written in the row of the common point. The completed matrix is sent through an iteration where the line is broken at first and last non-zeros in the column with any intermediate non-zero(s) in between then retained. At the end of the iteration the line is broken as per the connections of the line. The above procedure is demonstrated for the line in Figure 3.8(1).

$$\begin{array}{c}
 \left[ \begin{array}{c|ccc}
 1 & e2 & 0 & 0 \\
 2 & e2 & 0 & 0 \\
 3 & e2 & 0 & 0 \\
 4 & e2 & 0 & 0 \\
 5 & 0 & e3 & 0 \\
 6 & 0 & 0 & e4 \\
 7 & 0 & 0 & e4 \\
 8 & 0 & e3 & 0
 \end{array} \right] \\
 \rightarrow \\
 \left[ \begin{array}{c|ccc}
 1 & e2 & 0 & 0 \\
 2 & e2 & 0 & 0 \\
 3 & e2 & 0 & 0 \\
 4 & e2 & 0 & 0
 \end{array} \right] + \left[ \begin{array}{c|ccc}
 4 & e2 & 0 & 0 \\
 5 & 0 & e3 & 0
 \end{array} \right] + \left[ \begin{array}{c|ccc}
 5 & 0 & e3 & 0 \\
 6 & 0 & 0 & e4
 \end{array} \right] + \\
 \left[ \begin{array}{c|ccc}
 6 & 0 & 0 & e4 \\
 7 & 0 & 0 & e4
 \end{array} \right] + \left[ \begin{array}{c|ccc}
 7 & 0 & 0 & e4 \\
 8 & 0 & e3 & 0
 \end{array} \right]
 \end{array}$$

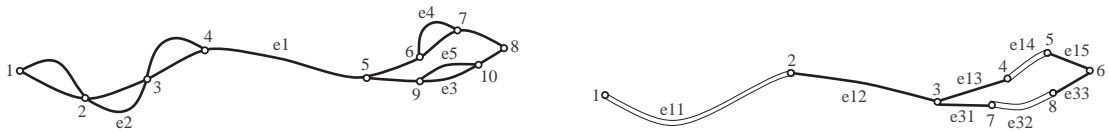
When this matrix is sent through the iteration mentioned before the line is broken into two in the first iteration: one line from points 1 to 4 and the other from 4 to 8. In the next iteration the line is broken into three: one line from 1 to 4, next from from 4 to 5 and the

third from 5 to 8. In the third and last iteration the line from 5 to 8 is broken down into three more, which are 5 to 6; 6 to 7; and 7 to 8.

Similarly for line  $e3$  the matrix will be

$$\left[ \begin{array}{c|cc} 5 & e1 & 0 \\ 9 & 0 & e5 \\ 10 & 0 & e5 \\ 8 & e1 & 0 \end{array} \right] \rightarrow \left[ \begin{array}{c|cc} 5 & e1 & 0 \\ 9 & 0 & e5 \end{array} \right] + \left[ \begin{array}{c|cc} 9 & 0 & e5 \\ 10 & 0 & e5 \end{array} \right] + \left[ \begin{array}{c|cc} 10 & 0 & e5 \\ 8 & e1 & 0 \end{array} \right]$$

and the broken lines will be 5 to 9; 9 to 10; and 10 to 8. Thus the number of iterations for each matrix is equal to the row space of the matrix.



(1) Levelling line before finding intersection points

(2) Levelling line segmented at the intersection points identified

Figure 3.8: An example for the *intersection point recognizing* algorithm

### 3.5.2 Removing open lines and loops

Open lines and loops are illustrated in Figure 3.9. Open lines are those lines, whose initial or end points have no other connections to them. For example, in the case of the network in Figure 3.9 the open line would be  $c-f$ , and  $f$  is the point that has no other connections other than the line  $c-f$ . Open lines occur frequently in levelling networks, because there is always a requirement for a tide gauge, a permanent GPS station, or a height control point for a construction site e.g., (dam, nuclear plant, bridge, industry, etc.) to be connected to the precise levelling network (personal communication with Mr. Véronneau).

Open lines are ought to be removed as they do not serve any purpose in the least squares adjustment of the network. The reason being that since one of the end points is not connected to any other line in the network, there is no redundancy involved at that point. And, redundancy is the holy grail of a least squares adjustment, which provides a proper check on the observations for the height value estimated for that point. Also, if such observations are removed from the network they will not have an impact in the outcome of the results.

Loops are those lines that start and end at the same point, whilst all the points forming the sections within those lines will have exactly two connections, for example, Figure 2.2. Loops are either an artefact of improper network design and planning, or done on purpose to do some local checks on the observation quality. The reason for removing loops are that when parametric least squares is used for estimation of the parameters, it will be impossible to represent the loop equation in the design matrix, and hence the normal matrix. Loops can be retained only if adjustment of condition equations is followed as they will provide a sound check for the point and observation in the loop, for example, the point  $e$  and the associated loop in Figure 3.9.

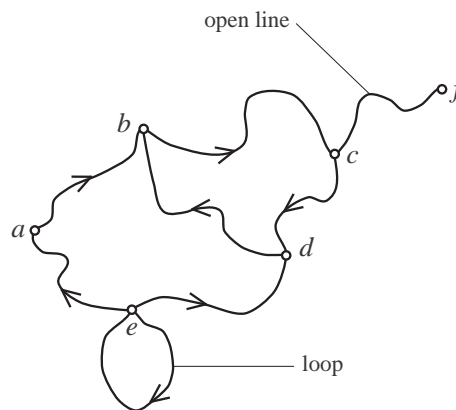


Figure 3.9: Illustration of the open line and loop in a levelling network

### 3.5.3 Reduction of levelling observations

It is recalled that in a kinematic levelling network the observations within a given epoch are assumed static (cf. section 2.5.2). This is the discretization of the continuous secular trend of the velocity signal. That is why releveling observations taken within the same epoch do not provide any velocity information. Also, from solvability analysis it was elucidated that if a point in the network has observations through it only in one epoch then it does not allow the parameterization of velocity parameter for that particular point (cf. section 3.3). Further, this is a bottleneck for the adjustment and estimation of heights and velocities as these parameters have to be fixed with constants thereby increasing the excess constraints.

In the reduction process it is sought to eliminate these excess constraints or, in the worst

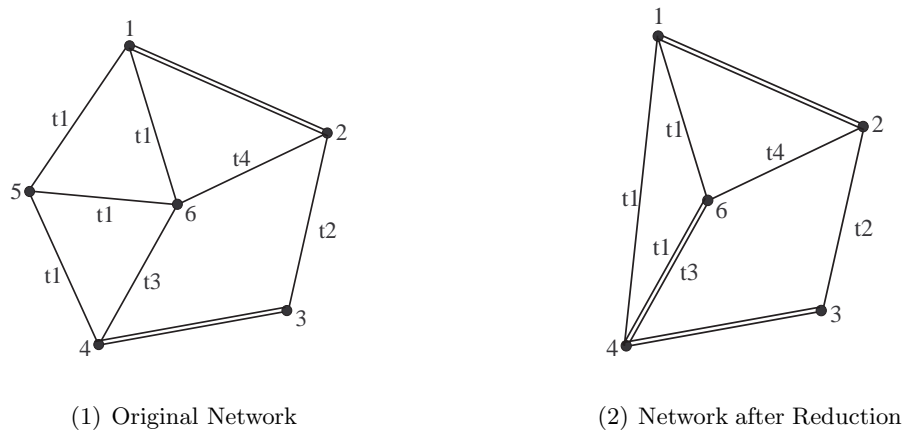


Figure 3.10: Illustration of Reduction process

cases to reduce the number of overconstraints in the network. So, first all the bottlenecks, i.e. the points whose incident observations were observed only in one epoch, are identified. Since all the observations in the same epoch are static, all the observations through each of those points can be combined and new pseudo-observations can be formed. This is referred to as *reduction*, which is borrowed from levelling network adjustment terminology and redefined. In static levelling network adjustment this procedure is applied to observations, which are in the middle of a long levelling line and are connected exactly by two observations – one at the initial point and the other at the end point of the observation. For example, in Figure 3.5 if all the intermediate white dots between the two black dots are combined to form two single levelling lines then this procedure would be called *reduction* in the classical sense.

Here, instead of sticking to observations that had only two connections, one at the initial point and one at the end point, observations with multiple connections are also considered for reduction. The reduction process algorithm that has been implemented for this research follows the following steps,

1. find and remove loops
2. find and remove open lines
3. find all points in the network that were visited by observations only in one epoch
4. for  $i = 1$  to  $p$  (the number of points from previous step)

- ```

4.1 combine all the observations meeting at point i --  $C_n^2$ 
4.2 check if the combined lines already exist in the observations with the
    same epoch
    4.2.1 if yes throw the pseudo-observation away
    4.2.2 else add and update the observation table
end for loop

5. remove all points with their observations from step 3 that are still present
    after reduction

```

The above algorithm is explained with the Figure 3.10 in which Figure 3.10(1) has already been explained previously. Now, in Figure 3.11(1) only point 5 has been visited by observations in only one epoch –  $t_1$ . So, only the observations passing through this point will be reduced by the algorithm: lines 1-5, 4-5, and 5-6 observed in epoch  $t_1$ . The number of combinations will be equal to  $C_3^2$ , which is 3, and the combinations are 1-4, 1-6, and 4-6 all with observation epoch  $t_1$ . Of these combinations line 1-6 with observation epoch  $t_1$  already exists in the network hence, it is rejected, but the other two combinations (pseudo-observations) are accepted. Thus, the reduced network looks like the Figure 3.10(2). Now, there are a few positive additions to the network, which are

- a) a new levelling line is formed – line 4-6.
- b) a new observation is added – line 1-4.

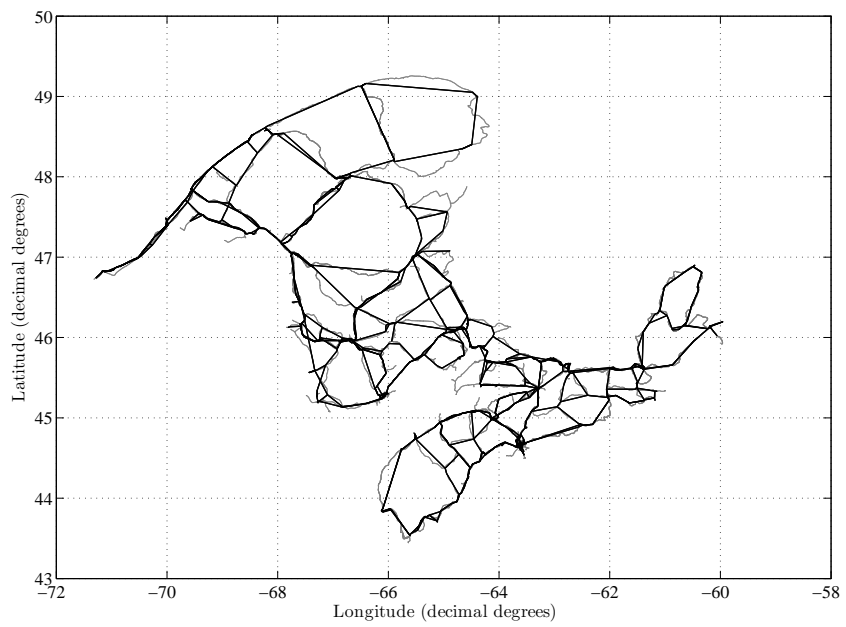
This reduction process reduces the number of excess constraints in the network and also, improves the redundancy in the network. In the above example, the number of excess constraints was reduced from 1 to 0 and the redundancy has improved from 0 to 2. This algorithm was applied to the levelling network in the study region. The resultant statistics of the network are shown in the next section.

### 3.6 Network configuration at various stages of data processing

The three figures in Figure 3.11 show the raw network, network after processing for intersection points and network after reduction of observations. Physically all three networks are the



(1) Original form of the network



(2) Network after finding the intersection points

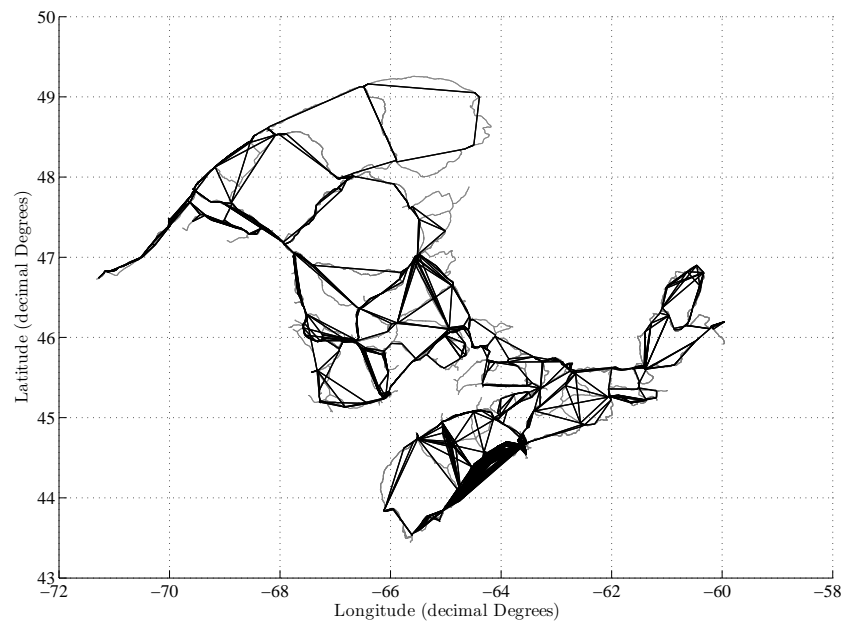
same in the sense that no new field observations were added to the raw network, but they are topologically different. This difference in topology changes the entire scenario of adjustment as the error estimates of the parameters and the weighting of the observations completely depend on the topology of the network. The latter is because, the observations are combined to reduce the number of parameters during the reduction process and hence, also their corresponding variances. Also, in the reduced network a lot of pseudo-observations are generated because of the  $C_n^2$  combinations at each point whose observations all have the same year of observation. When  $2 \leq n \leq 3$  ( $n$  - degree of vertex of a point) the reduction process generates the same number of observations that were present before reduction. But, when  $n$  is any bigger than that then the reduction process will generate a lot more pseudo-observations than what has been observed. This phenomenon in the original network is shown in the following figures.

In Figure 3.12(3), when compared to Figure 3.12(2), there are a lot of pseudo-observations formed just by using the combination  $C_n^2$  in the reduction algorithm. In one sense it is good to have more observations, but they are just combinations of original data and connecting points that were not directly connected by observations taken in the field. The justification for such a method comes from a need to reduce the parameters that are being estimated rather than anything else. Further, the extra observations add redundancy and stabilize the inverse of the normal matrix. To prove the last point a simple example is sought for elucidation.

### 3.6.1 Equivalence of estimated parameters from networks before and after reduction

In order to elucidate the physical equivalence and the topological non-equivalence of the networks before and after reduction, observations were simulated for the networks shown in Figure 3.13. The observations were simulated by assuming the following velocities for those points in the network.

Further, the loop misclosures for the simulated observations were kept within  $4\sqrt{K}$  mm $\sqrt{\text{km}}$ , where  $K$  is the distance in km. A kinematic adjustment and a static adjustment were performed to demonstrate the physical equivalence of the networks before and after reduction.

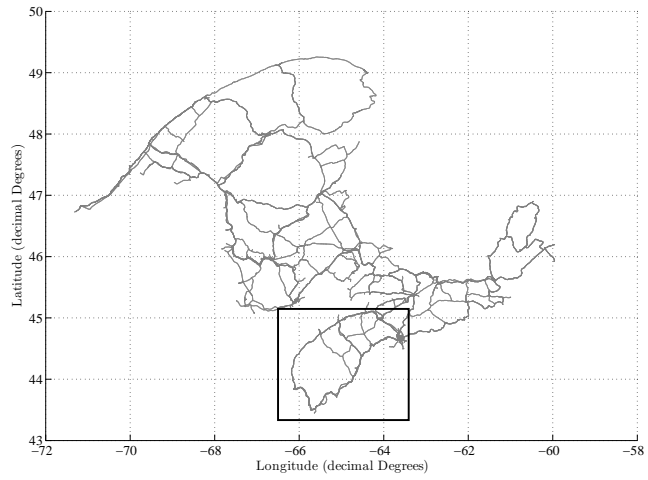


(3) Network after reduction process

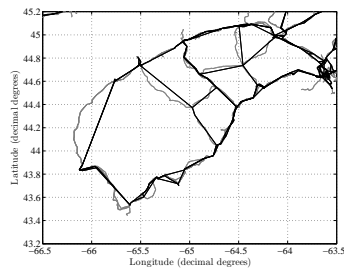
Figure 3.11: Raw network and network at various stages of data processing

| S.No. | Velocities<br>mm/yr |
|-------|---------------------|
| 1.    | 6.0                 |
| 2.    | 6.0                 |
| 3.    | 6.2                 |
| 4.    | 6.5                 |
| 5.    | 4.3                 |
| 6.    | 5.0                 |

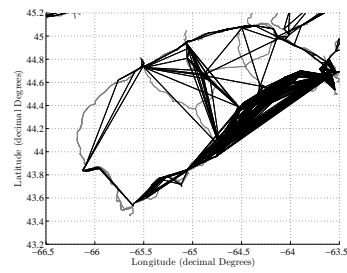
Table 3.4: Velocity at each height point



(1) Area with excess pseudo-observations is highlighted

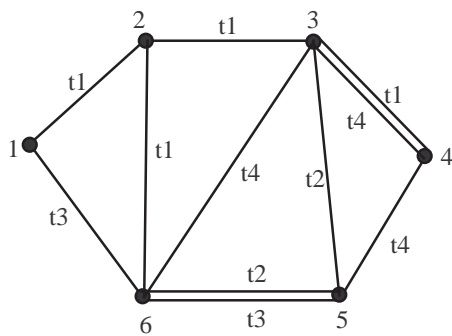


(2) After finding intersection points

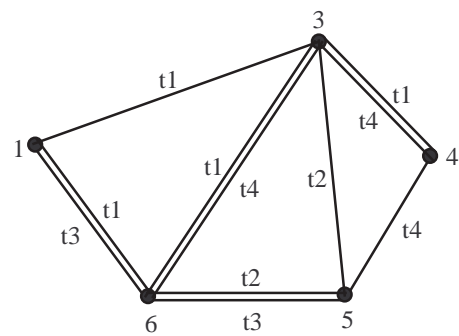


(3) After network reduction

Figure 3.12: Figure shows the excess pseudo-observations after network reduction



(1) Before network reduction



(2) After network reduction

Figure 3.13: Simulated examples to show the equivalence of the network estimates before and after reduction.

---

| Network          | Observations | Parameters | Rank Defect | Datum points                      |
|------------------|--------------|------------|-------------|-----------------------------------|
| Before Reduction | 11           | 12         | 9           | 1 (height) and 2 and 5 (velocity) |
| After Reduction  | 11           | 10         | 8           | 1 (height) and 5 (velocity)       |

---



---

| Points | Before reduction   | After reduction    |
|--------|--------------------|--------------------|
|        | m                  | m                  |
| 3      | $1.712 \pm 0.026$  | $1.712 \pm 0.019$  |
| 4      | $1.431 \pm 0.029$  | $1.427 \pm 0.021$  |
| 5      | $19.359 \pm 0.032$ | $19.351 \pm 0.024$ |
| 6      | $21.196 \pm 0.024$ | $21.195 \pm 0.017$ |

---

Table 3.5: Height estimates of points

From the results shown in Tables 3.5, 3.6, and 3.7, it can be seen that the values of the points before and after reduction do change, but not drastically. The changes are very minimal, and it can be said that both the networks are physically equivalent even though topologically non-equivalent. Also, it can be observed that the values from the reduced network approach the originally assumed values.

### 3.6.2 Heights estimated from networks before and after reduction process

In order to prove the equivalence of the networks before and after reduction for the levelling network used for this research, the networks before and after reduction were considered as static networks and the height values of the points in the network were estimated. Only a static adjustment of these networks is possible, because the original network had too many

---

| Points | Before reduction<br>mm/yr | After reduction<br>mm/yr |
|--------|---------------------------|--------------------------|
| 1      | $5.5 \pm 0.5$             | $5.7 \pm 0.4$            |
| 3      | $5.8 \pm 0.4$             | $6.0 \pm 0.3$            |
| 4      | $6.2 \pm 0.4$             | $6.3 \pm 0.3$            |
| 6      | $4.7 \pm 0.4$             | $4.8 \pm 0.3$            |

---

Table 3.6: Velocity estimates of points

---

| Points | Before reduction<br>m | After reduction<br>m |
|--------|-----------------------|----------------------|
| 3      | $1.705 \pm 0.027$     | $1.693 \pm 0.021$    |
| 4      | $1.411 \pm 0.031$     | $1.399 \pm 0.030$    |
| 5      | $19.412 \pm 0.030$    | $19.422 \pm 0.027$   |
| 6      | $21.236 \pm 0.023$    | $21.250 \pm 0.020$   |

---

Table 3.7: Height estimates of points from static adjustment

excess constraints (cf. Table 3.8) and it would not be meaningful to fix all those values given the size of the network.

| Network type     | Observations | Parameters | Rank Defect |
|------------------|--------------|------------|-------------|
| Before reduction | 3324         | 3422       | 560         |
| After reduction  | 3730         | 2292       | 24          |

Table 3.8: Observations, parameters, and rank defect of the networks before and after reduction; considering them as kinematic levelling networks

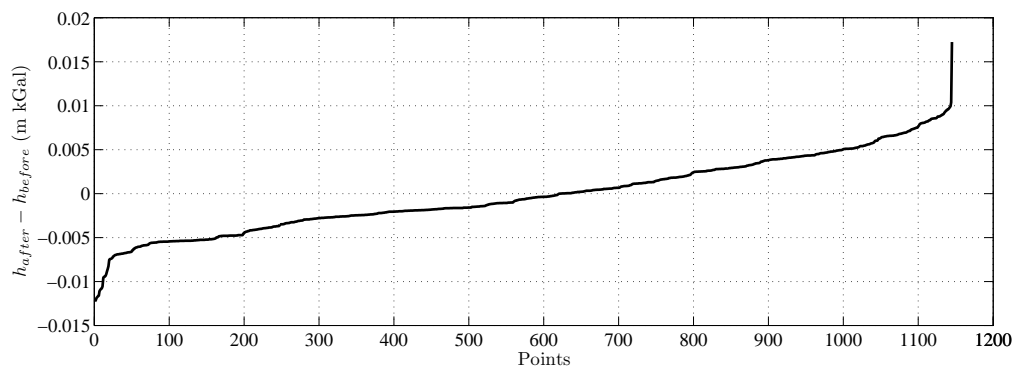


Figure 3.14: Plot of the differences in height estimates from networks after applying the reduction process and after finding the intersection points

The results of the tests from the static levelling networks indicate that the height estimates do not differ by much. Especially, in Figures 3.14 and 3.15, the difference values are concentrated between  $\pm 10\text{mm}$ . Considering the size of the network the differences are very small. The differences in the estimates come from, as mentioned previously, the change in topology of the network.

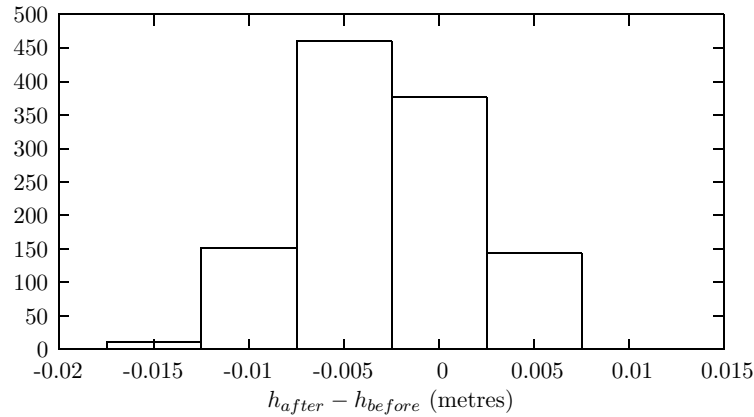


Figure 3.15: Histogram of the differences in height estimates from networks after applying the reduction process and after finding the intersection points

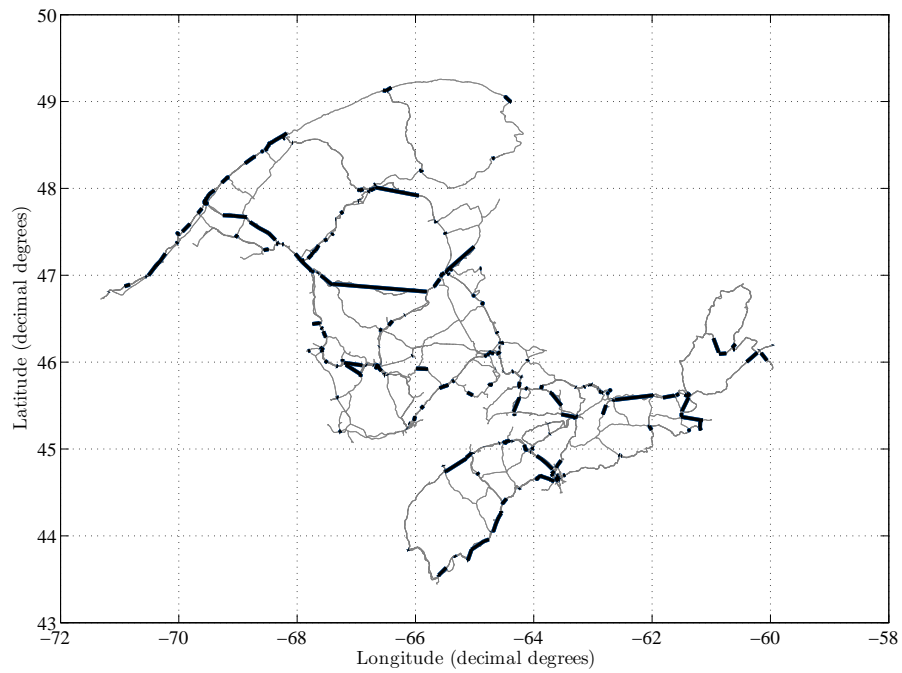
### 3.7 Relevellings at various stages of processing

In the Figures 3.4, 3.16(1), and 3.16(2), the relevellings before any processing was done is shown in addition to relevellings after finding out the intersection points and relevellings after reduction of the network. A closer look at the figures reveals that after every processing stage the length of the relevelling lines seems to be growing, but also with the addition of a few (in the southeast corner of the network in Figure 3.16(2)) after network reduction. This addition is due to the generation of pseudo-observations after network reduction (cf. section 3.5.3). Thus, the processing of the observations has helped in the following ways:

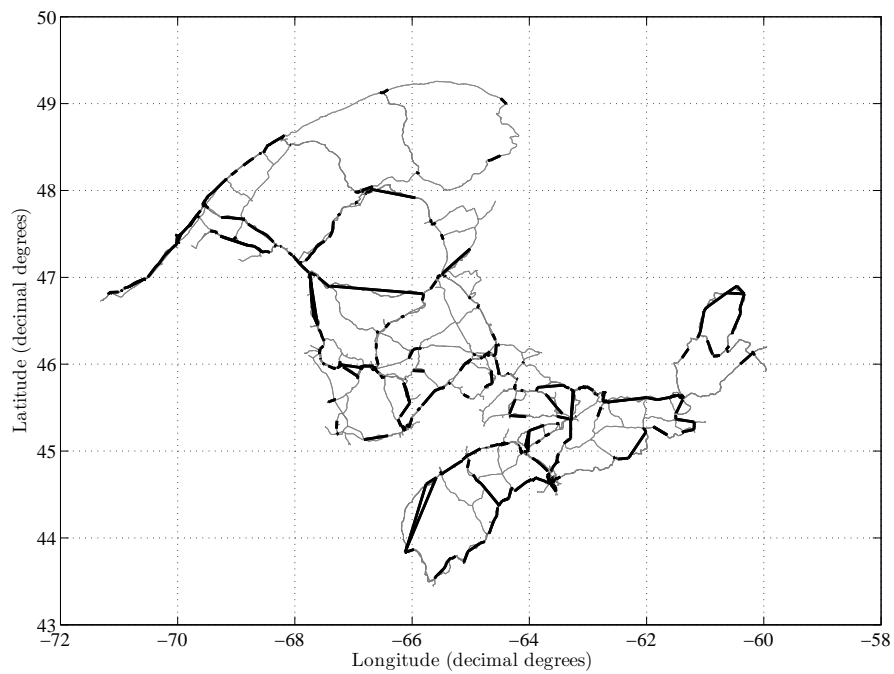
1. it combined the observations through points that were all observed only in one epoch thereby reducing the parameters needed to be estimated and the excess constraints needed to be fixed; and
2. the combination of observations brought out the hidden relevelling information and provided strength to the estimation of crustal motion.

### 3.8 Chapter summary

The chapter focussed on bringing the observations to ready-to-adjust format. The important points that have to be noted in this chapter are as follows:



(1) Relevellings in the network after finding the intersection points



(2) Relevellings in the network after reduction process

Figure 3.16: Relevellings in the network from the raw data and at various stages of data processing

1. a review of the levelling network history revealed that no effort was made to perform releveling over the entire network, but the heartening fact is that the accuracy of the observations are homogeneous with the range being  $(4\sqrt{K} - 0-2\sqrt{K})$  mm;
2. the data storage format revealed the location of releveling in the dataset, however, it was not sufficient for retrieving them from the dataset;
3. the network in its original form gave an underdetermined problem, which was overcome by applying three different data processing steps, viz., finding intersection points, removing loops and open lines, and reduction;
4. the reduction process improved the situation from a rank deficiency of 560 to a rank deficiency of 24, thus bringing the rank deficiency to manageable proportion; and
5. since the reduction process changed the topology of the network, the networks before and after reduction were shown to be equivalent by estimating heights from static adjustment of either network.

## Chapter 4

# Pre-adjustment Analysis of the Levelling Network

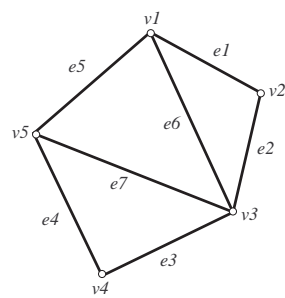
### 4.1 Graph theory: A brief overview

Graph theory deals with the analysis of *graphs*. A *graph*  $G(V, E)$  is defined as a set of vertices  $V\{v_1, v_2, \dots, v_n\}$  connected by a set of edges  $E\{e_1, e_2, \dots, e_m\}$ . In other words, a graph is a geometric structure defined for a set of vertices (points) by the interconnecting edges (lines or arcs). The structure of the connections between the vertices enabled by the edges is called the *topology* of the graph. Graphs are broadly classified into *directed graphs* or *digraphs*, and *undirected graphs*. The classification is based on whether the edges connecting the vertices are oriented in direction or not, as shown in Figure 4.1. A digraph is also referred to as a *network* especially, when the edges carry a quantitative significance to them. For example, pipeline networks, transportation networks, social networks, geodetic networks, etc.

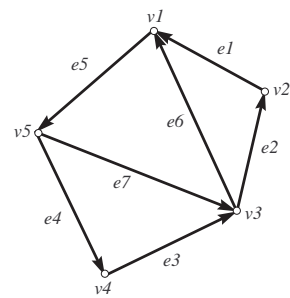
Also, there are other types of classifications of graphs that are common to both undirected and directed graphs: *simple graphs*, *multigraphs*, *complete graphs*, and *regular graphs*. A *multigraph* is a graph, where a pair of vertices have multiple edges connecting them and/or have loops in them. For example Figure 4.1(3) is a multigraph in which edges  $e_3$  and  $e_8$  are multiple edges of the pair of vertices  $v_3$  and  $v_4$ . Further, edge  $e_9$  is loop at vertex  $v_1$ . A *simple graph* is a graph that does not have any multiple edges or loops. Figures 4.1(1) and 4.1(2) are examples of a simple graph. A *complete graph* is a graph in which every vertex is connected to every other vertex in the graph. A triangle is a simple example of a complete graph, where every vertex of a triangle is connected to every other vertex. A *regular graph* is a graph where every vertex has equal number of connections. A rectangle, triangle, or in general, a polygon is an example of a regular graph where every vertex has two connections. It should be noted that every complete graph is a regular graph.

#### 4.1.1 Degree of vertex

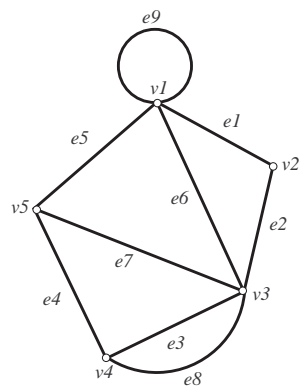
The term *connections* in the above paragraph was used to mention the number of edges (lines) culminating or starting at a vertex. This is referred to as the *degree of vertex* in graph theory,



(1) Undirected graph



(2) Directed graph



(3) Multigraph

Figure 4.1: Types of graphs

and these two terms, connections and degree of vertex, will be hereafter used interchangeably. For example, in Figure 4.1(1) vertex  $v_3$  has a degree of vertex of 4 as there are four edges starting from or culminating into it. In addition, the starting point of a node will be referred to as *from point* and the culminating or end point of an edge will be referred to as *to point*. This from-and-to information is relevant and important only in the case of directed graphs as directions are considered.

### 4.1.2 Representations of graphs

Graphs are commonly represented in three different ways, which are *edge-node list*, *adjacency matrix* and *incidence matrix*. Edge-node lists are more suited for storage purposes, while adjacency and incidence matrices are well suited for computational purposes. Here, the three different representations of Figures 4.1(1) and 4.1(2) are given.

#### Edge-node lists

| Edge  | From point | To point |
|-------|------------|----------|
| $e_1$ | $v_2$      | $v_1$    |
| $e_2$ | $v_3$      | $v_2$    |
| $e_3$ | $v_4$      | $v_3$    |
| $e_4$ | $v_5$      | $v_4$    |
| $e_5$ | $v_1$      | $v_5$    |
| $e_6$ | $v_3$      | $v_1$    |
| $e_7$ | $v_5$      | $v_3$    |

Table 4.1: Edge-node list of the directed graph of Figure 4.1(2). For the undirected graph of Figure 4.1(1), the list will be the same except for the fact that the directions will have no meaning and are interchangeable.

### Adjacency matrices

The matrix representations need some more explanation. First, the adjacency matrix is dealt with. The adjacency matrix is a square matrix with the dimensions of the number of points in the graph  $n \times n$ . The matrix contains entries of only 0 and 1, where 0 indicates the points are not connected by a line, or in other words, the points are not adjacent. And, an entry of 1 indicates that the pair of points are connected/adjacent. In the case of an undirected graph the adjacency matrix has entries in cells  $v_i v_j$  as well as  $v_j v_i$ , and hence, the *adjacency matrix is a symmetric matrix for the undirected case*. In the case of a directed graph, the adjacency matrix has an entry for  $v_i v_j$  if there is a line connecting  $i$  and  $j$  starting from the former and ending at the latter points. There will be an entry for  $v_j v_i$  only if there is a line starting from  $j$  and ending at  $i$ . Hence, the adjacency matrix of a directed graph is not symmetric.

Adjacency matrix of an undirected graph

Adjacency matrix of a directed graph

$$\begin{array}{c} \left[ \begin{array}{cccccc} & v_1 & v_2 & v_3 & v_4 & v_5 \\ v_1 & 0 & 1 & 1 & 0 & 1 \\ v_2 & 1 & 0 & 1 & 0 & 0 \\ v_3 & 1 & 1 & 0 & 1 & 1 \\ v_4 & 0 & 0 & 1 & 0 & 1 \\ v_5 & 1 & 0 & 1 & 1 & 0 \end{array} \right] \end{array} \qquad \begin{array}{c} \left[ \begin{array}{cccccc} & v_1 & v_2 & v_3 & v_4 & v_5 \\ v_1 & 0 & 0 & 0 & 0 & 1 \\ v_2 & 1 & 0 & 0 & 0 & 0 \\ v_3 & 1 & 1 & 0 & 0 & 0 \\ v_4 & 0 & 0 & 1 & 0 & 0 \\ v_5 & 0 & 0 & 1 & 1 & 0 \end{array} \right] \end{array}$$

A careful look at the matrices would indicate that the diagonal elements are all zero suggesting that the points are not connected to themselves by a line. However, if there is a loop at one of those points then the diagonal entry has a 1 for that particular point.

### Incidence matrices

The incidence matrix is a rectangular matrix with the dimensions of the rows equivalent to the number of lines and the columns equivalent to the number of points in the graph – a  $m \times n$  matrix. The entries of the matrix comprise of  $-1$ ,  $0$ , and  $1$  for a directed graph, and  $0$  and  $1$  for an undirected graph. The word incident refers to the fact that the points are incident upon the line. Hence, an entry of  $1$  in the matrix indicates the points are incident in that particular line. This further implies that every row has a pair of entries in the case of graph with lines.

If there are arc lines, and the arc lines are described/formed by more than a pair of points, then each row has more than two entries. Also, if there are loops in the graph then there is only one entry in that particular row indicating that only one point is incident upon the line. For the directed graph case,  $-1$  entry indicates the *from point* and  $1$  indicates the *to point*.

Incidence matrix of an undirected graph

Incidence matrix of a directed graph

$$\begin{array}{c} \left[ \begin{array}{cccccc} & v_1 & v_2 & v_3 & v_4 & v_5 \\ e_1 & 1 & 1 & 0 & 0 & 0 \\ e_2 & 0 & 1 & 1 & 0 & 0 \\ e_3 & 0 & 0 & 1 & 1 & 0 \\ e_4 & 0 & 0 & 0 & 1 & 1 \\ e_5 & 1 & 0 & 0 & 0 & 1 \\ e_6 & 1 & 0 & 1 & 0 & 0 \\ e_7 & 0 & 0 & 1 & 0 & 1 \end{array} \right] \end{array}$$

$$\begin{array}{c} \left[ \begin{array}{cccccc} & v_1 & v_2 & v_3 & v_4 & v_5 \\ e_1 & 1 & -1 & 0 & 0 & 0 \\ e_2 & 0 & 1 & -1 & 0 & 0 \\ e_3 & 0 & 0 & 1 & -1 & 0 \\ e_4 & 0 & 0 & 0 & 1 & -1 \\ e_5 & -1 & 0 & 0 & 0 & 1 \\ e_6 & 1 & 0 & -1 & 0 & 0 \\ e_7 & 0 & 0 & 1 & 0 & -1 \end{array} \right] \end{array}$$

### Properties of the adjacency and incidence matrices

The main interests of this research lies in the properties of the adjacency and incidence matrices of the undirected graphs; and incidence matrices of the digraphs, and hence, only these will be discussed. The properties of the above mentioned matrices are given as follows,

- The column and row sums of the adjacency matrices, and the column sum of the incidence matrices of undirected graphs give the degree of vertex of the set of points in the graphs.
- The incidence matrix of a directed and an undirected graph always have a column rank deficiency of 1.
- The adjacency matrix of an undirected and a digraph is of full rank.
- Both the incidence and adjacency matrices of any graph are sparse matrices.

### Relationship between the adjacency and incidence matrices

Let  $\mathcal{A}$  be the adjacency matrix and  $\mathcal{I}$  be the incidence matrix. Then  $\mathcal{A}$  and  $\mathcal{I}$  are related in the following manner,

$$\mathcal{A} = \mathcal{D} - \mathcal{I}^T \mathcal{I} \quad (4.1)$$

$$\mathcal{L}(G) = \mathcal{I}^T \mathcal{I} \quad , \quad (4.2)$$

where

$\mathcal{L}(G)$  is called the *Laplacian* of the graph and is the inner product of the incidence matrix, and

$\mathcal{D}$  is a diagonal matrix containing the degree of vertices as its diagonal entries.

The above relationship is true only for the incidence matrices of the undirected graphs. It is also true for incidence matrices of the digraphs, but the resultant adjacency matrices are the adjacency matrices of the underlying undirected graph of a digraph<sup>1</sup>. Equation (4.1) implies that provided the incidence matrix of any graph, the adjacency matrix of the underlying undirected graph can be constructed. In addition to that, the *Laplacian matrix* and its variants formed from the inner product of the incidence matrix are used in the *spectral analysis of graphs*.

## 4.2 A detailed excursion through least squares adjustment of a levelling network

In this section a link will be made between graph theory and least squares adjustment of a levelling network. Also, a link will be created to the sections following in order to emphasize the importance of looking into the statistics before attempting an adjustment of the levelling network. To illustrate the adjustment by least squares Figure 4.1(2) is considered as a levelling network here. For reasons of simplicity, the points will only be referred to in the mathematical equations below without the prefix  $v$ . Recalling the levelling observation equation given by,

$$\Delta H_{ij} = H_j - H_i + \epsilon \quad , \quad (4.3)$$

---

<sup>1</sup>For every digraph there is an underlying undirected graph obtained by removing the directions of the digraph

where

$\epsilon$  is the unknown error term in the observation.

Applying this observation equation to the entire network in Figure 4.1(2) will give us the following set of equations,

$$\begin{aligned}
 e_1 &= H_1 - H_2 + \epsilon_1 \\
 e_2 &= H_2 - H_3 + \epsilon_2 \\
 e_3 &= H_3 - H_4 + \epsilon_3 \\
 e_4 &= H_4 - H_5 + \epsilon_4 \\
 e_5 &= H_5 - H_1 + \epsilon_5 \\
 e_6 &= H_1 - H_3 + \epsilon_6 \\
 e_7 &= H_3 - H_5 + \epsilon_7 .
 \end{aligned}$$

Writing the above equations in matrix format will give us,

$$\begin{bmatrix} e_1 \\ e_2 \\ e_3 \\ e_4 \\ e_5 \\ e_6 \\ e_7 \end{bmatrix} = \begin{bmatrix} 1 & -1 & 0 & 0 & 0 \\ 0 & 1 & -1 & 0 & 0 \\ 0 & 0 & 1 & -1 & 0 \\ 0 & 0 & 0 & 1 & -1 \\ -1 & 0 & 0 & 0 & 1 \\ 1 & 0 & -1 & 0 & 0 \\ 0 & 0 & 1 & 0 & -1 \end{bmatrix} \begin{bmatrix} H_1 \\ H_2 \\ H_3 \\ H_4 \\ H_5 \end{bmatrix} + \begin{bmatrix} \epsilon_1 \\ \epsilon_2 \\ \epsilon_3 \\ \epsilon_4 \\ \epsilon_5 \\ \epsilon_6 \\ \epsilon_7 \end{bmatrix} . \quad (4.4)$$

Representing the observations with  $\Delta H$  and the parameters as  $H$  the equation (4.4) can be written in a simpler form, which becomes,

$$\Delta H = AH + \epsilon , \quad (4.5)$$

where

$A$  is called the design matrix.

The  $A$  matrix is an exact replica of the incidence matrix mentioned in section 4.1.2 of the Figure 4.1(2). Also, (4.5) is the linear equation as in (2.15), which is again solved by the linear equality constrained least squares as the incidence matrix is rank deficient (cf.

section 2.4). The solution is given by equation (2.19), which is recalled here and replaced by the appropriate terms for observations and parameters.

$$\hat{\mathbf{H}} = (\mathbf{A}^T \mathbf{A} + \mathbf{D}\mathbf{D}^T)^{-1}(\mathbf{A}^T \Delta \mathbf{H} + \mathbf{D}\mathbf{c}) \quad , \quad (4.6)$$

where

$\mathbf{D}$  is the datum matrix. The equation (4.6) is applicable only if the datum matrix method is used. If the constraints are applied to the observations prior to the estimation of parameters then appropriate number of columns are removed from the design matrix. This can be mathematically expressed as follows;

applying the constraints to the observations prior to estimation

$$\Delta \mathbf{H}' = \Delta \mathbf{H} - \mathbf{A}\mathbf{D}\mathbf{c} \quad ; \quad (4.7)$$

removing the appropriate number of columns from the design matrix – in the static levelling case one column is removed,

$$\mathbf{A} \rightarrow \mathbf{A}' \quad ;$$

then the solution to equation (4.5) becomes,

$$\hat{\mathbf{H}} = (\mathbf{A}'^T \mathbf{A}')^{-1}(\mathbf{A}'^T \Delta \mathbf{H}') \quad . \quad (4.8)$$

If the observations are provided with weights then the solutions (4.6) and (4.8) become,

$$\hat{\mathbf{H}} = (\mathbf{A}^T \mathbf{P}\mathbf{A} + \mathbf{D}\mathbf{D}^T)^{-1}(\mathbf{A}^T \mathbf{P}\Delta \mathbf{H} + \mathbf{D}\mathbf{c}) \quad (4.9)$$

$$\hat{\mathbf{H}} = (\mathbf{A}'^T \mathbf{P}\mathbf{A}')^{-1}(\mathbf{A}'^T \mathbf{P}\Delta \mathbf{H}') \quad , \quad (4.10)$$

where

$\mathbf{P}$  is the weight matrix.

The terms  $(\mathbf{A}^T \mathbf{A} + \mathbf{D}\mathbf{D}^T)$ ,  $(\mathbf{A}'^T \mathbf{A}')$ ,  $(\mathbf{A}^T \mathbf{P}\mathbf{A} + \mathbf{D}\mathbf{D}^T)$ , and  $(\mathbf{A}'^T \mathbf{P}\mathbf{A}')$  are the *normal matrices* of the equations (4.6), (4.8), (4.9), and (4.10) respectively. The terms  $(\mathbf{A}^T \mathbf{A})$ ,  $(\mathbf{A}'^T \mathbf{A}')$ ,  $(\mathbf{A}^T \mathbf{P}\mathbf{A})$  are the Laplacian and weighted Laplacian (if the weight matrix  $\mathbf{P}$  is involved) matrices, and hence, involve the degree of vertices of the points in the network and adjacency matrix as well. However, the point of interest is the degree of vertices.

The advantage of using least squares is that it provides estimates of the variances of the estimates. The error variances for the solutions in equations (4.6), (4.8), (4.9), and (4.10) are respectively,

$$\mathbf{Q}_{\hat{H}} = (\mathbf{A}^T \mathbf{A} + \mathbf{D}\mathbf{D}^T)^{-1} \quad (4.11)$$

$$\mathbf{Q}_{\hat{H}} = (\mathbf{A}'^T \mathbf{A}')^{-1} \quad (4.12)$$

$$\mathbf{Q}_{\hat{H}} = (\mathbf{A}^T \mathbf{P}\mathbf{A} + \mathbf{D}\mathbf{D}^T)^{-1} \quad (4.13)$$

$$\mathbf{Q}_{\hat{H}} = (\mathbf{A}'^T \mathbf{P}\mathbf{A}')^{-1} \quad , \quad (4.14)$$

where

$\mathbf{Q}_{\hat{H}}$  is the variance-covariance matrix of the estimates. This variance-covariance of the estimates involves the Laplacian, and its weighted variant, matrix of the network. In the case of column removal approach of estimation, the variance-covariance matrix is the direct inverse of the Laplacian of the network devoid of the row and column of the point whose column is removed from the incidence (design) matrix. This relationship between graph theory and levelling network adjustment is brought out here to emphasize that the degree of vertex dictates the variance-covariance estimates of the parameters. According to Strang (1986), the higher the values of the diagonal elements when compared to the off-diagonal elements, the more stable is the inverse of the matrix. Thus, an analysis of the degree of vertices will give *a priori* information about the stability of the inverse. Also, the degree of vertex of a point indicates the response of the point to the least squares adjustment as a higher number of observations leading to a point provide better check on the estimated height values at that point.

The geodetic literature indicates that there have been a few attempts in utilizing graph theory to solve geodetic problems in the vertical (Snay, 1978), horizontal (Grafarend & Mader, 1989), three-dimensional (Even-Tzur, 2001), and solvability of kinematic levelling networks (Kleijer et al., 2001). Linkwitz (1999) provides a complete overview of network analysis by starting off with the role of graph theory in such an analysis. Further, Borre (2001) provides a comprehensive overview of the spectral analysis of the normal matrix of a network both from a graph theoretical point of view as well as from the geodetic network analysis point of view. The role of graph theory should not be overestimated, because it is only an efficient and effective tool for the intuitive understanding of the character of a network.

The above ideas can also be extended to the kinematic levelling network. Recalling the

kinematic observation equation model (2.24) from section 2.5.1,

$$\Delta H_{ij}(t_k) = H_j(t_0) - H_i(t_0) + (v_j - v_i)(t_k - t_0) + \epsilon$$

For reasons of simplicity and better understanding the  $\Delta t_0$  term has been neglected and assumed as constant. Applying this model to the Figure 3.13(2), which is illustrated here in Figure 4.2 again for reasons of clarity.

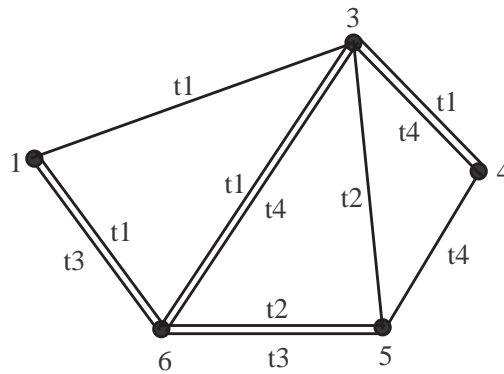


Figure 4.2: Illustration for explaining the kinematic levelling network design matrix

$$\begin{bmatrix} \Delta H_{13}(t_1) \\ \Delta H_{34}(t_1) \\ \Delta H_{36}(t_1) \\ \Delta H_{61}(t_1) \\ \Delta H_{53}(t_2) \\ \Delta H_{56}(t_2) \\ \Delta H_{56}(t_3) \\ \Delta H_{61}(t_3) \\ \Delta H_{34}(t_4) \\ \Delta H_{36}(t_4) \\ \Delta H_{45}(t_4) \end{bmatrix} = \begin{bmatrix} -1 & 1 & 0 & 0 & 0 \\ 0 & -1 & 1 & 0 & 0 \\ 0 & -1 & 0 & 0 & 1 \\ 1 & 0 & 0 & 0 & -1 \\ 0 & 1 & 0 & -1 & 0 \\ 0 & 0 & 0 & -1 & 1 \\ 0 & 0 & 0 & -1 & 1 \\ 1 & 0 & 0 & 0 & -1 \\ 0 & -1 & 1 & 0 & 0 \\ 0 & -1 & 0 & 0 & 1 \\ 0 & 0 & -1 & 1 & 0 \end{bmatrix} \begin{bmatrix} -1 & 1 & 0 & 0 & 0 \\ 0 & -1 & 1 & 0 & 0 \\ 0 & -1 & 0 & 0 & 1 \\ 1 & 0 & 0 & 0 & -1 \\ 0 & 2 & 0 & -2 & 0 \\ 0 & 0 & 0 & -2 & 2 \\ 0 & 0 & 0 & -3 & 3 \\ 3 & 0 & 0 & 0 & -3 \\ 0 & -4 & 4 & 0 & 0 \\ 0 & -4 & 0 & 0 & 4 \\ 0 & 0 & -4 & 4 & 0 \end{bmatrix} \begin{bmatrix} H_1 \\ H_3 \\ H_4 \\ H_5 \\ H_6 \\ \text{---} \\ v_1 \\ v_3 \\ v_4 \\ v_5 \\ v_6 \end{bmatrix} + \begin{bmatrix} \epsilon_{13} \\ \epsilon_{34} \\ \epsilon_{36} \\ \epsilon_{61} \\ \epsilon_{53} \\ \epsilon_{56} \\ \epsilon_{56} \\ \epsilon_{61} \\ \epsilon_{34} \\ \epsilon_{36} \\ \epsilon_{45} \end{bmatrix} \quad (4.15)$$

In equation (4.15) there is a partition to indicate one part of the design matrix refers to the height part of the matrix and the other part refers to the velocity part of the matrix. Hereafter, the height part of the matrix will be represented as  $\mathbf{A}^H$  and the velocity part of the matrix will be represented as  $\mathbf{A}^v$ . Rewriting equation (4.15),

$$\Delta \mathbf{H}(t) = [\mathbf{A}^H | \mathbf{A}^v] \begin{bmatrix} \mathbf{H} \\ \text{---} \\ \mathbf{v} \end{bmatrix} + \boldsymbol{\epsilon} \quad (4.16)$$



matrix of the kinematic levelling network, it can be expanded as follows,

$$\mathbf{A}^T \mathbf{A} = \left[ \mathbf{A}^{HT} | \mathbf{A}^{HT} \mathbf{T}^T \right]^T \left[ \mathbf{A}^H | \mathbf{T} \mathbf{A}^H \right] \quad (4.21)$$

$$= \left[ \begin{array}{c|c} \mathbf{A}^{HT} \mathbf{A}^H & \mathbf{A}^{HT} \mathbf{T} \mathbf{A}^H \\ \hline \mathbf{A}^{HT} \mathbf{T}^T \mathbf{A}^H & \mathbf{A}^{HT} \mathbf{T}^T \mathbf{T} \mathbf{A}^H \end{array} \right] \quad (4.22)$$

Here, it can be seen that all the four elements of the expanded inner product of the kinematic levelling network design matrix are Laplacian and its variant matrices. These Laplacian matrices are the Laplacian of the incidence matrix of the underlying multigraph of the network. Here, the variants of the Laplacian are weighted by the epoch of observation: in some cases it is epoch and in others it is square of the epoch. Thus, the role of the degree of vertices in the stable inverse of the normal matrix for the kinematic levelling network is explained.

### 4.3 Statistics of the levelling network

The following statistics of the network are presented in this section.

1. Number of observations in a releveling line.
2. Number of the different epochs of observations at each point in the network.
3. Time interval between the first and the last observation in a releveling line.
4. Length of levelling lines before and after reduction.
5. Degree of vertices.
6. Time interval between the first and last observations through each point in the network.

All these statistics will provide a good characterization of the network in terms of its strengths and weaknesses, and further enabling a rigorous analysis of the results from least squares estimation of parameters. Again, the value of these statistics should not be overestimated as they provide only an intuitive understanding of the network.

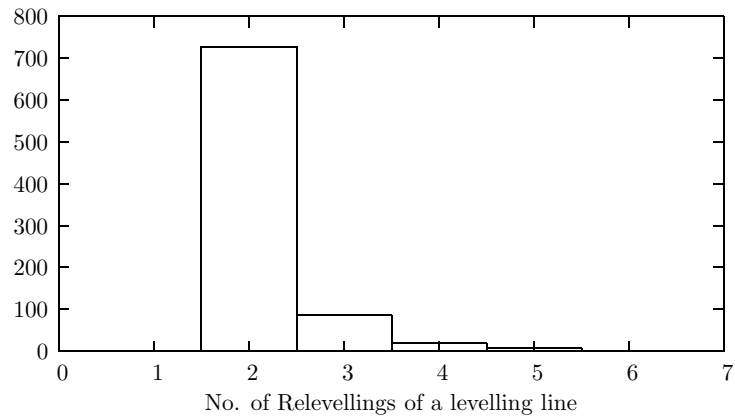


Figure 4.3: Histogram of the number of relevellings of the relevelled levelling lines

#### 4.3.1 Number of observations in the relevelling lines

This statistic provides information on how often the observations have been repeated in the network for the purpose of vertical crustal motion determination. In the Figure 4.3 it can be clearly seen that the number of observations for a relevelling line is predominantly 2, which indicates that it can only give velocities and also, these velocities cannot be checked for their accelerations if any or, if they are only secular over time. It can be recalled that this was one of the reasons why a linear model (section 2.5.1) was chosen for modelling the vertical crustal motion.

#### 4.3.2 Number of the different epochs of observations at each point in the network

This statistic is similar to the previous one, but it differs only in that it emphasizes on the other form of velocity information in the network, i.e., the information in the single levelling observations observed at different epochs and incident at a point in the network. Again, it is clearly seen that the points all have been visited by observations only in two different epochs. This again indicates that only velocities can be estimated and they cannot be checked for their accelerated trend, if any, in the region.

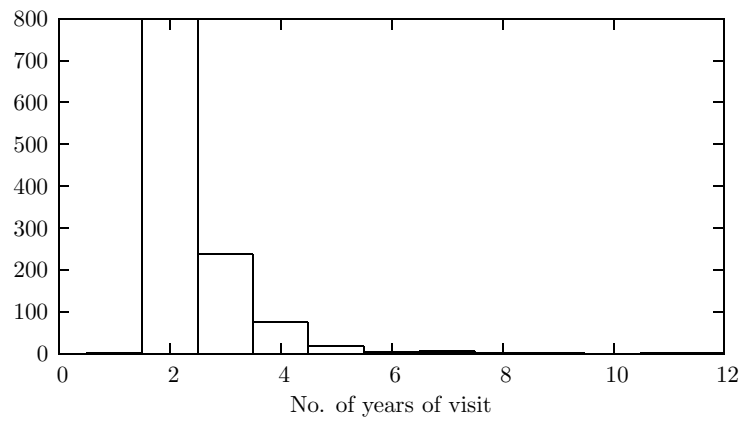


Figure 4.4: Histogram of the number of years (epochs) in which the observations were observed through each point in the network

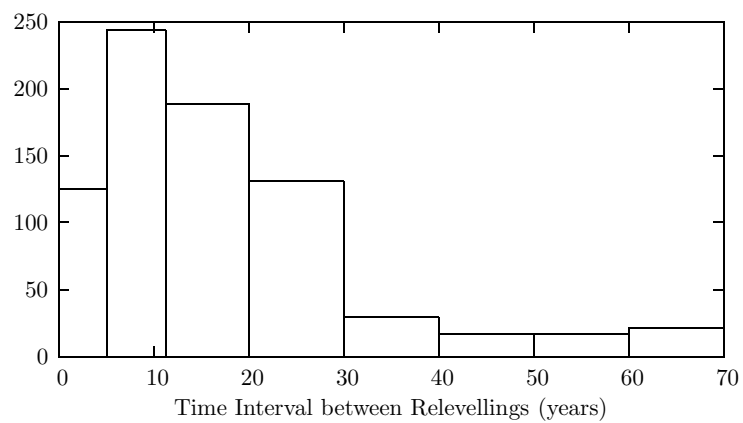


Figure 4.5: Histogram of the time interval between the epochs of observation in the releveling lines

### 4.3.3 Time interval between epochs of observation in the levelling lines

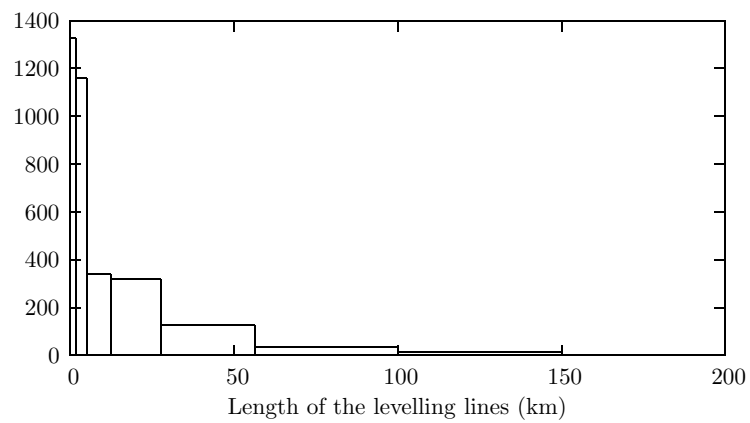
This statistic provides information about the time resolution available in the network: bigger the time resolution easier the identification of velocities. Considering the accuracy of levelling observations (minimum of  $4\sqrt{K}\text{mm}\sqrt{\text{km}}$ ) and the rate of vertical crustal motion (in  $\text{mm}/\text{year}$ ), it can be said that in order get meaningful velocities from the relevellings the time interval must be a minimum of 10 years. Eventhough 1 year would be sufficient enough theoretically, the velocity estimates will not be reliable. An analogy would be the rounding off the decimal places, where when only three decimal digits are required it is always good practice to round off at the fourth or even the fifth digit. Figure 4.5 shows a rather uniform distribution of the time intervals 0-5, 6-10, 11-20, and 21-30. After that the numbers become insignificant. The histogram shows that more than 80% of the time intervals are close to 10 years or more. This indicates that the relevellings will more often provide us a signal (velocities) rather than noise (errors), because of a good time resolution.

### 4.3.4 Length of levelling lines before and after reduction

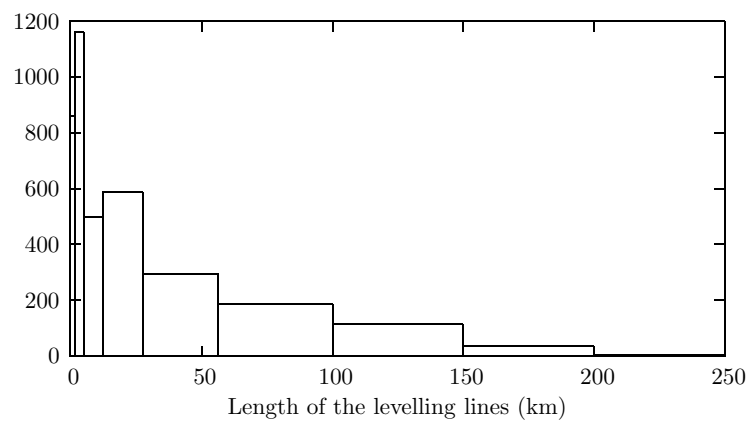
This statistic provides an insight into the global or local nature of the signal that has been estimated from the network. Also, it indicates the homogeneity of the network geometry. In this case fig. 4.6(1) shows a predominantly homogeneous network of shorter levelling lines before reduction whereas, after reduction the network shows a lot more inhomogeneity than that was present before, fig. 4.6(2). This can be attributed to the combining nature of the reduction algorithm.

### 4.3.5 Degree of vertices

Degree of vertex of a point in a network is the number of observations observed through that point. The analysis of the degree of vertices of the network provides a clear insight into the robustness of the network towards errors in the observations. If the points of a height network have more than two observations observed through them then it can be presumed that the parameters associated with that point will be estimated with better accuracy. This comes from the fact that the variance-covariance matrix of the estimates is the inverse of the weighted Laplacian matrix, and the Laplacian matrix is a variant of the adjacency matrix.



(1) Before reduction



(2) After reduction

Figure 4.6: Histograms of length of levelling lines before and after reduction

The adjacency matrix depicts the connectedness of each point in a network of the levelling type.

$$\mathbf{Q}_{\hat{x}} = (\mathbf{A}^T \mathbf{P} \mathbf{A})^{-1} \quad , \quad (4.23)$$

where

$\mathbf{Q}_{\hat{x}}$  is the variance-covariance matrix of the parameter estimates,

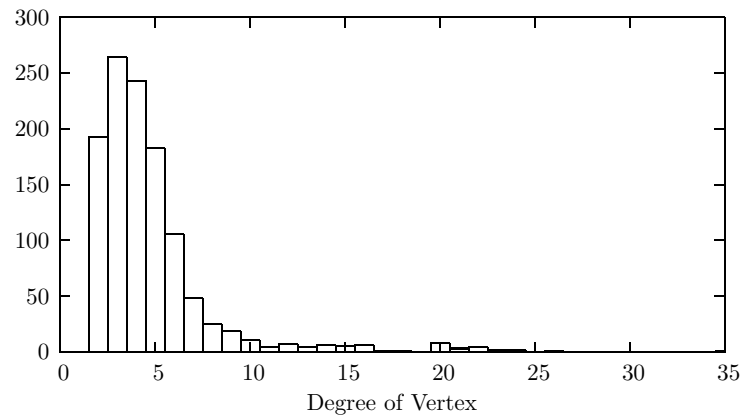
$\mathbf{A}$  is the design matrix with no rank defect, and

$\mathbf{P}$  is the weight matrix of the observations, and here, it is the inverse of variance-covariance matrix of the observations.

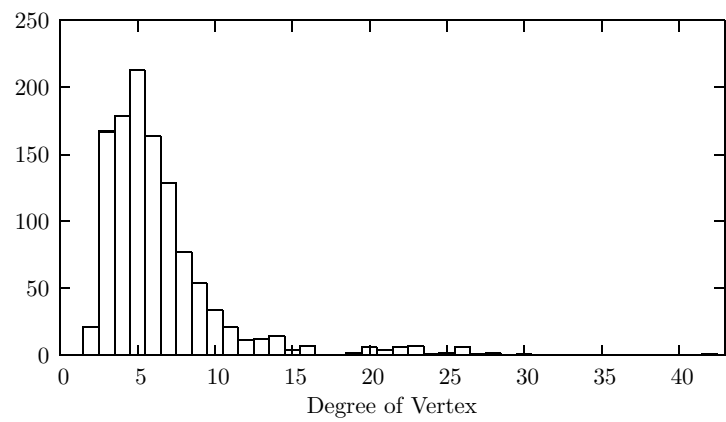
The histograms (Figures 4.7(1) and 4.7(2)) and the spatial plots (Figures 4.8(1) and 4.8(2)) of the degree of vertices of the network are shown. The histogram provides a quantitative overview of the predominant degree of vertex of the points in the network while the spatial plot of the degree of vertex shows how they are distributed in the network. In both figures the network replete of the relevellings is also taken into account, because only this configuration determines the geometric strength of the network and hence, controls error variances of the estimates. The plots with the relevellings added to them are just to show how different the degree of vertices of the network looks after adding those relevellings.

The distribution of the degree of vertex of the network without relevellings ranges from 2 to 10, and after that it dies out. A similar pattern can be observed in the case with relevellings. Also, the predominant degrees of vertex are 3 and 5 in the without and with relevellings cases respectively. This goes to show that the network has good geometric strength. The spatial distribution plot of the same for both cases supports the above reasoning. However, there is cause for concern as obvious from Figure 4.7(1).

The cause for concern is that there are atleast two hundred points (out of 1146, which is close to 20%) that have a degree of vertex of only two in the network without relevellings. This shows that there is no strong redundancy check for these points except for the fact that they are in the network. Such points sometimes do not make it into loop circuits as they might be weak connections between two big or small networks. So, a review of the spatial plot of only the degree 2 vertices is done with Figure 4.9. The plot indicates no such problems, and also, indicates that it is distributed all over the network. Further, most of them are present in loop circuits, which provide those points with adequate check for errors. The ones that

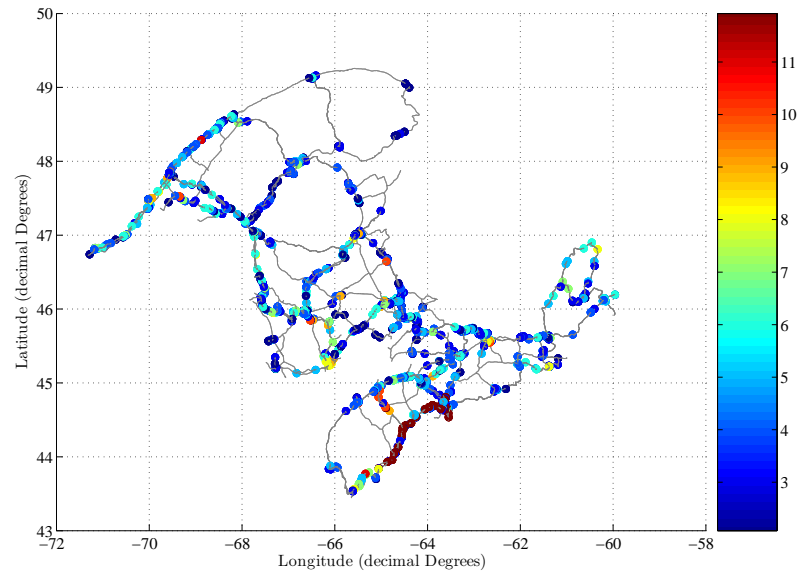


(1) Without relevelings

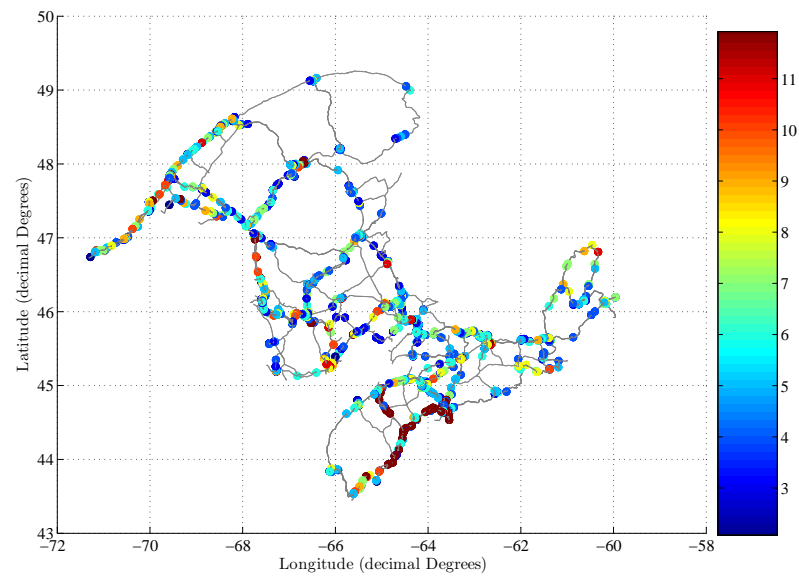


(2) With relevelings

Figure 4.7: Histograms of the degree of vertices of the network points without and with relevelings taken into consideration



(1) Without relevelings



(2) With relevelings

Figure 4.8: Spatial plots of the degree of vertices of the network point without and with relevelings taken into consideration. The degree of vertices of the network points without relevelings determine the response of the network to the adjustment.

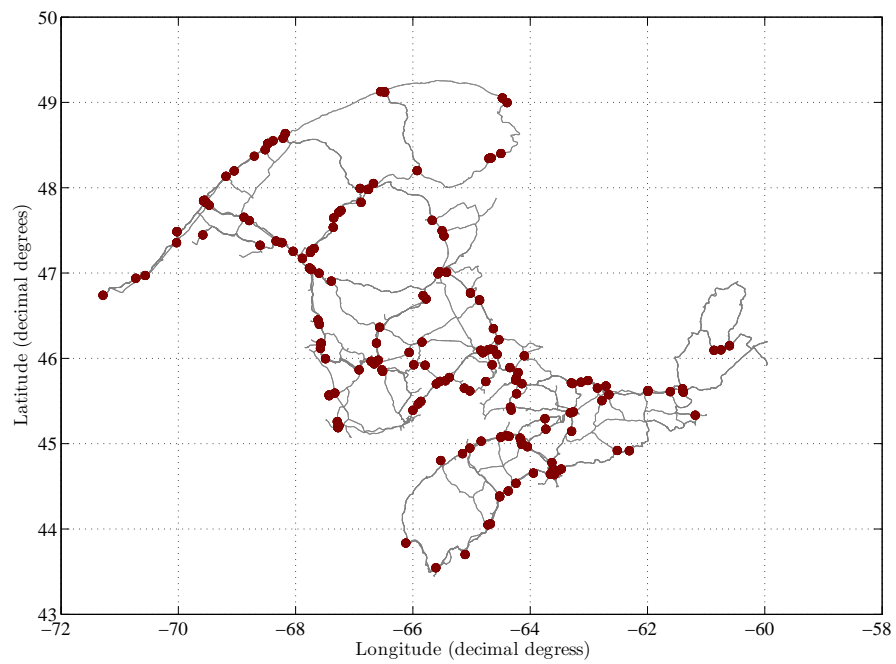


Figure 4.9: Spatial distribution of the degree 2 vertices in the network. The degree 2 vertices are spread out all over the network, and also substantial in quantity.

are critical are all located on the tail portion of the network in the northwest corner that is extending in the southwestern direction.

Apart from the above concern, the entire network is filled with very good degree of vertex interspersed by minimum degree of vertex (2) and other higher values. This shows that the network is close to homogeneity in terms of degree of vertex. However, the southern most part of the network does not share this homogeneity as a brown streak can be seen indicating very high degree of vertex in that region. This is due to the combination effect explained in section 3.6. It is the presumption and expectation of the author that such a kind of inhomogeneity will show up in the error estimates of the parameters.

#### 4.3.6 Time interval between the first and last observations through each point in the network

The kinematic height model used here is recalled for reasons of clarity, which is given as,

$$H_p(t_k) = H_p(t_0) + v_p \Delta t \quad ,$$

where

$H_p$  is the height of a point  $p$ ,

$v_p$  is the height velocity of point  $p$ , and

$\Delta t = t_k - t_0$  is the time difference between the reference epoch and the observation epoch.

This model was compared with the equation of a line, and it is recalled again here for reasons of clarity. The abscissa in the adjustment model is the time, ordinate is the height of the point, the slope is the vertical velocity, and the constant is the height value at the reference epoch. If the pairs of values of the abscissa and the ordinate are known, it is possible to determine the equation of the line. The equation of the line is defined by  $m$  (velocity  $v$ ) and  $c$  (height at  $t_0$ ). If the errors in the values of the ordinates are equivalent to the value of the slope then it is common sense that larger abscissa intervals are required to determine the slope value. In other words, if the slope of the line is too flat then we need higher abscissa intervals to find out the change in ordinate values.

It is exactly the same situation that is dealt with in here. The heights determined via spirit levelling have a precision of millimetre and the velocities have a magnitude of mm/year. This means that a larger time interval is required for the determination of velocities from

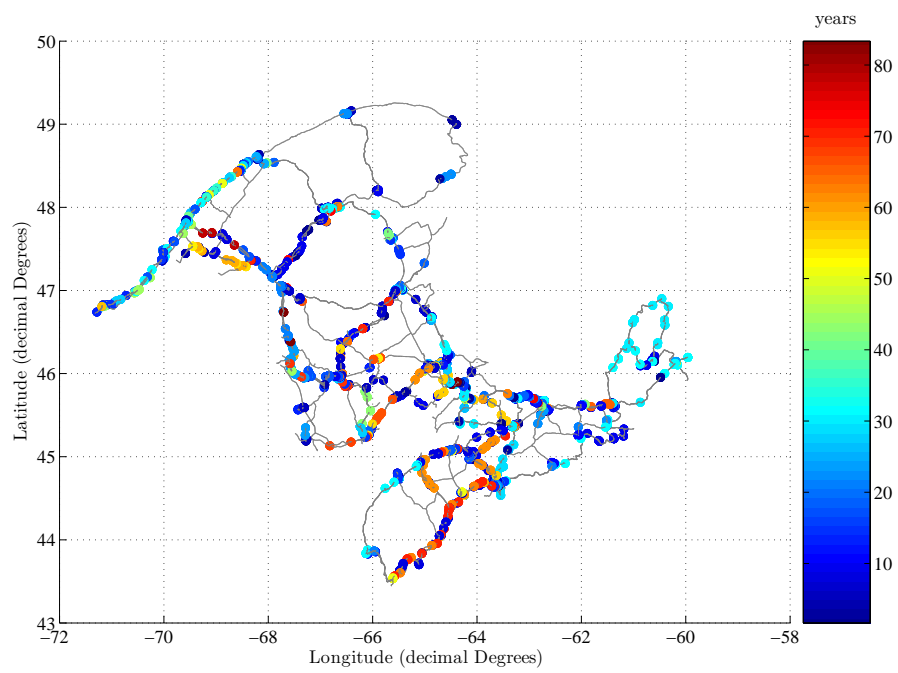


Figure 4.10: Spatial plot of the time difference,  $\Delta t$ , between the first and the last observations through each point in the network

height differences. Thus, in the present case the retrieval of velocity information at a point depends on the time interval between the first and last observations through that point. It depends only on this time interval, because the first and the last times of observation provide a boundary for the velocity information content at that point.

In the spatial plot of the time interval (Figure 4.10) it can be seen that there is a mixed distribution of the time interval values. However, the time interval values are predominantly in the cyan and blue zone of the colorbar. This is proven by the histogram plot (Figure 4.11), where the predominant values are concentrated between 1 and 32 years. The three peak time intervals 7, 8, and 9 years are seen more often in the middle of the network, and they are bordered by the higher values on the northern, southern, and western boundaries of the network. Also, starting from the south western end of the network there is a zig-zag streak of red and dark yellow values going until the middle of the network. In summary, the distribution of the  $\Delta t$  is mixed all over the network, and, the peak values at 7, 8, and 9 years indicate that errors might dominate the deformation information.

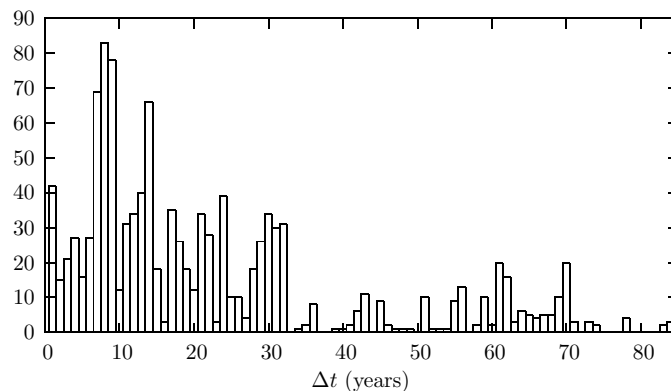


Figure 4.11: Histogram of  $\Delta t$  between the first and last observations through each point in the network.

#### 4.4 Trend analysis of the relative velocities from multiple relevellings

Here, the term *trend analysis* is similar to *time-series analysis*, but it is not in the real sense of the conventional time series analysis, which requires observations to be taken at short and usually equal intervals of time. The observations that are analysed do not fall into this frame;

however, the aim is to find out the consistency in the trend of the crustal motion over time. To perform this analysis a levelling line must have been observed atleast in three different epochs (years), which gives two relative velocities for comparison.

Now, the computation of relative velocities is explained. First, the relevelings of a levelling line are identified and sorted with respect to ascending order of time. Then, the following computation is performed.

$$\left| \begin{array}{c} h_{ij}(t_1) \\ h_{ij}(t_2) \\ h_{ij}(t_3) \\ \vdots \\ h_{ij}(t_{n-1}) \\ h_{ij}(t_n) \end{array} \right| \left| \begin{array}{c} \frac{h_{ij}(t_2)-h_{ij}(t_1)}{t_2-t_1} \\ \frac{h_{ij}(t_3)-h_{ij}(t_2)}{t_3-t_2} \\ \vdots \\ \frac{h_{ij}(t_n)-h_{ij}(t_{n-1})}{t_n-t_{n-1}} \end{array} \right|$$

In the following Figures 4.12(1)–4.12(105), the relative velocities are plotted as a bar graph in the left-hand-side (LHS) of each figure and the corresponding time interval bars in the right-hand-side (RHS) of that figure.

Consistency in the trend of crustal deformation relative velocities is defined in the following manner: *The relative velocities in a series must be equal or atleast close enough in magnitude irrespective of the time interval between the observations.* This formulation comes from the assumption that the crustal deformation trend for the region considered is *secular*. This is a very important assumption and the interpretation of the results are good only as far as the assumption.

When the bar graphs are analyzed it is found that only one Figure – 4.12(14) – appears convincing; however, there are a few doubtful cases. The doubtful ones are Figures 4.12(20), 4.12(27), 4.12(30), 4.12(39), 4.12(63), and 4.12(87). In Figure 4.12(14), what is seen is that the magnitudes of relative velocities are similar and the time intervals for the two relative velocities are not the same. The difference in time interval gives a very good indication that the relative velocities are signals of the crustal deformation along that levelling line. It is

surprising that all the other graphs do not show any consistency (apart from the doubtful ones), and these can be regarded as errors. The reason for considering the rest of the graphs as errors is because of the following reasons.

1. The relative velocities switch between positive and negative, which means there is both uplift and subsidence along same levelling line. This is impossible unless and otherwise for an earthquake changing (episodically) the deformation direction. So, these can be classified as errors. The best example for this type of a graph is Figure 4.12(60), where there are four relative velocities possible with one year time interval, and the negative and positive values alternate. The other good examples that have different year intervals, but still show the positive negative switch are Figures 4.12(3), 4.12(17), and 4.12(40).
2. In some graphs, for example, in Figures 4.12(1), 4.12(2), 4.12(13), 4.12(15), 4.12(34), 4.12(41), and 4.12(48) it can be seen that the relative velocities are higher when the time interval is small and vice versa. This could be, because they are simply errors in the observations and they get smoothed out as the time interval increases. This suggests that they are ratios of error differences and the time interval between them.
3. In some other graphs, for example, in Figures 4.12(51), 4.12(54) and 4.12(68) it can be seen that the time intervals are very similar, but the relative velocities are completely disparate values. So, this may be an indication that these are not signals of crustal deformation, but again the ratio mentioned above. Although, it could also be the inability of the linear model to capture episodic and non-linear motion.
4. Further, there are graphs, where the relative velocity magnitudes are directly proportional to the time intervals. This is again an inconclusive situation, because nothing can be said about the values; however, they can be classified as errors. Some examples for this situation are 4.12(9), 4.12(78), 4.12(88), 4.12(90), and 4.12(97).

The doubtful cases mentioned above are doubtful in that they have very similar time intervals and very similar relative velocity magnitudes. It cannot be said with confidence that these values are relative velocities, because from the general trend of the figures in the time series, the relative velocities are inversely proportional to the time interval. So, the doubt remains as to whether the values have to be classified as relative velocities or as errors.

In addition to the above, one important trend that can be observed from the time series is that if the time intervals are shorter –  $1 \leq \Delta t \leq 10$  – then the jumps, switches, and inconsistencies are more common than with observations taken over longer periods of time. This is an important observation, because this gives a hint to utilize time as weights for the adjustment. Also, it is expected that levelling measurements provide accuracies at the millimeter level and the signal that is being pursued is also at the millimeter level. This means that there has to be a sufficient time interval between observations for the signal to be pronounced and extracted from the observations. Thus, this analysis clearly reveals if there is any deformation information at all in the observations and if they have been smeared by errors – mostly by unaccounted systematic errors – in the observations.

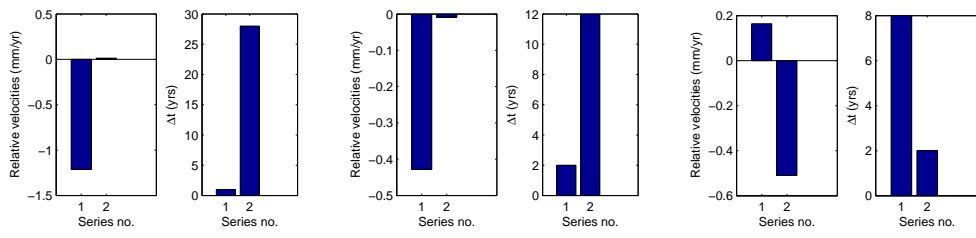
In summary, the pre-adjustment analysis shows that the network has a good geometric strength, and nominal resolution in terms of time interval between repeated observations. Although the trend analysis shows some inconsistencies, it is a true that repeated observations over time do contain information about the motion, if there is any. From geodynamic models and GPS studies it is known that the area has some postglacial rebound motion going on, and hence, it is a strong belief that the adjustment of the network for velocities will show some signals pertaining to the vertical motion. Further, the number of levelling lines that could be analysed are only 106 of about 2800 levelling lines in the network (as in the underlying simple graph of the network), which is less than the 4% of the lines.

## 4.5 Chapter summary

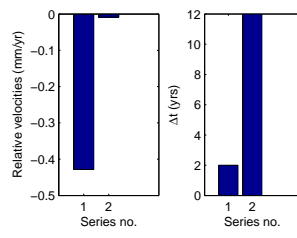
Pre-adjustment analysis of the network was analysed in this chapter to get an insight into the nature of the network, and also to get an idea about the quality of the estimates from the adjustment of the network. The important points from this chapter are as follows:

1. the ability of graph theory to help visualise the network and give an intuitive understanding was demonstrated;
2. the relationship between the degree of vertices of the network and the variance-covariance estimate of the parameters was illustrated;
3. a number of statistics were computed for the network of concern, viz.,

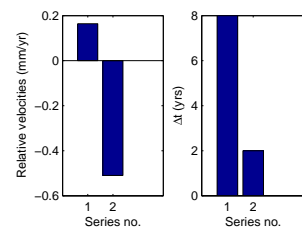
- number of observations in a releveling line;  
The predominant number was 2 in this case and hence, indicated only velocities can be estimated, and a check cannot be made if there is any acceleration in the velocity values.
  - number of the different epochs of observations at each point in the network;  
This statistic again showed the predominance of two epochs at most of the points, which further confirmed that only a linear model of vertical crustal motion can be applied to the data.
  - time interval between the first and the last observation in a releveling line;  
The time interval statistic showed that the network had equal share of short and long time intervals, which augurs well for the vertical crustal motion estimation.
  - length of levelling lines before and after reduction;  
The length of the levelling lines increased only marginally after reduction when compared to the lengths before reduction.
  - degree of vertices;  
The degree of vertices of the network without relevelings will reflect the strength of the network. In that sense, the degree of vertices of the simple graph indicates that the network has a number of degree 2 vertices, which suggests that the adjustment will not be able to check for errors at these points.
  - time interval between the first and last observations through each point in the network;  
This statistic showed that most of the network points fall under the time  $\leq 10$  years indicating only a nominal time interval between epochs.
4. the statistics showed that the network was a nominal network for the estimation of vertical crustal motion; and
  5. trend analysis of relative velocities calculated from multiple relevelings was performed, which indicated the relevelings were ridden with errors. However, this formed only 4% of the available levelling lines and so, it can be said that this analysis cannot be extrapolated to the entire network.



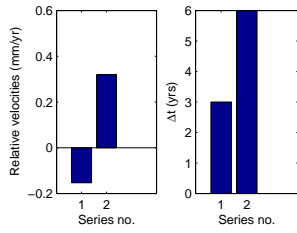
(1)



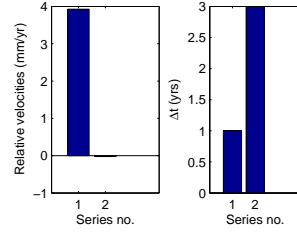
(2)



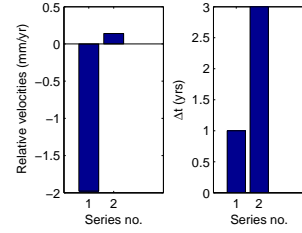
(3)



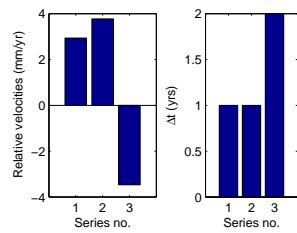
(4)



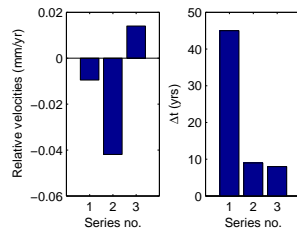
(5)



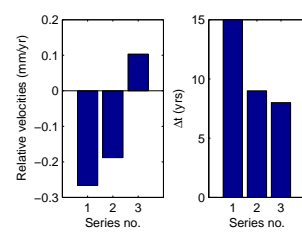
(6)



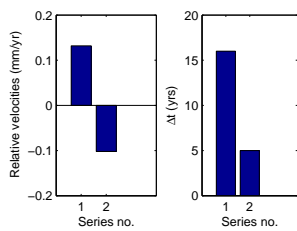
(7)



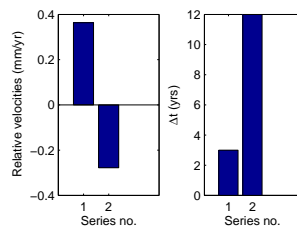
(8)



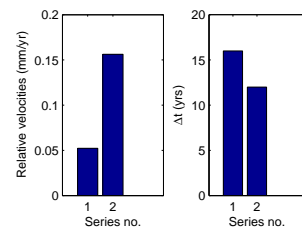
(9)



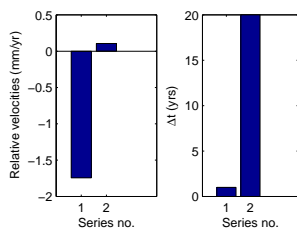
(10)



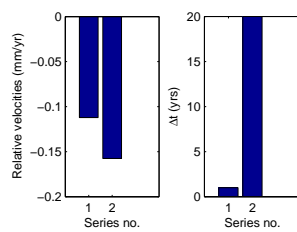
(11)



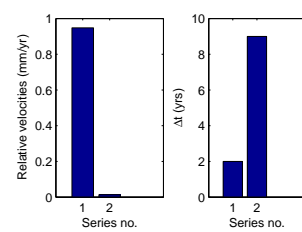
(12)



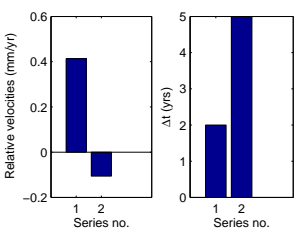
(13)



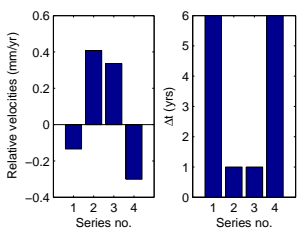
(14)



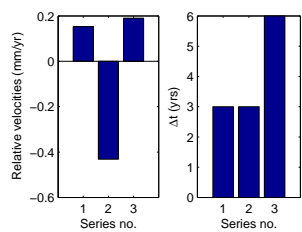
(15)



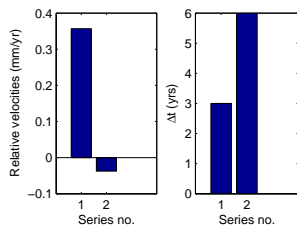
(16)



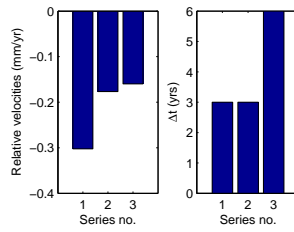
(17)



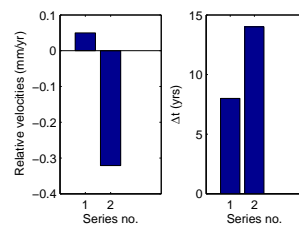
(18)



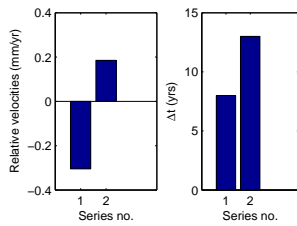
(19)



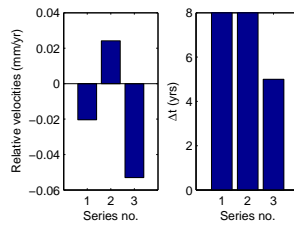
(20)



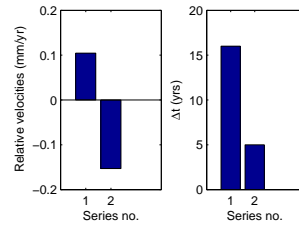
(21)



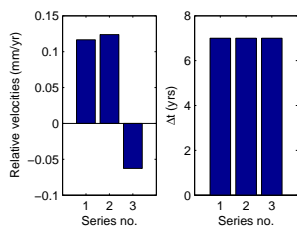
(22)



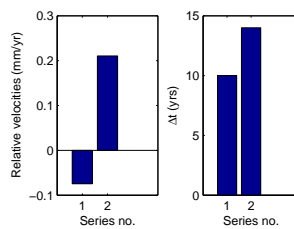
(23)



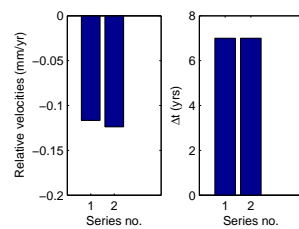
(24)



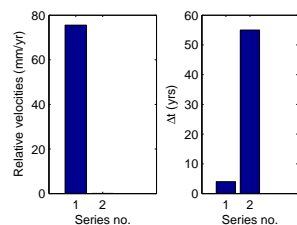
(25)



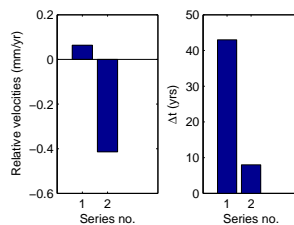
(26)



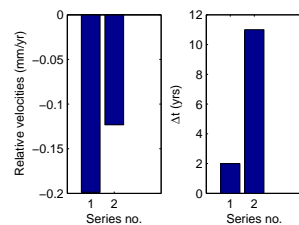
(27)



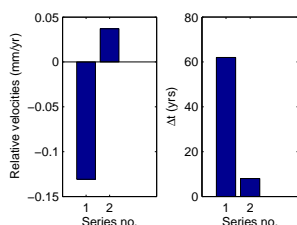
(28)



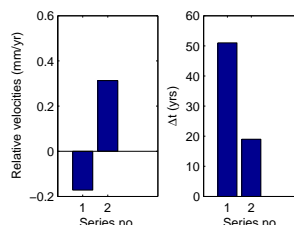
(29)



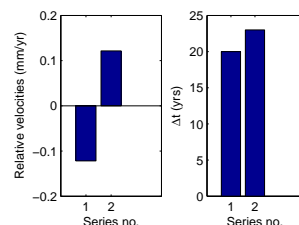
(30)



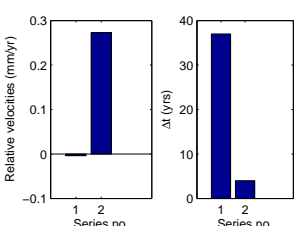
(31)



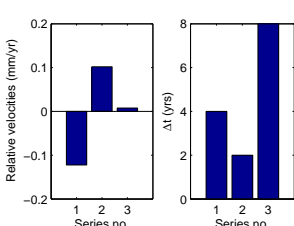
(32)



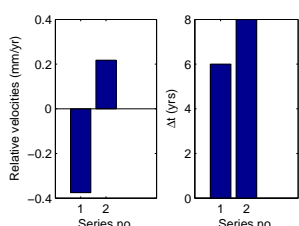
(33)



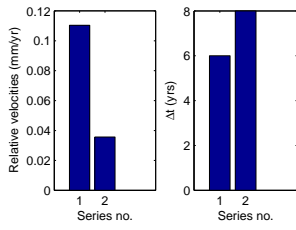
(34)



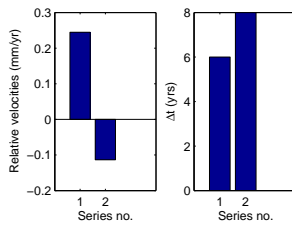
(35)



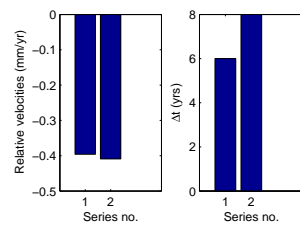
(36)



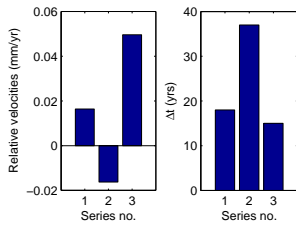
(37)



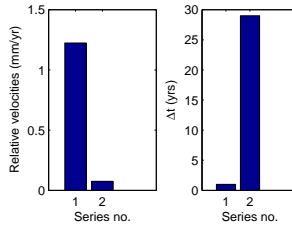
(38)



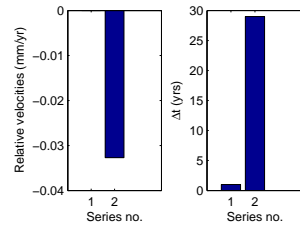
(39)



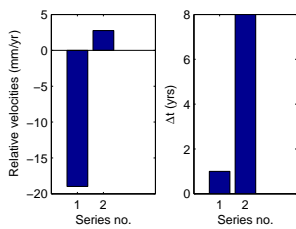
(40)



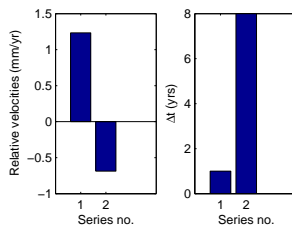
(41)



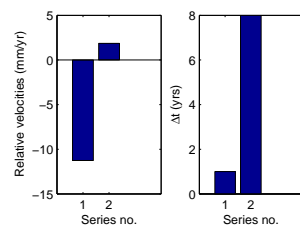
(42)



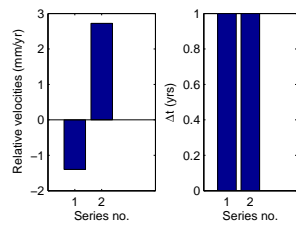
(43)



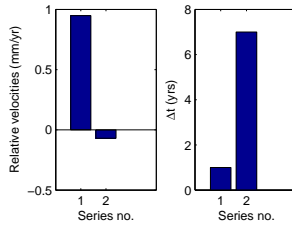
(44)



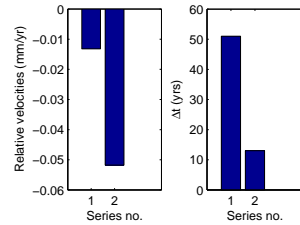
(45)



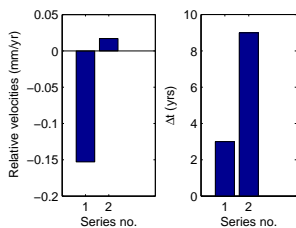
(46)



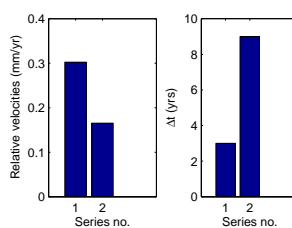
(47)



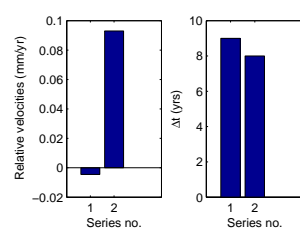
(48)



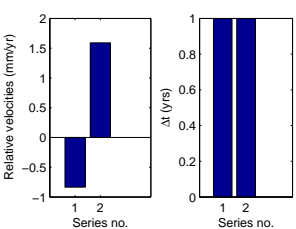
(49)



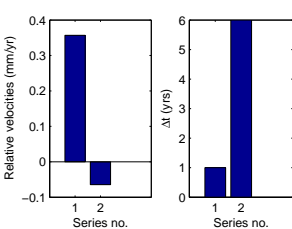
(50)



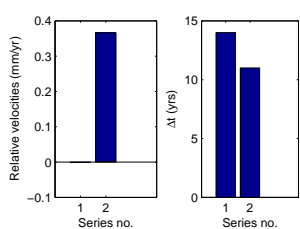
(51)



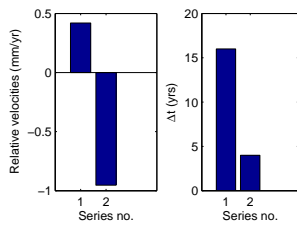
(52)



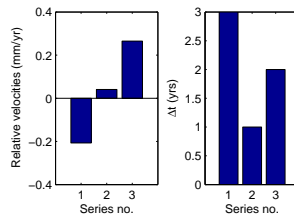
(53)



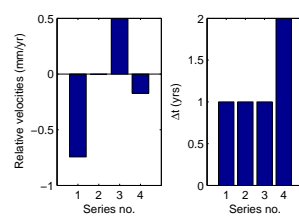
(54)



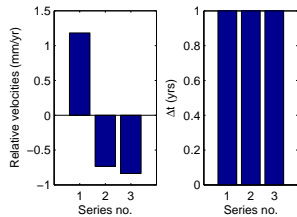
(55)



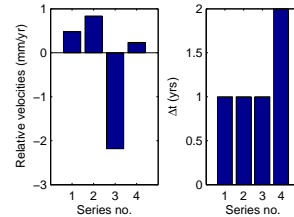
(56)



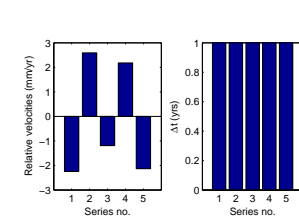
(57)



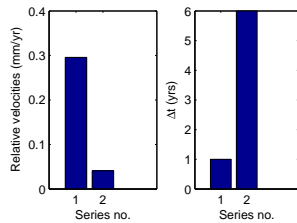
(58)



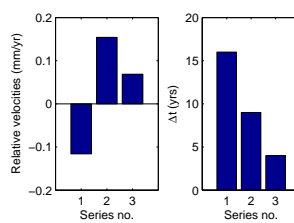
(59)



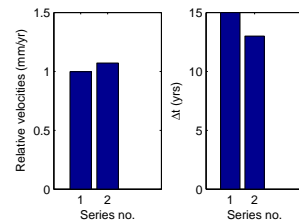
(60)



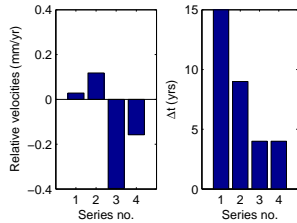
(61)



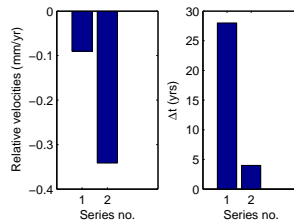
(62)



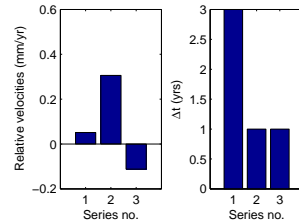
(63)



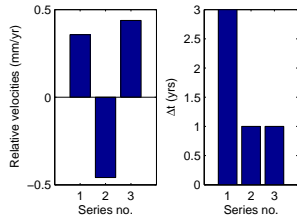
(64)



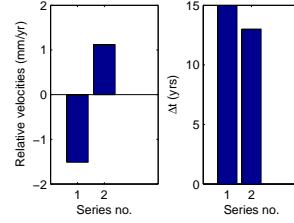
(65)



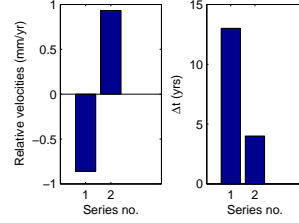
(66)



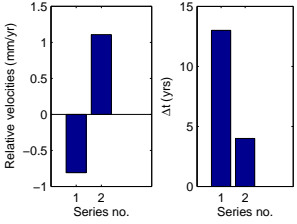
(67)



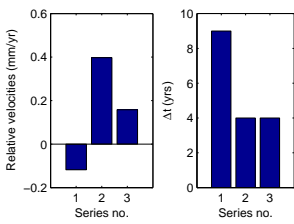
(68)



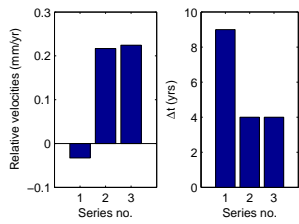
(69)



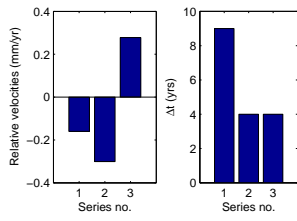
(70)



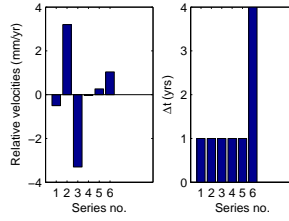
(71)



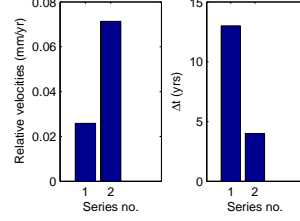
(72)



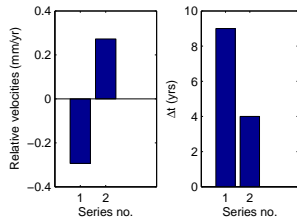
(73)



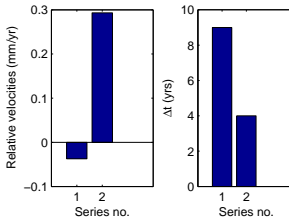
(74)



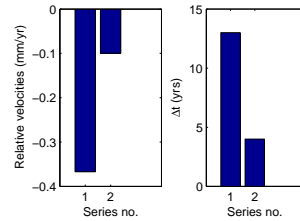
(75)



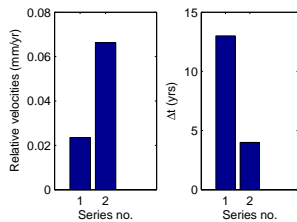
(76)



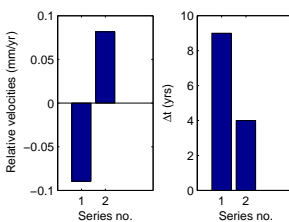
(77)



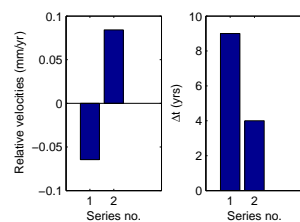
(78)



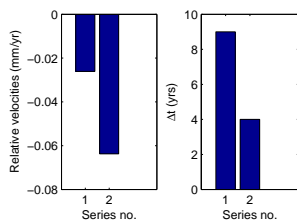
(79)



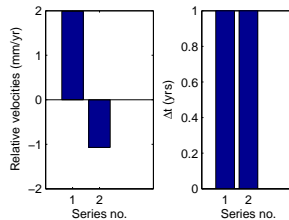
(80)



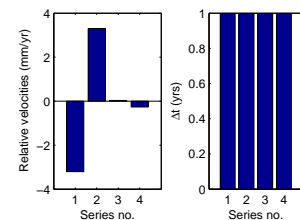
(81)



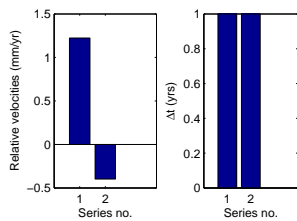
(82)



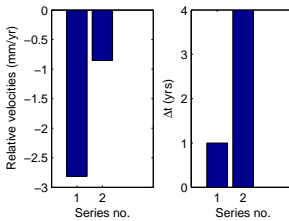
(83)



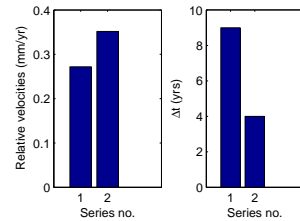
(84)



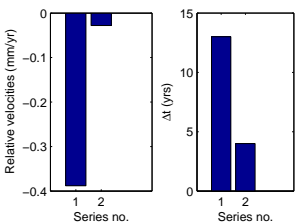
(85)



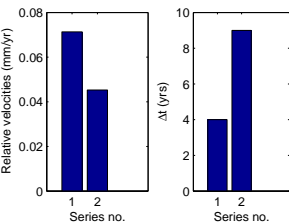
(86)



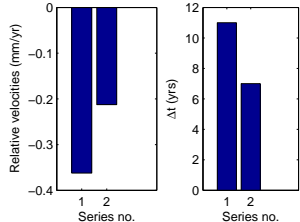
(87)



(88)



(89)



(90)

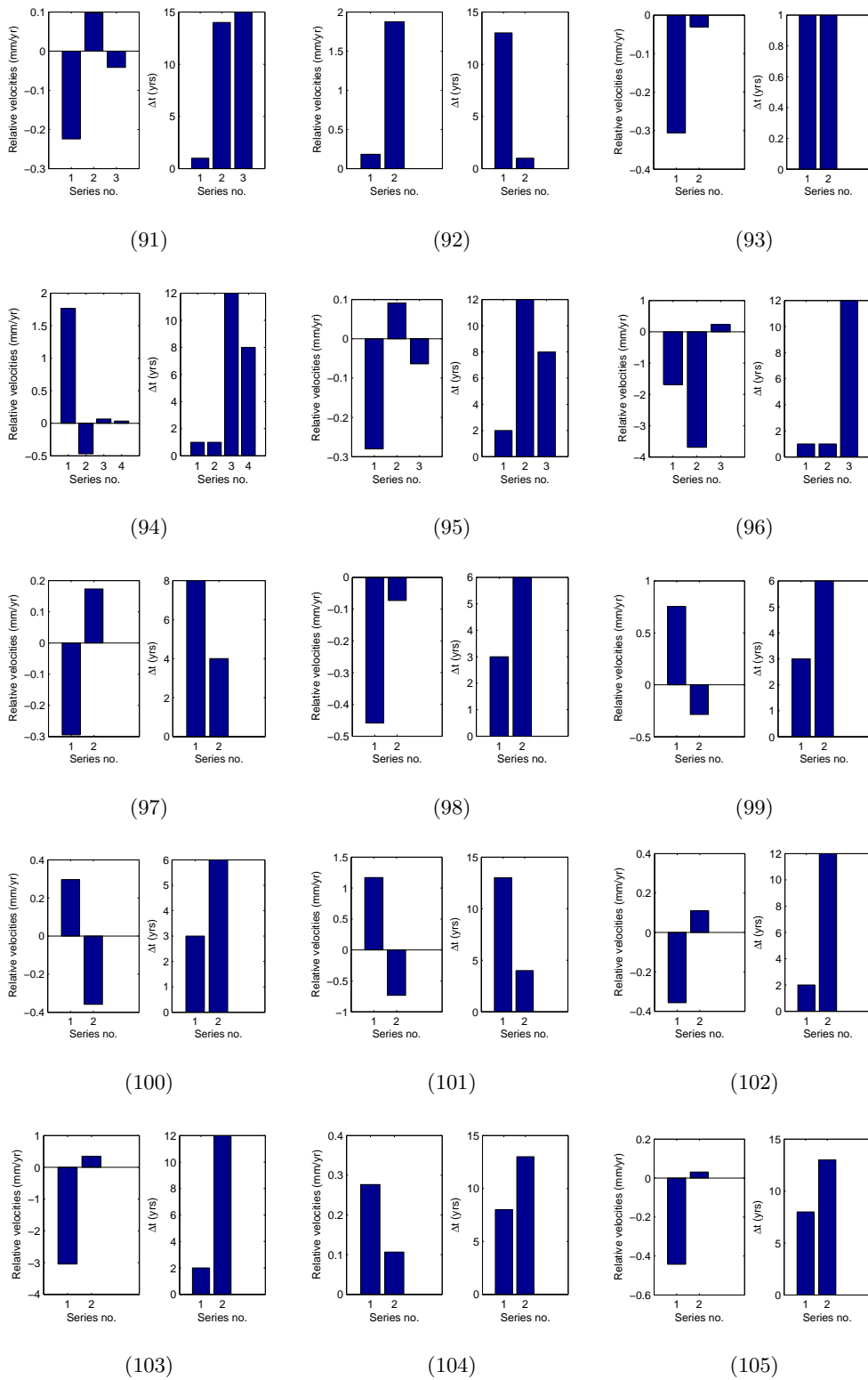


Figure 4.12: Trend analysis of relative velocities derived from multiple relevelings of a levelling line

## Chapter 5

# Realisation of a Kinematic Vertical Datum for the Levelling Network

After a thorough investigation of the characteristics of the network concerned for vertical crustal motion determination, a linear constrained least squares adjustment of the network is carried out. The method of adjustment followed is the parametric least squares method as it provides the parameters directly, and integrates the datum definition problem into it. Since the adjustment takes care of the datum problem of the scattered kinematic levelling network concerned here, the least squares adjustment of the network is referred to as the *realisation of a kinematic vertical datum*. In this chapter, the method of adjustment and the source of the velocity constraints are explained in sections 5.1, 5.2, and 5.3, and then the estimated parameters and the adjusted observations are analysed and statistically tested in sections 5.4 and 5.5.

### 5.1 Subset matrix selection from the kinematic design matrix

The network that was adjusted was the network after the reduction process. The network had 3730 observations, and 2292 parameters with half of the parameters representing heights and the other half representing the velocities of the points in the network. The kinematic design matrix of the network had a rank deficiency of 24 indicating that the network had a multiple rank deficiency. As mentioned in section 3.3.3, the network now has 23 different interconnected subnetworks (as every kinematic network has a minimum rank deficiency of 2) that have an extra rank deficiency. The problem then was to find these groups, or to find those columns that were linearly dependent on the other columns. This problem can be solved in two ways, either by graph-theoretical methods, or by matrix calculus methods.

Initially, the graph-theoretical method was preferred and an implementation was attempted, but was not successful. As mentioned by Snay (1978), it is a challenging task to devise graph-theoretical methods to solve networks that have their points parameterized by more than one parameter. So, the matrix calculus methods were chosen here. In matrix

calculus, the above mentioned problem is solved by finding out the subset of the design matrix whose columns are the most linearly independent columns. Hence, this method is called the *subset selection* method.

The subset matrix can be selected based on either *QR factorization with pivoting*, *Cholesky decomposition*, or *singular value decomposition*. All these methods are discussed in detail in Golub & van Loan (1996) (cf. chapter 12). Here, the method based on QR factorization was used to identify the subset of most linearly independent columns from the kinematic design matrix. In Kleijer et al. (2001), the method based on Cholesky decomposition has been used. The choice of the QR factorization based method was because of the ease of implementation of the method and ease of interpretation of the results.

A point to be noted here is that the S-transformation of Baarda facilitates in finding out the subset of the most linearly independent columns. The reason being, only the most linearly independent columns will give a good condition number: in other words, a condition number closer to unity. Or, in the terms of Lanczos (1997) (cf. section 2.3.2), the subset that has the most linearly independent columns retains close to complete information available in the complete matrix, and hence, provides the minimum condition number possible. Thus, such a subset indicates the points in the network that can be constrained to obtain the best datum, and which in turn minimizes the error estimates of the parameters.

Mostly, the points chosen by mathematical methods cannot be implemented in practice due to historical reasons, or theoretical reasons. For example, in a static height network the point that provides the best possible datum will be close to the centre of the network, but only tide gauges along the coast lines are preferred (this might not be true for land-locked countries) in order to define a geoid. Further, tides gauges that have records over a long period of time are preferred due to their historical significance, and also, for the sheer amount of sea-level data.

## 5.2 Methods of applying the constraints in an excess constraints situation

It is recalled that the kinematic design matrix of the network concerned has multiple rank deficiency. In such situations the excess constraints can be applied in the following ways (cf. section 3.3.3),

1. minimum constraints are fixed with one height and one velocity, and rest of the excess constraints are all fixed with velocities,
2. minimum constraints are fixed with one height and one velocity, and rest of the excess constraints are all fixed with heights, and
3. minimum constraints are fixed with one height and one velocity, and rest of the excess constraints are fixed with a combination of heights and velocities.

The first method has a disadvantage, because all the heights and velocities that are estimated from the excess constraint adjustment are distorted by the excess constraint velocities fixed. It is trivial that there will not be a distortion when the excess constraints are the true values of the velocities. But this is rarely possible as they are often taken from *a priori* geophysical/geodynamical models, or from other forms of geodetic measurements (GPS, SAR/InSAR, and tide gauges). The second method has a very good advantage in that if heights of points are known to an nominal accuracy, all taken in the same epoch, and having the same reference frame, then the heights and velocities of all the other points can be estimated without any significant distortion. This allows the interpretation of the velocities in terms of vertical crustal motion without any assumptions and biases from geophysical/geodynamical models. The third method is not a sensible method at all as it will not be possible to interpret the results either based on the heights, or based on the source of the velocities. In this research the first two methods were used.

### 5.3 Results from adjustment for the realisation of a kinematic vertical datum

As mentioned in Table 3.8 the network had a rank deficiency of 24 and the corresponding subnetworks were identified using subset matrix selection method. However, the condition number of the subset matrix was large, which blew up the error values of the estimates. Hence, one more column had to be removed to bring down the value of the condition number. Thus, in the end 25 different points were fixed out of which 23 are excess constraints. The 25 datum points are depicted in Figure 5.1

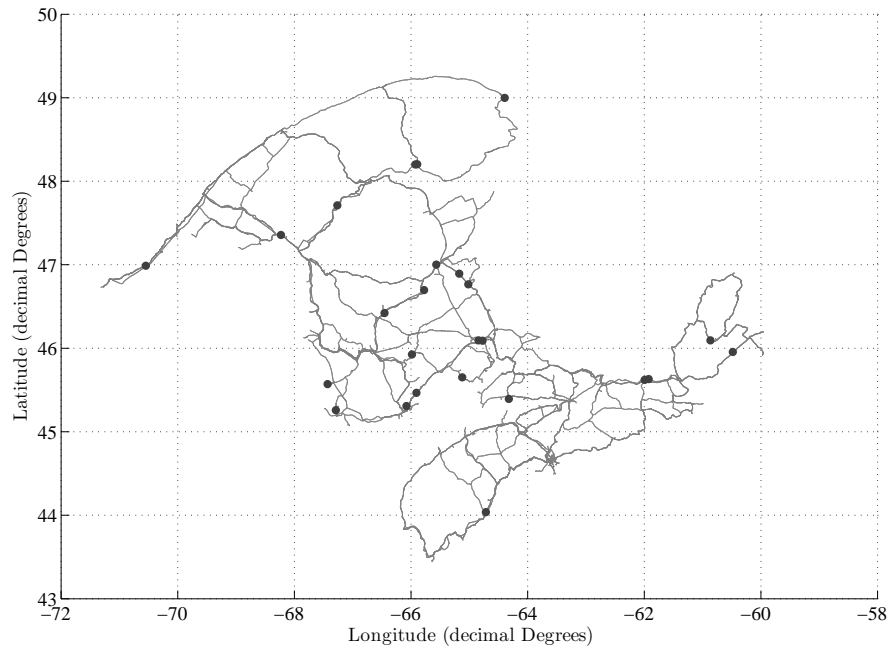
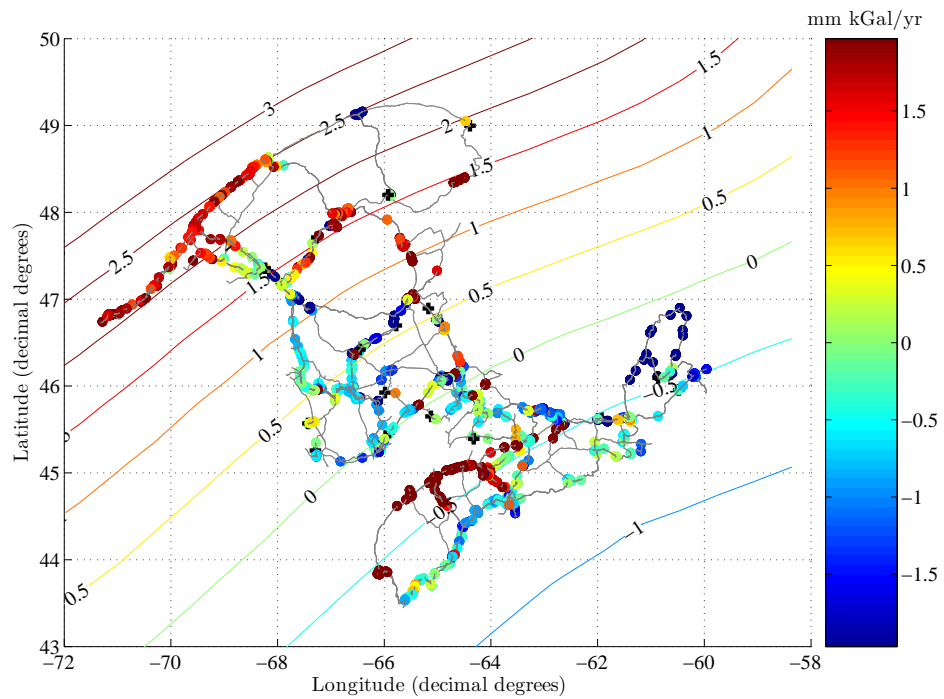


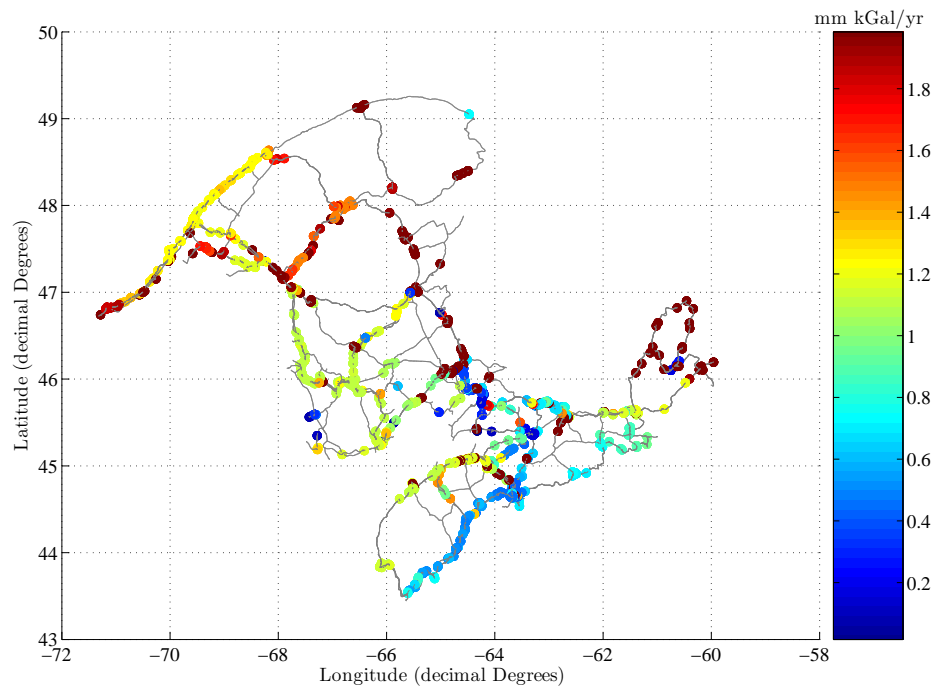
Figure 5.1: The 25 datum points fixed for all the adjustments carried out in the research

### 5.3.1 Fixing the excess constraints with velocities

For fixing the excess constraint velocities five different post glacial rebound models were used, which provided the velocity values for the excess constraints. The post glacial rebound models are computed on approximated spherical Viscoelastic Maxwell type 2 (VM2) Earth models (Peltier, 2002) with six layers, and with ICE-3G (Tushingham & Peltier, 1991) (Figure 5.2(1)) and ICE-4G models (Peltier, 2002) (Figures 5.3(1), 5.3(2), 5.3(3), and 5.3(4)), which provide information on the ice loading history (cf. Table 6.1). The numerical modelling of the post glacial rebound models are explained in Rangelova et al. (2005). It has to be noted that it is not a matter of concern as some arbitrary values for the velocities can also be taken. As it will be shown later that fixing the velocity excess constraints to zero does not alter the results significantly. A geophysical/geodynamical model is preferred instead of arbitrary values, because the models come from scientific and logical reasoning. Nevertheless, it has to be kept in mind that an excess constraint adjustment only provides distorted values no matter what values are used.

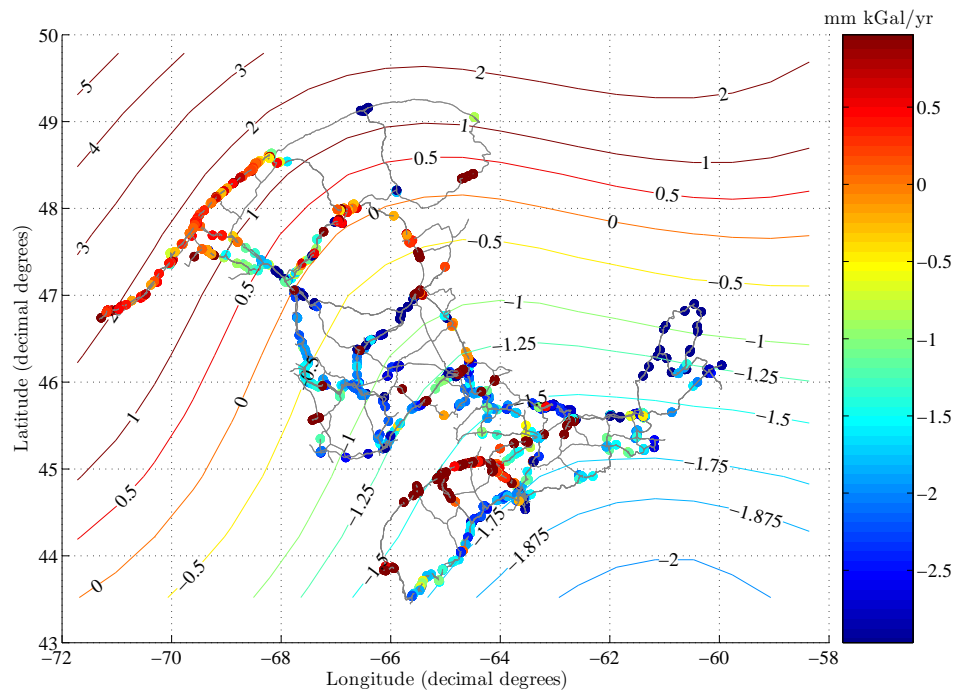


(1) Estimates of velocities by using velocities from model 1 for excess constraints and with precision of the observations as weights

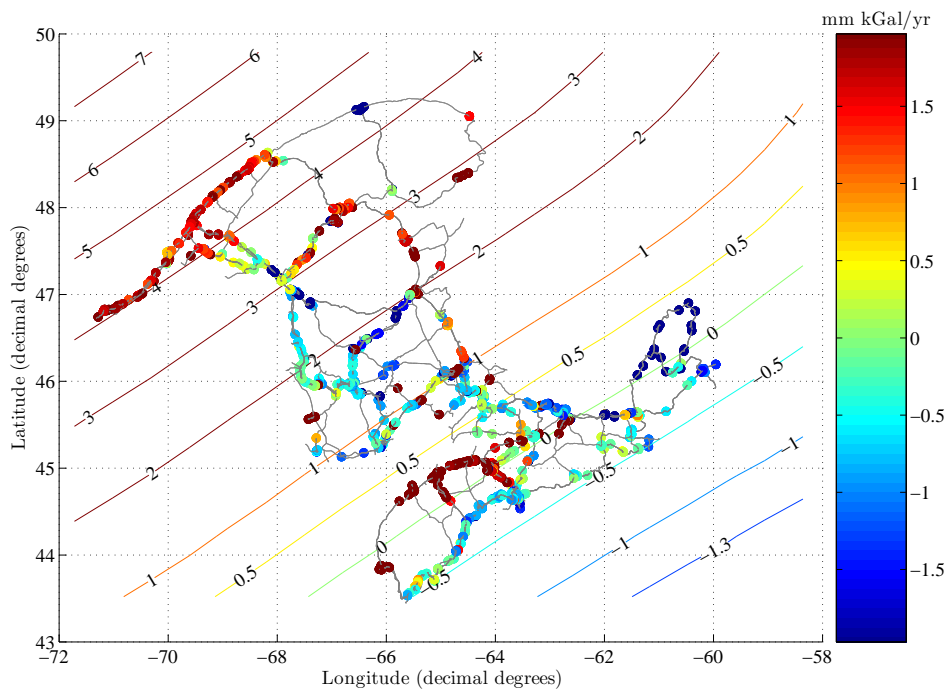


(2) Error estimates of velocities using velocities from model 1 for excess constraints and with precision of the observations as weights

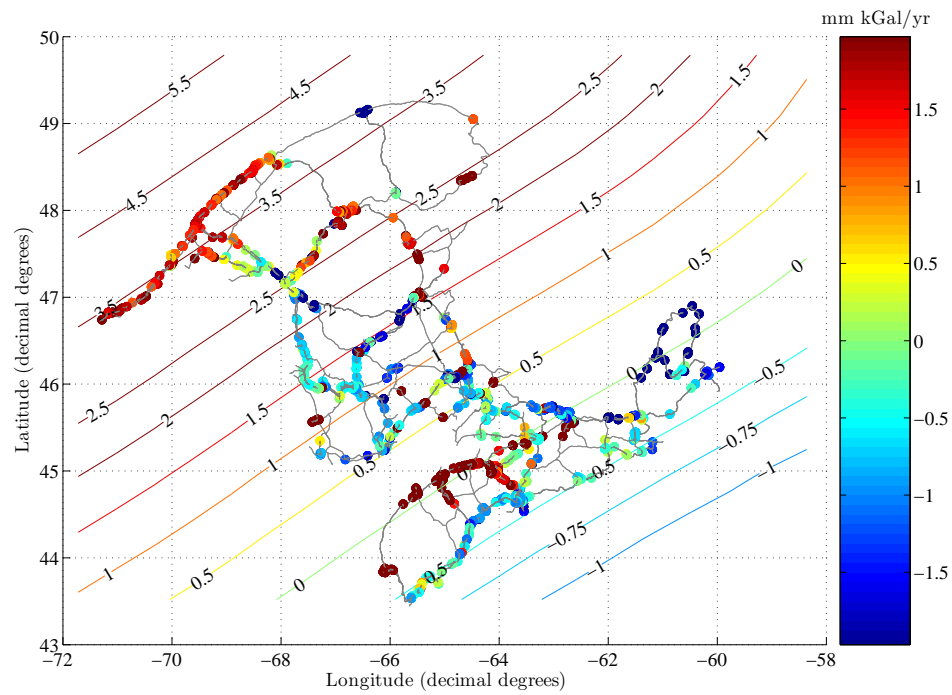
Figure 5.2: Velocities and their errors estimated using velocity excess constraints from model 1 and with weights as the precision of the observed data



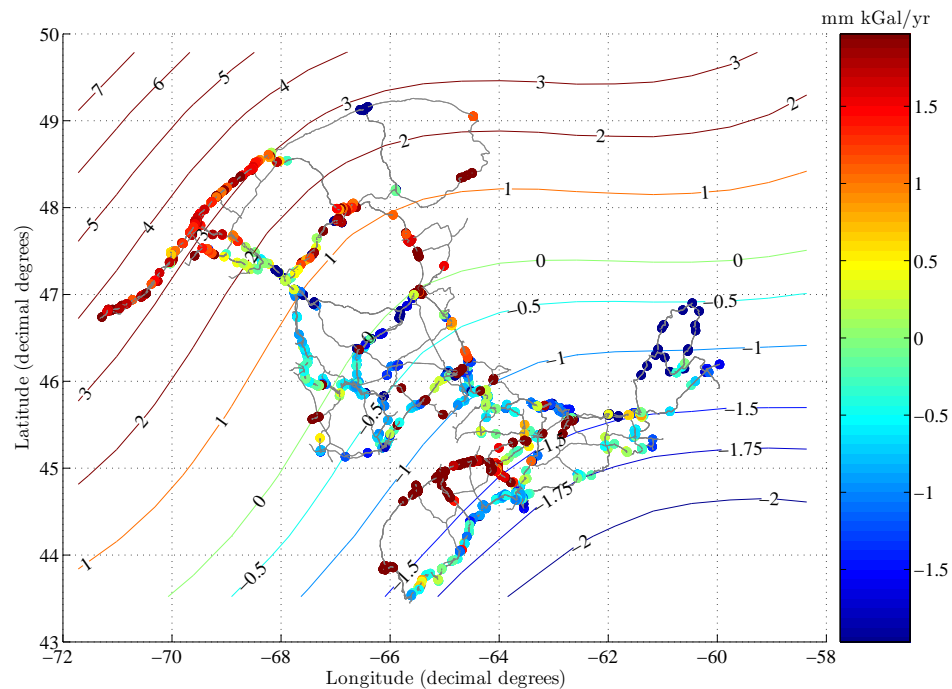
(1) Velocity estimates using velocity excess constraints from model 2 and with precision of the observations as weights



(2) Velocity estimates using velocity excess constraints from model 3 and with precision of the observations as weights



(3) Velocity estimates using velocity excess constraints from model 4 and with precision of the observations as weights



(4) Velocity estimates using velocity excess constraints from model 5 and with precision of the observations as weights

Figure 5.3: Velocities estimated from the network with the use of different *a priori* postglacial rebound models

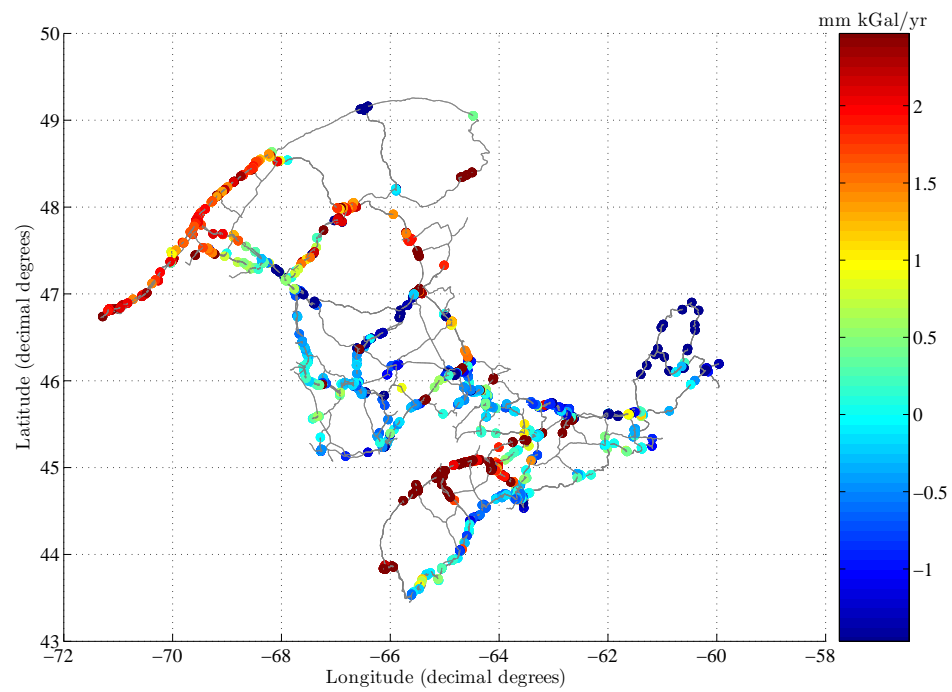


Figure 5.4: Velocities estimated from the network by fixing all the constraints with zero and using precision of the observations as weights

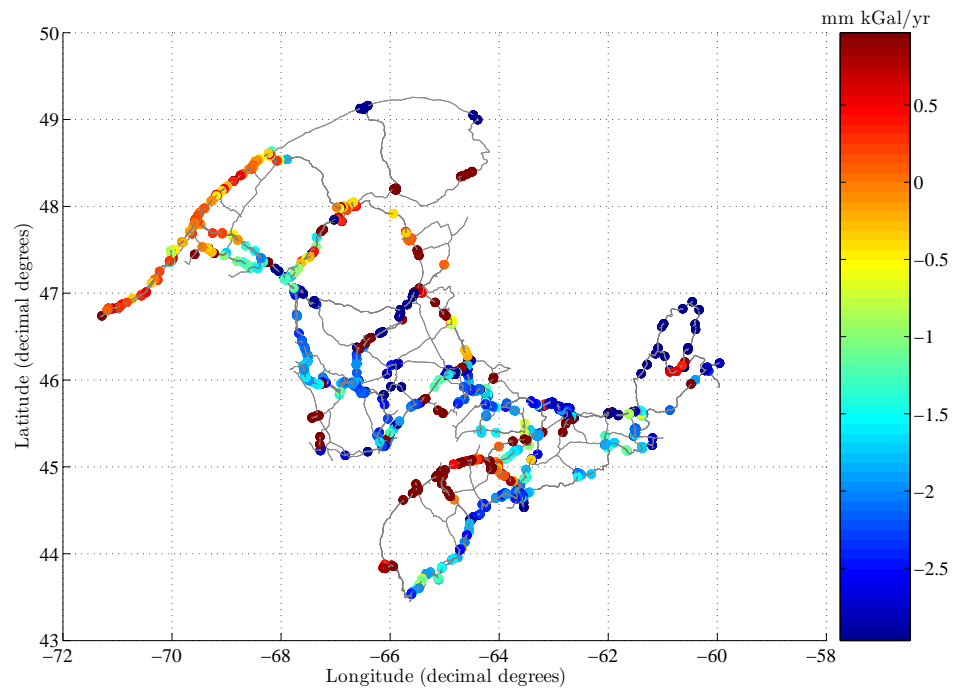
### 5.3.2 Fixing the excess constraints with heights

It was realized that if heights from a source are used as excess constraints it is easier to validate their true value and their accuracy when compared to velocities as excess constraints. Also, there are a lot of sources for obtaining reliable height values when compared to velocities, viz., GPS/levelling, and SAR/InSAR. As mentioned before, if certain precautions are taken care of, the estimated velocities can be interpreted without any bias or assumptions. Thus, it is felt that in multiple rank deficiency cases this is the best possible solution that can be arrived at.

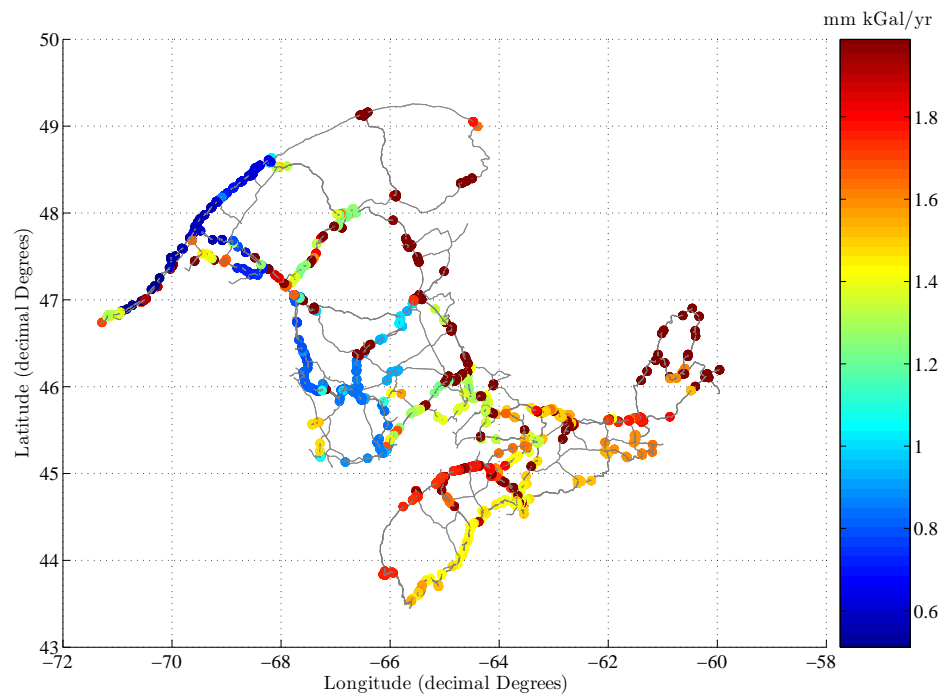
In the adjustments carried out in this research three different height sources were considered: heights calculated by Geodetic Survey Division, Natural Resources Canada, from Canadian Precise Levelling Network adjustment, heights from Shuttle RADAR Topography Mission (SRTM), and GPS/levelling heights. It can be argued that heights estimated from the network are used to estimate velocities of the same network points is incorrect, but it is performed to see what effect it has on the outcome. A better source is the digital elevation models (DEMs) obtained from SRTM data. The advantage of SRTM is that all the heights obtained are in the same year (2000), and this suits extremely well with the time discretization used for this study, which is year. Hence, there will not be any signal of vertical crustal motion. However, the serious disadvantages are that the accuracy is extremely low, viz.,  $\leq 15\text{m}$ . Further, the SRTM heights are orthometric heights based on EGM96 geoid model, which was truncated at the metre level accuracy (personal communication with Dr. A. Braun). So, it was decided not to use SRTM data for adjustment. GPS/levelling was considered as an alternative, but the idea had to be dropped because of the lack of GPS measurements on levelling benchmark stations that were needed to be fixed in the adjustment.

### 5.3.3 Discussion of the results

The least squares adjustment of the network was performed by inverting the normal matrices of the column removed design matrices. For the velocity excess constraints and the height excess constraints adjustments, the inverse of the diagonal variance-covariance matrix, formed from the precision provided with data, was used as the weight matrix. The results are shown from Figure 5.2 through Figure 5.5(1). In all those figures, if an *a priori* post glacial rebound



(1) Velocity estimates



(2) Error estimates of velocities

Figure 5.5: Velocities and their errors estimated from the network by fixing the excess constraints with heights estimated by Geodetic Survey Division, Natural Resources Canada

model is used then the isolines of the vertical rates are plotted. Since the errors of the estimates do not change with the change of the values of the constraints, only one error plot is shown for all those figures.

The units of the velocity estimates are  $\text{mm kGal}/\text{year}$ , which indicates that the crustal motion is explained in terms of variation in geopotential over time. This can be interpreted directly as  $\text{mm}/\text{year}$ , because the gravity values vary around 980 Gal ( $1 \text{ Gal} = 1 \text{ cm}/\text{s}^2$ ), which if expressed in kGal ( $1 \text{ kGal} = 1000 \text{ Gal}$ ) will be equal to 0.98kGal. If this value is rounded off, it will give unity. The other reason for using these units is that the data was received from Geodetic Survey Division, Natural Resources Canada, in the form of geopotential numbers, and it was decided not to use gravity data to convert them back to height differences, which will then introduce errors from such conversions.

The striking similarity between all the Figures 5.2 through 5.5(1) is that the color pattern and the range of the velocities are very similar. In all those figures the velocities from the cyan and blue zone of the colourmap dominate the whole network. Also, three different local patterns can be seen: 1. The red streaks on the northern part of the network, which is the region south of the St. Lawrence river; 2. the ‘A’ shaped patch of dark blue patch in the southeast corner of the network, which is the Cape Breton Island east of Nova Scotia; and, 3. the dark red ‘boomerang-shaped’ patch in the southwest parts of the network, which is Nova Scotia. Further, a close inspection of the velocity values shows the presence of uplift values next to subsidence values. This is a pattern that was shown to be in the relevelings in the trend analysis (section 4.4), where there was hardly a trend in the relative velocities and it was interpreted to be the unaccounted systematic errors or remnant errors in the observations.

Figure 5.2(2) provides an illustration of the spatial distribution of error estimates of the velocities. The figure shows a slow gradation from higher error estimates in the northern part of the network to lower error estimates in the southern part of the network. The predominant error values range from  $0.5 - 1.5 \text{ mm}/\text{yr}$ . However, the eastern boundary of the network presents itself with large error values, along with a small island of large error values in the the south eastern corner of the network. The error estimates closer to the datum points do not have smaller values, which might be due to the over-constrained adjustment of the network. In addition to the above the error estimates show the patterns that were seen in the velocity estimates plot (Figure 5.2(1)). The three different exaggerated local patterns in the velocity

estimates, which are distinct from the ‘seemingly’ global pattern of the network might also be because of the weighting of the observations. So, other weights for the observations were also used to perform the adjustment.

In order to verify if the patterns are an outcome of the post glacial rebound models, all the velocity constraints were fixed to zero. The spatial plot of the velocities is shown in Figure 5.4. The patterns show up even if the velocities are fixed with some arbitrary values. Hence, the patterns cannot be an outcome of the *a priori* models used. The other possibilities are either the variance-covariance matrix, the geometry of the network, or the nature of the vertical crustal motion. Each of these three possibilities are treated individually in the sequel.

#### 5.3.4 Results from adjustment using different weight matrices

Three different types of weight matrices were applied apart from the precision of observations supplied by Geodetic Survey Division, Natural Resources Canada with the levelling data: normalized precision of the data as weights; unit weights for all observations or, in other words, equal weights for all observations; and time interval between the observations as weights. It can be argued that all these three different weights do not provide any information on the stochastics of the information, but the concept of weights adopted in the context of this research is that weights are just numbers that provide a logical scheme to give importance to certain observations rather than others. So, in order to counteract the units of the weights formed, it is assumed that all the weights formed are normalized by their unit values ( $1\{\text{unit}\}$ ).

##### Unit weights for all observations

In the unit weighted adjustment, the velocity estimates (Figure 5.6(1)) seem to provide a decreasing gradient pattern from north to south, but still the inconsistencies remain as in the case of using precision of observations as weights. In other words, the estimates have been smoothed out throughout the network. The major changes are the red “boomerang” has disappeared; however, positive values prevail in that region. Also, in the southern most part a greenish-yellow patch can be seen, which was dark blue when the observation precision was used as weights. In addition, the mid-western boundary values have risen in their magnitude substantially – negative values have become positive values. The error estimates for the unit

weights case (Figure 5.6(2)) has shown a further shift to the higher error values, and again in the order of  $0.1 - 0.2 \text{ mm kGal/yr}$ , but this is insignificant.

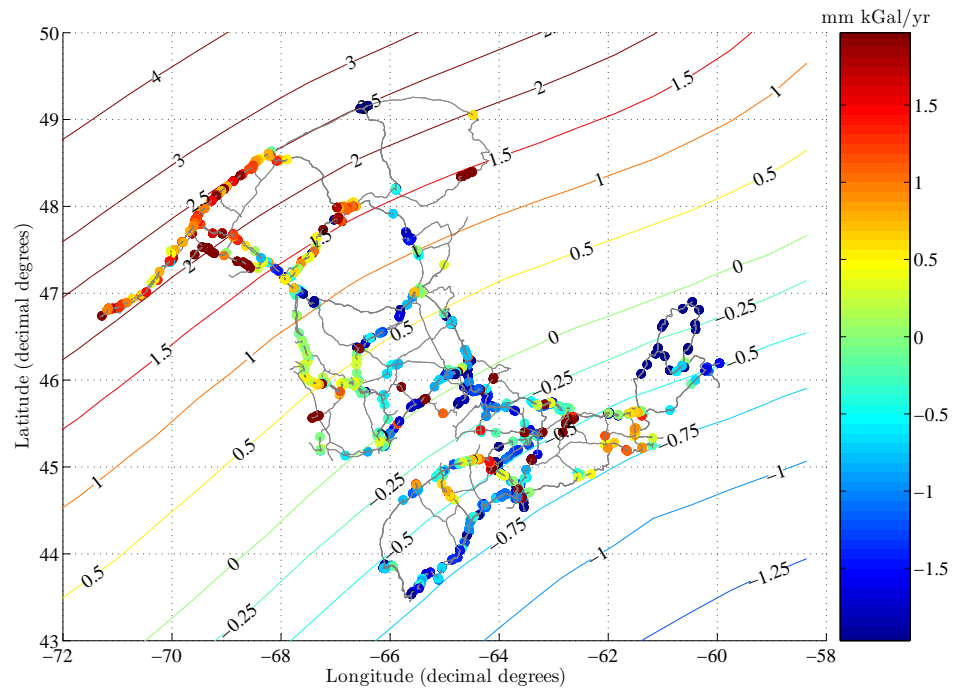
### Time interval between observations as weights

For the adjustment using the time interval between relevellings, forming the weight matrix was not straight forward. The reason is that not all the observations in the network are relevelled and hence, a different approach was required to be adopted for the single levelling lines. First the relevellings were identified and then the time difference between the relevellings were calculated. Then based on the idea that every relevelling observation holds the vertical crustal motion information from the time it was observed last time until the time the relevelling itself was measured, the observation was provided with a weight of this time difference. This is explained in Table 5.1.

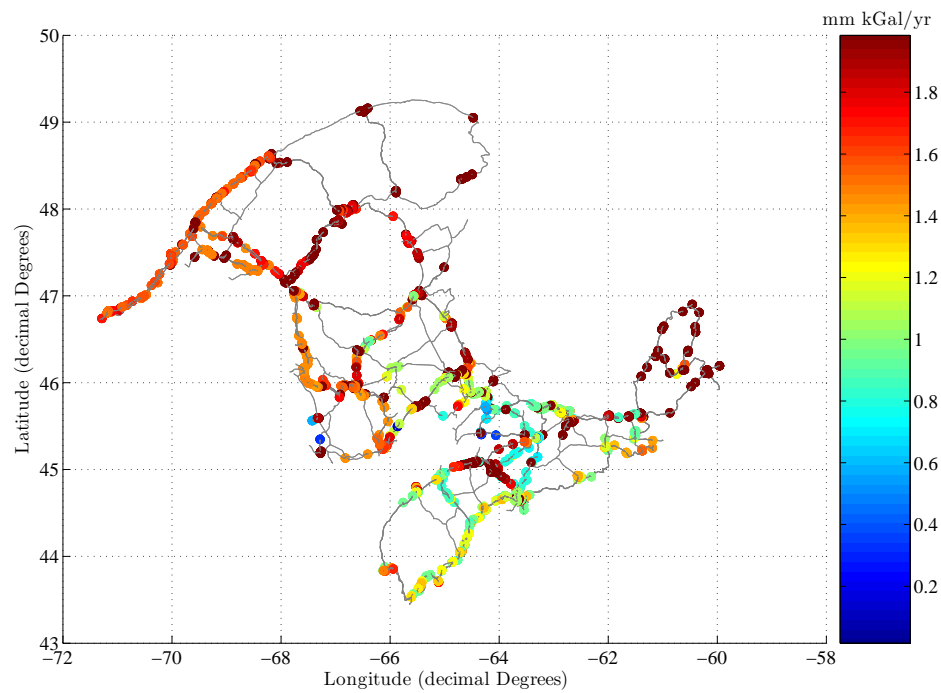
| Observations        | Time intervals  | Weights                 |
|---------------------|-----------------|-------------------------|
| $\Delta H(t_1)$     |                 | $\Delta t_{12}$         |
|                     | $t_2 - t_1$     |                         |
| $\Delta H(t_2)$     |                 | $\Delta t_{12}$         |
|                     | $t_3 - t_2$     |                         |
| $\Delta H(t_3)$     |                 | $\Delta t_{23}$         |
| $\vdots$            | $\vdots$        | $\vdots$                |
| $\Delta H(t_{n-1})$ |                 | $\Delta t_{(n-2)(n-1)}$ |
|                     | $t_n - t_{n-1}$ |                         |
| $\Delta H(t_n)$     |                 | $\Delta t_{(n-1)n}$     |

Table 5.1: Table showing the weighting scheme based on the time interval between observations for relevelling lines

However, as it can be seen in the table that a problem was encountered in assigning a

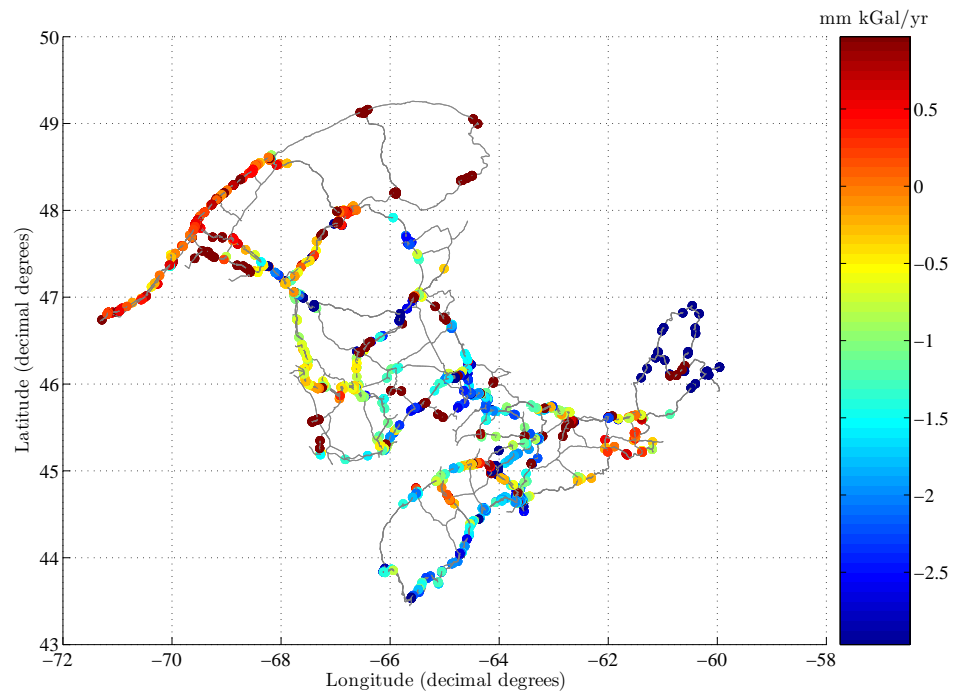


(1) Estimates of velocities

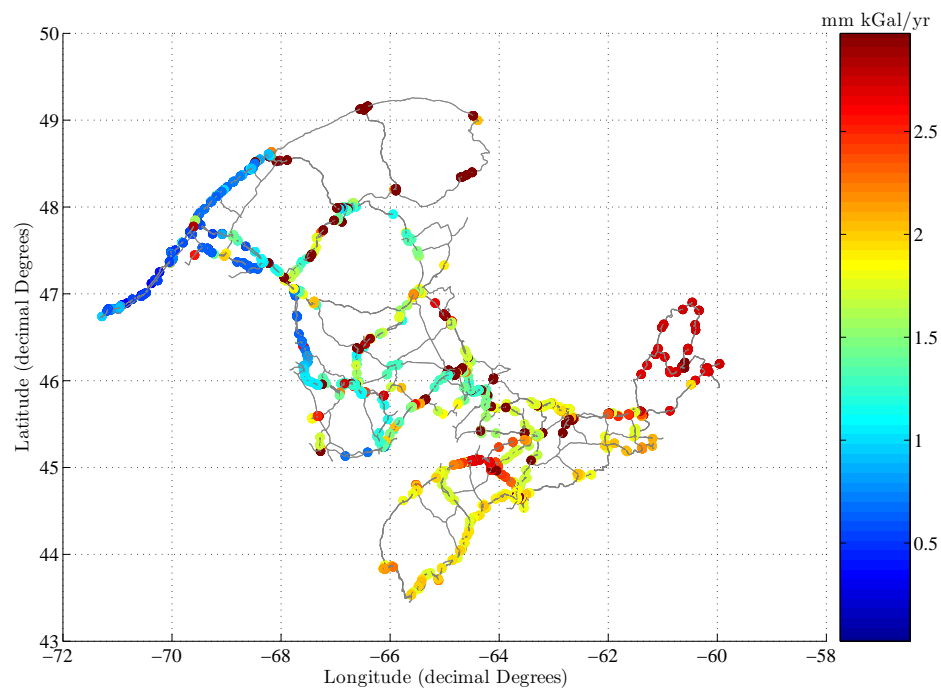


(2) Error estimates of velocities

Figure 5.6: Velocities and their errors estimated with unit weights for all observations and fixing the excess constraints with velocities from model 1



(1) Estimates of velocities



(2) Error estimates of velocities

Figure 5.7: Velocities and their errors estimated with unit weights for all observations and fixing the excess constraints with heights obtained from static adjustment by Geodetic Survey Division, Natural Resources Canada

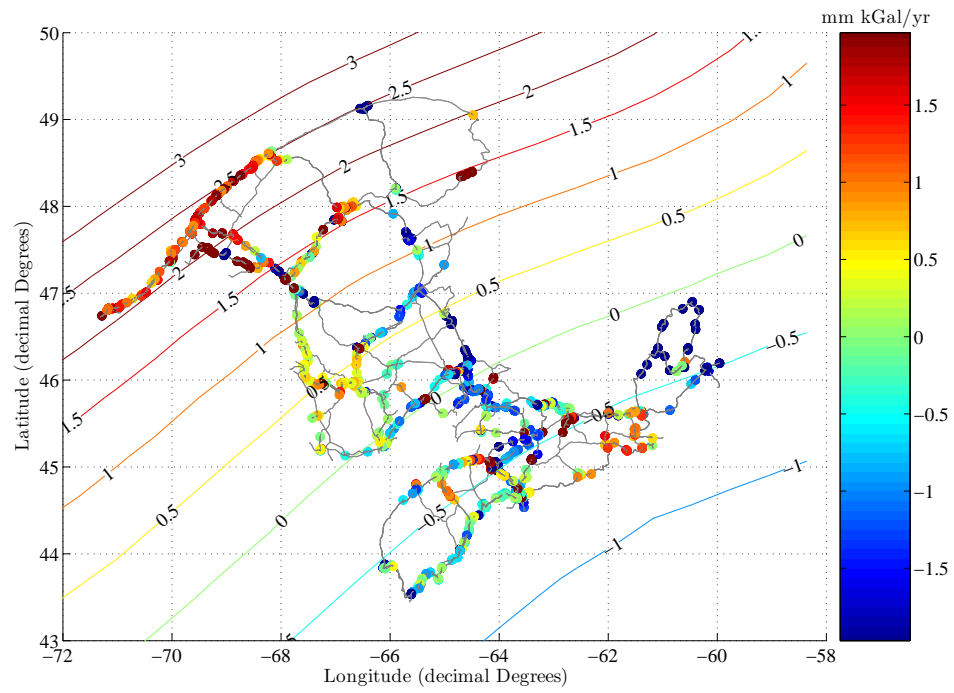
weight for the initial observation. A weight of zero cannot be applied as this will make the weight matrix singular and hence, normal matrix inversion impossible. So, it was decided to provide the first observation with the same weight as the next immediate releveling. The weight calculation can be done only when there is a releveling for an observation. If there is only a single levelling observation along a levelling line then the following method is applied. For all the observations there is a from and to point, and every point in the network has observations taken in different years. So, for every single levelling observation, the years of observation at each point involved in the particular observation are taken and sorted. Then the time difference between the year of the observation of the single levelling and the immediate year of observation before the observation of concern was calculated. This is clearly explained in Table 5.2.

| Observation          | Years of observation through each point         | Sorted years              | Weight          |
|----------------------|-------------------------------------------------|---------------------------|-----------------|
| $\Delta H_{ij}(t_4)$ | $i - t_1, t_2, t_4$<br>$j - t_2, t_3, t_4, t_7$ | $t_1, t_2, t_3, t_4, t_7$ | $\Delta t_{34}$ |

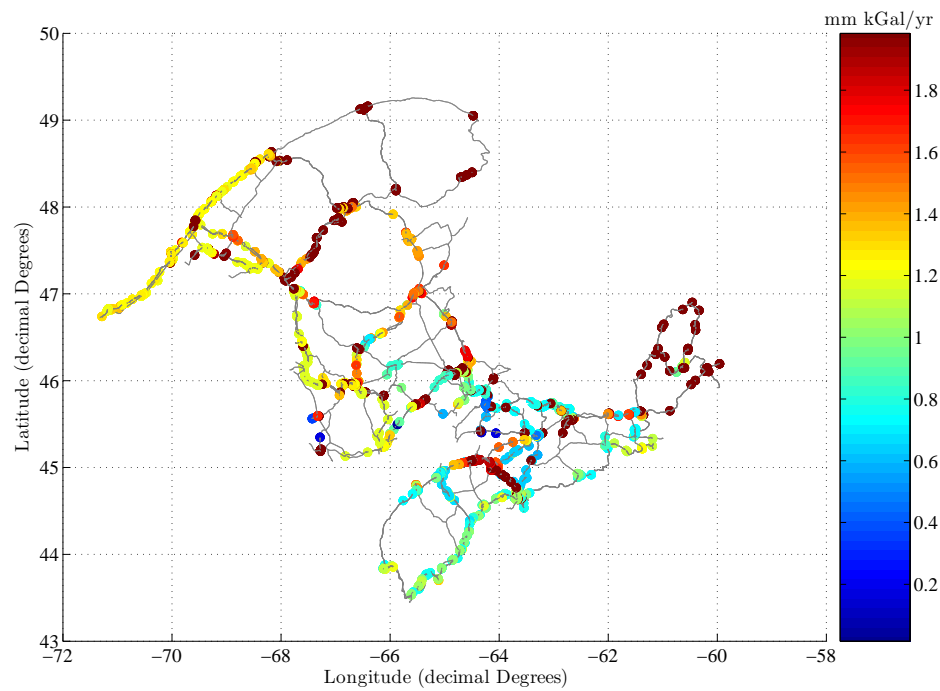
Table 5.2: Table showing the weighting scheme based on the time interval between observations for single levelling lines

The results from the adjustment with this weighting scheme are shown in Figures 5.8 and 5.9. The velocity estimates in Figure 5.8(1) show similar patterns as seen in Figure 5.6(1), but there are minor differences. The same can be said of the estimates from excess constraints fixed with heights shown in Figure 5.9(1). It can be said with confidence that the time interval weighting scheme does not influence the observations except for minor changes.

From the use of different schemes it has been established that the local patterns, described in section 5.3.3, are in fact an outcome of the weights formed from the precision values of the observations provided by the Geodetic Survey Division, Natural Resources Canada.

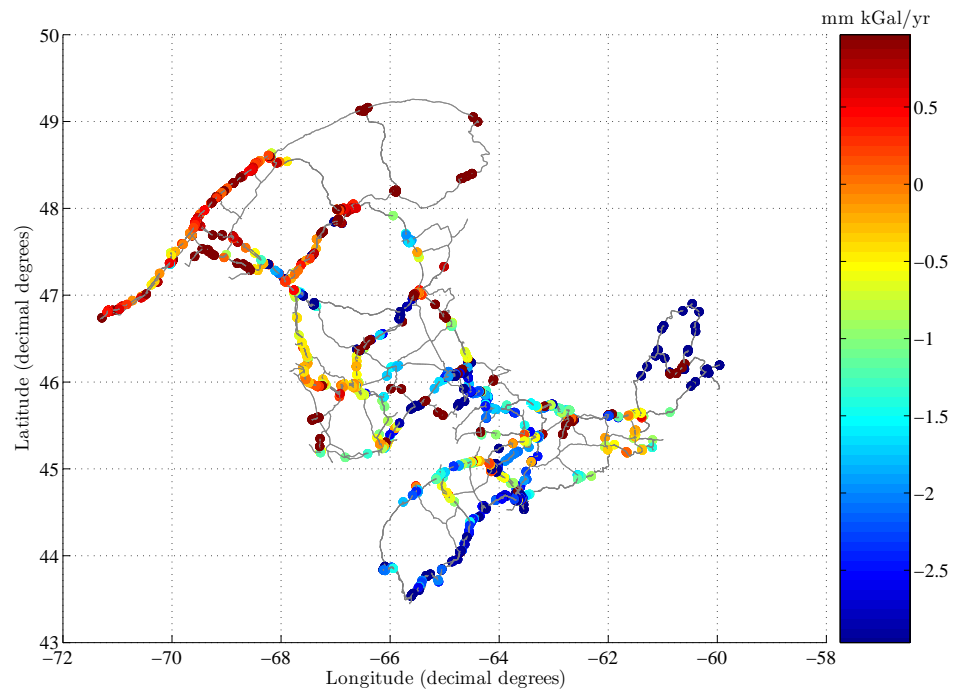


(1) Velocity estimates

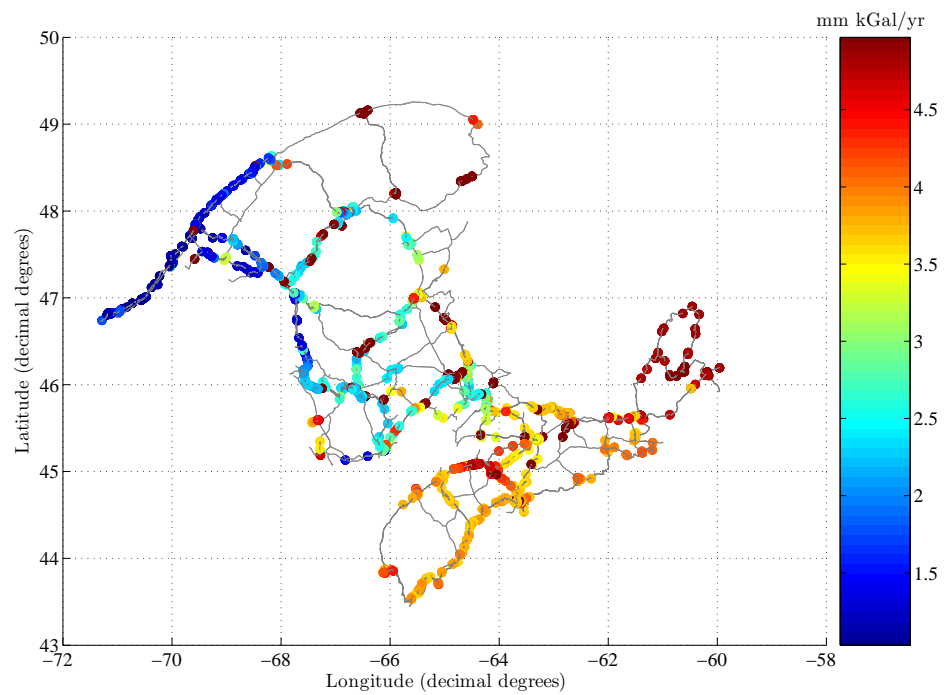


(2) Error estimates of velocities

Figure 5.8: Velocities and their errors estimated by applying time interval between observations as weights for the observations and fixing the excess constraints with velocities from model 1



(1) Estimates of velocities



(2) Error estimates of velocities

Figure 5.9: Velocities and their errors estimated with time interval between observations as weights for the observations and fixing the excess constraints with heights obtained from static adjustment by Geodetic Survey Division, Natural Resources Canada

Nevertheless, it has to be kept in mind that these precision values were carefully chosen based on field experience, instrument types used for measurement, and knowledge of local phenomena (personal communication with Mr. Véronneau).

It can be inferred from the above results that the precision weights provided with the data exaggerates the velocity estimates. However, the appearance of similar patterns inspite of the use of different excess constraints still needs to be answered. The reason being that the excess constraints were expected to behave like overconstraints and give a different distorted picture everytime, but this is not the case here. The results appear to come out of a minimum constraint adjustment, where the pattern remains the same, but with a shift depending upon the values of the constraints. This similarity in pattern could either be a response of the network geometry to the adjustment, or the nature of the vertical crustal motion itself. If the latter is true, then one major objective of the study is fulfilled.

Also, note has to be made of the pattern of the error estimates when the excess constraints are fixed with heights. The patterns in Figures 5.5(2), 5.7(2), and 5.9(2) follow a slow gradation from low error values at the North of the network to high values towards the south of the network. This gradation of error values occur only in minimum constraint adjusted networks, where the network points closer to the constrained/datum point have lower error estimates than the ones that are located away from the constrained/datum point. This is demonstrated by Baarda (1981) for a 2-D horizontal network. Thus, this provides ample proof that when the excess constraints are fixed with heights that have a nominal accuracy, they can be used to estimate vertical crustal motion rates that can be interpreted without any *a priori* geophysical/geodynamical information.

In order to support the above discussion and further analyses, Table 5.3 provides some statistics that summarize the results in Figures 5.2–5.9. The values in the table indicate that the maximum and minimum values of the velocities are large and unrealistic values, especially in the case of height excess constraints, where the values are huge. These are unrealistic considering the nature of uplift in the region. Also, the means of the parameter estimates with respect to the height excess constraints are unrealistic as well. The reason for this being that there are about 10% of the total velocity estimates, using height excess constraints, whose values are more than  $100 \text{ mm kGal/year}$ . This shoots up the mean values to unrealistic levels. However, care must be taken in interpreting the reason for these extreme

| Figure        | Ex. Cnstrnt. | Weights | Velocity (mm kGal/yr) |         |      | Std. Dev. (mm kGal/yr) |      |      |
|---------------|--------------|---------|-----------------------|---------|------|------------------------|------|------|
|               |              |         | Max.                  | Min.    | Mean | Max.                   | Min. | Mean |
| Figure 5.2(1) | V1           | P       | 46.9                  | -108.3  | 0.1  | 310.4                  | 0.0  | 2.1  |
| Figure 5.3(1) | V2           | P       | 45.8                  | -109.4  | -1.0 | 310.4                  | 0.0  | 2.1  |
| Figure 5.3(2) | V3           | P       | 47.2                  | -108.0  | 0.4  | 310.4                  | 0.0  | 2.1  |
| Figure 5.3(3) | V4           | P       | 47.1                  | -108.1  | 0.3  | 310.4                  | 0.0  | 2.1  |
| Figure 5.3(4) | V5           | P       | 47.1                  | -108.1  | 0.3  | 310.4                  | 0.0  | 2.1  |
| Figure 5.4    | Z            | P       | 47.4                  | -107.8  | 0.6  | 310.4                  | 0.0  | 2.1  |
| Figure 5.5    | H            | P       | 628.6                 | -1301.4 | 10.2 | 310.5                  | 0.0  | 2.3  |
| Figure 5.6    | V1           | U       | 56.5                  | -51.2   | 0.1  | 75.4                   | 0.1  | 2.2  |
| Figure 5.7    | H            | U       | 628.4                 | -1303.7 | 10.6 | 76.1                   | 0.3  | 2.3  |
| Figure 5.8    | V1           | Y       | 51.0                  | -86.7   | 0.4  | 161.8                  | 0.5  | 3.7  |
| Figure 5.9    | H            | Y       | 628.3                 | -1307.3 | 10.4 | 163.8                  | 0.4  | 3.9  |

Table 5.3: Statistics summarizing the results in Figures 5.2–5.9. The statistics here show the maximum, minimum, and mean values of all the estimation results: both the parameters and their error estimates. V1, V2, V3, V4, and V5 – velocities excess constraints from models 1, 2, 3, 4, and 5, respectively; H – height excess constraints; Z – zero values for all excess constraints; P – precision of observations used as weights; U – unit weights; Y – time interval between observations as weights

values. In addition to the above, it can be clearly seen from the table that other than estimates from height excess constraints rest of the means of estimates are significantly smaller than their estimated error means. This is a serious drawback if the estimates have to be interpreted geophysically. Further analysis of the estimates are provided in section 5.6.

## 5.4 Least squares error analysis

In order to understand the role of the data and the constraints and how they impact the estimated parameters, resolution matrices and redundancy matrices are analysed. These matrices are related to the comparison of *a priori* and *a posteriori* variances of the data and the parameters. These matrices provide insight into the response of the network toward the adjustment.

### 5.4.1 Resolution matrices

The term *resolution matrices* comes from the fact that these matrices resolve the contributions from data and *a priori* information on the parameters, for example excess constraints, towards the estimation of parameters. The resolution matrices are dealt with in regularization literature, where ill-conditioned matrices are regularized with the aid of *a priori* information on the parameters. The design matrices of networks are similar to ill-conditioned in that they need *a priori* information to invert their normal matrices due to the inherent rank deficiency in them. Hence, the resolution matrices will provide information on the contributions of the *a priori* information and the observations.

Recalling equation 4.9 here,

$$\hat{\mathbf{H}} = (\mathbf{A}^T \mathbf{P} \mathbf{A} + \mathbf{D} \mathbf{D}^T)^{-1} (\mathbf{A}^T \mathbf{P} \Delta \mathbf{H} + \mathbf{D} \mathbf{c}) \quad .$$

Substituting  $\mathbf{A} \mathbf{H} + \mathbf{v}$  for  $\Delta \mathbf{H}$  and  $\mathbf{D}^T \mathbf{H}$  for  $\mathbf{c}$  and taking the expectation of the estimator  $\hat{\mathbf{H}}$  gives,

$$\mathbb{E}\{\hat{\mathbf{H}}\} = (\mathbf{A}^T \mathbf{P} \mathbf{A} + \mathbf{D} \mathbf{D}^T)^{-1} (\mathbf{A}^T \mathbf{P} \mathbb{E}\{\mathbf{A} \mathbf{H} + \mathbf{v}\} + \mathbf{D} \mathbb{E}\{\mathbf{D}^T \mathbf{H}\}) \quad . \quad (5.1)$$

On simplification equation (5.1) gives,

$$\mathbb{E}\{\hat{\mathbf{H}}\} = (\mathbf{A}^T \mathbf{P} \mathbf{A} + \mathbf{D} \mathbf{D}^T)^{-1} (\mathbf{A}^T \mathbf{P} \mathbf{A} \mathbf{H} + \mathbf{D} \mathbf{D}^T \mathbf{H}) \quad (5.2)$$

$$\mathbf{H} = (\mathbf{A}^T \mathbf{P} \mathbf{A} + \mathbf{D} \mathbf{D}^T)^{-1} (\mathbf{A}^T \mathbf{P} \mathbf{A} + \mathbf{D} \mathbf{D}^T) \mathbf{H} \quad . \quad (5.3)$$

In the above equation (5.3), the R.H.S. of the equation can be split up into two matrices, viz.,

$$\mathbf{R}_y = (\mathbf{A}^T \mathbf{P} \mathbf{A} + \mathbf{D} \mathbf{D}^T)^{-1} \mathbf{A}^T \mathbf{P} \mathbf{A} \quad (5.4)$$

$$\mathbf{R}_x = (\mathbf{A}^T \mathbf{P} \mathbf{A} + \mathbf{D} \mathbf{D}^T)^{-1} \mathbf{D} \mathbf{D}^T \quad . \quad (5.5)$$

The matrices  $\mathbf{R}_y$  and  $\mathbf{R}_x$  are the resolution matrices of the observations and the *a priori* information, respectively. The resolution matrices are square matrices with the size of the number of parameters required to be estimated.

The implication from equation (5.3) is that

$$(\mathbf{A}^T \mathbf{P} \mathbf{A} + \mathbf{D} \mathbf{D}^T)^{-1} (\mathbf{A}^T \mathbf{P} \mathbf{A} + \mathbf{D} \mathbf{D}^T) = \mathbf{I} \quad , \quad (5.6)$$

which further implies,

$$\mathbf{R}_y + \mathbf{R}_x = \mathbf{I} \quad . \quad (5.7)$$

The diagonal elements of the resolution matrices vary between 0 and 1. If the values of  $\text{diag}(\mathbf{R}_y)$  are 1 then those parameters are purely estimated by the observations and if the values of  $\text{diag}(\mathbf{R}_x)$  are 1 then those parameters are completely estimated by the *a priori* information provided. If the values are between 0 and 1 then they suggest the percentage contribution of the observations and the *a priori* information.

In a minimum constraint datum adjustment, the parameters that are fixed, i.e. the parameters through which the *a priori* information is supplied, are solely determined by the parameter side, and the rest of the parameters are solely determined by the observations. This means that for the fixed parameters the  $\mathbf{R}_x$  values are 1, and the  $\mathbf{R}_y$  values are 0, and vice-versa for the other parameters. In an overconstraint network adjustment, the parameters that are fixed are partially determined by the *a priori* information and partially by the observations, and the rest of the parameters are solely determined by the observations. This means that the  $\mathbf{R}_x$  and  $\mathbf{R}_y$  will not be 1 and 0 respectively for the fixed parameters, but will add up to unity. A numerical example is shown for the static levelling network of Figure 4.1(2). Figure 5.10 shows the numerical results, which stand proof to the explanation given above.

Figure 5.11 shows the diagonal values of the resolution matrices with different datum matrices, viz., velocity excess constraint (Figure 5.11(1)) and height excess constraint (Figure 5.11(2)) datum matrices. It can be clearly seen that the adjustments exhibit minimum

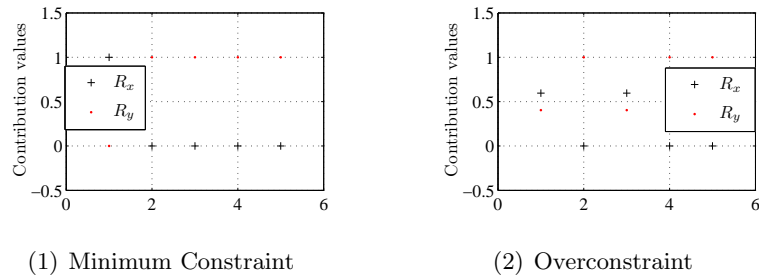


Figure 5.10: Resolution matrices of minimum and overconstraint adjustments of the static leveling network in Figure 4.1(2). For the minimum constraints adjustment, point 1 was fixed, and for overconstraints adjustment, point 3 was fixed additionally

constraint like behaviour, whence overconstraint behaviour is expected. However, the network shows overconstraint behaviour at two points. The explanation for this comes from the fact that if the subset matrix of the design matrix was selected the least singular value of the SVD of the subset and its second-least singular value had a difference in the order of  $10^2$ . This blew up the error estimates of the parameters and hence, one more parameter was required to be fixed. This is the reason for the partial values at the two points.

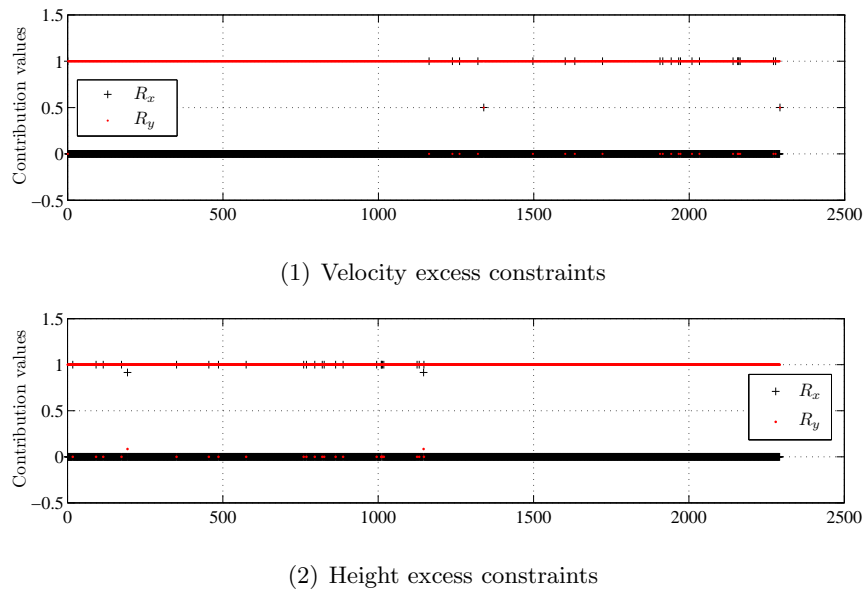
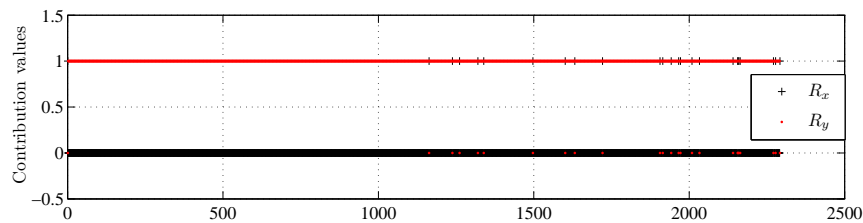


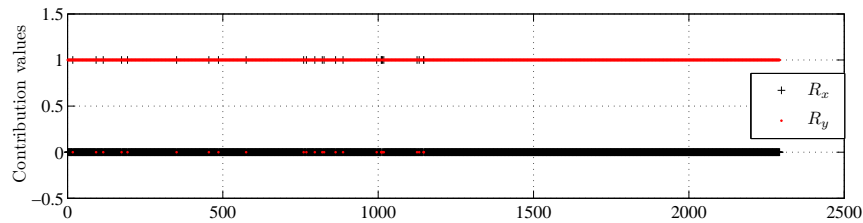
Figure 5.11: Diagonal elements of the resolutions matrices of the observations ( $R_y$ ) and the parameters ( $R_x$ ) with precision of the observations as weights

It can be seen that there is a slight difference in the way the excess constraints are treated,

if heights are fixed as excess constraints and if velocities are fixed as excess constraints. When heights are fixed, the contribution values approach 1, but when velocities are fixed the contribution values are shared half and half by the constraints and the observations. According to Zelt (1999), if the contribution values exceed 0.5–0.7 then those parameters can be considered to be fully estimated by the parameters fixed or observations, wherever the value occurs. Thus, in the case concerned the two height excess constraints, showing partial contribution values, are solely estimated by the heights fixed, while the two velocity constraints, exhibiting partial contribution values, have contribution from both fixed parameters and observations. The implications are that the height excess constraints distort the network to a lesser extent than the velocity excess constraints.



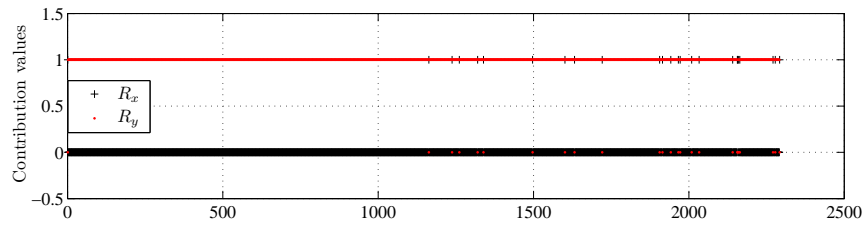
(1) Velocity excess constraints



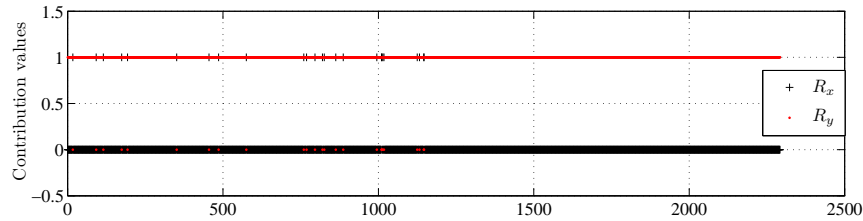
(2) Height excess constraints

Figure 5.12: Diagonal elements of the resolutions matrices of the observations ( $\mathbf{R}_y$ ) and the parameters ( $\mathbf{R}_x$ ) with unit weights for all observations

In Figures 5.12 and 5.13, where different weight matrices are applied, it is clearly seen that there are no partial resolution values, which clearly indicates that the network behaves like a group of minimum constraint networks. This also implies that the behaviour of the network in Figure 5.11, with partial resolution values, is a consequence of the weight matrices used and not the rank deficient network itself. Nevertheless, it can be said with adequate confidence that the behaviour of the network adjustment being close to the minimum constraint adjustment



(1) Velocity excess constraints



(2) Height excess constraints

Figure 5.13: Diagonal elements of the resolutions matrices of the observations ( $R_y$ ) and the parameters ( $R_x$ ) with heights as excess constraints

behaviour is an explanation to the constancy in pattern of the occurrence of vertical crustal motion estimates. In other words, it can be recalled that when there is a multiple rank deficiency in the kinematic network then there are groups in the network, and they can be adjusted individually as well (section 3.3.3). Hence, the similarity in the vertical crustal motion pattern could be because of this group behaviour of multiple rank deficient kinematic networks. The derivations for the resolution matrices explained in this section were all followed based on Sneeuw (2000).

#### 5.4.2 Redundancy matrices

The advantage of least squares estimation is the ability of the technique to utilize the redundancy in the observations, i.e. the excess observations, to cross-check the observations for their errors. The utilization of the excess observations in a geodetic network in general, depends on the geometry of the network. The tool that provides insight into whether the observations are cross-checked by other observations connected to them is the *redundancy matrix*.

Recalling the observation equation of the kinematic levelling network (4.16),

$$\Delta \mathbf{H}(t) = \mathbf{A} \mathbf{H} + \boldsymbol{\epsilon} \quad .$$

After applying least squares estimation the estimated residuals become,

$$\hat{\boldsymbol{\epsilon}} = \Delta \mathbf{H}(t) - \mathbf{A} \hat{\mathbf{H}} \quad (5.8)$$

$$\hat{\boldsymbol{\epsilon}} = \Delta \mathbf{H}(t) - \Delta \hat{\mathbf{H}}(t) \quad . \quad (5.9)$$

Applying the variance-covariance propagation law for the residuals gives the variance-covariance matrix of  $\hat{\boldsymbol{\epsilon}}$ ,

$$\mathbf{Q}_{\hat{\boldsymbol{\epsilon}}} = \mathbf{Q}_{\Delta H} - \mathbf{Q}_{\Delta \hat{H}} \quad (5.10)$$

$$\mathbf{Q}_{\hat{\boldsymbol{\epsilon}}} = \mathbf{Q}_{\Delta H} - \mathbf{A}(\mathbf{A}^T \mathbf{P} \mathbf{A} + \mathbf{D} \mathbf{D}^T)^{-1} \mathbf{A}^T \quad (5.11)$$

$$\mathbf{Q}_{\hat{\boldsymbol{\epsilon}}} = \mathbf{Q}_{\Delta H} - \mathbf{A} \mathbf{Q}_{\hat{H}} \mathbf{A}^T \quad . \quad (5.12)$$

Post-multiplying  $\mathbf{P}$  to equation (5.12) gives the redundancy matrix,

$$\mathbf{Q}_{\hat{\boldsymbol{\epsilon}}} \mathbf{P} = \mathbf{Q}_{\Delta H} \mathbf{P} - \mathbf{A} \mathbf{Q}_{\hat{H}} \mathbf{A}^T \mathbf{P} \quad (5.13)$$

$$\mathbf{Q}_{\hat{\boldsymbol{\epsilon}}} \mathbf{P} = \mathbf{I} - \mathbf{A} \mathbf{Q}_{\hat{H}} \mathbf{A}^T \mathbf{P} \quad (5.14)$$

$$\mathbf{Q}_{\hat{\boldsymbol{\epsilon}}} \mathbf{P} = \mathbf{I} - \mathbf{Q}_{\Delta \hat{H}} \mathbf{P} \quad (5.15)$$

The redundancy matrix is a square matrix with the dimensions of the number of observations as it is derived from the variance-covariance matrix of the residuals. The diagonal elements of the redundancy matrix are called the *local redundancy numbers*, which provide information on whether the particular observation was cross-checked by the redundancy in the network. The diagonal elements can be expressed in the following manner based on equation (5.15) (Sneeuw, 2000),

$$r_i = 1 - \frac{\sigma_{\Delta \hat{H}}^2}{\sigma_{\Delta H}^2} \quad , \quad (5.16)$$

where

$r_i$  is the local redundancy number, and

$\sigma^2$  are the variances of the estimates and the observations.

Equation (5.16) indicates that the values of the local redundancy number are a ratio of the change in variance of the observations before and after estimation and the variance

before estimation. The values of the local redundancy number vary from 0 to 1, where 0 indicates no improvement from the adjustment, i.e. the observation was not cross-checked by the redundancy in the network, and 1 indicates the opposite.

A careful look at the expanded form of the redundancy matrix in equation (5.13) will show that the *a posteriori* variance-covariance matrix is strongly dependent on the network geometry, because it is a combination of the Laplacian matrix and the edge-edge adjacency matrix  $\mathbf{AA}^T$ . Thus, this expanded form of the redundancy matrix is ample indication of the fact that the matrix acts as an indicator of how the geometry adjusts and improves the observations closer to their true values. Ding & Coleman (1996) provide a technique to utilize this information in finding multiple gross errors. A remarkable property of the redundancy matrix is that the trace of the redundancy matrix provides the number of redundant observations in the network (Sneeuw, 2000).

$$\text{tr}(\mathbf{Q}_{\hat{\epsilon}}\mathbf{P}) = m - n + d \quad (5.17)$$

$$\sum_{i=1}^m r_i = m - n + d \quad , \quad (5.18)$$

where

$m$  is the number of observations,

$n$  is the number of parameters, and

$d$  is the datum (rank) deficiency of the network design matrix.

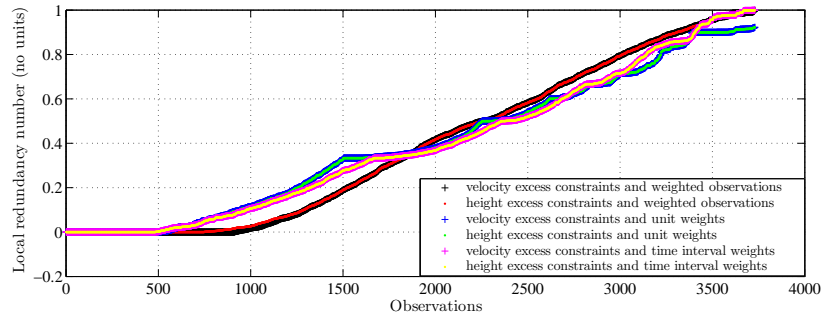


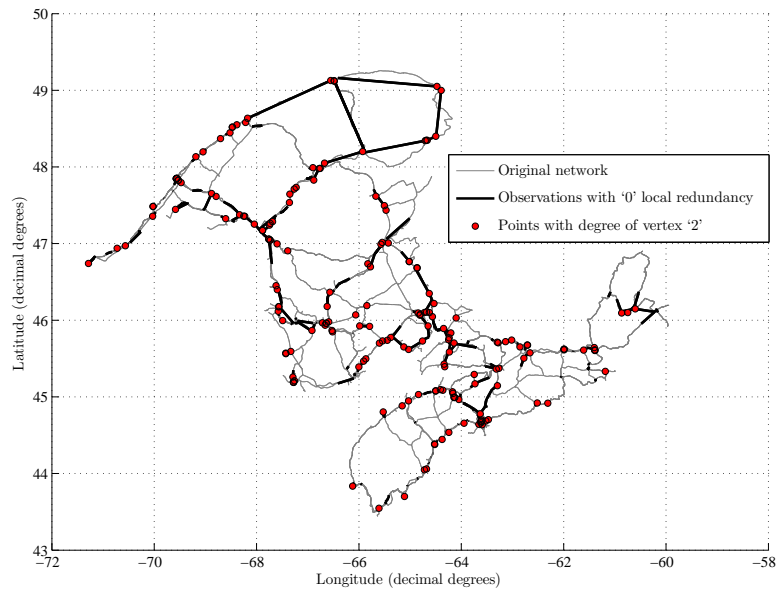
Figure 5.14: Local redundancy values of each of the observations in the network

Figure 5.14 shows the local redundancy numbers when heights and velocities are used as excess constraints. Also, the three different weight matrices applied for the estimation were taken into consideration. The figure shows that there is no difference in using heights

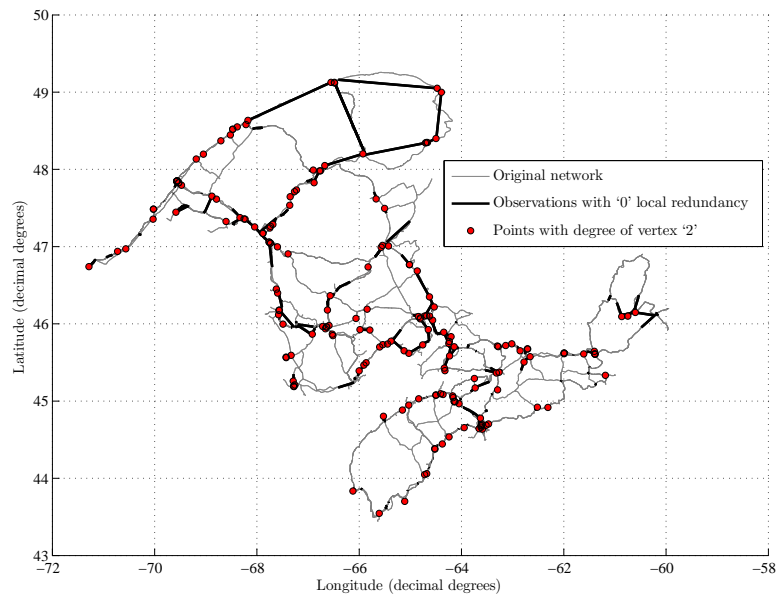
as excess constraints or velocities as excess constraints as there is only a marginal difference between the local redundancy numbers obtained from the two different types of adjustments. There is a visible difference only when precision of observations are used as weights. The difference is thought to come from the influence of the variance-covariance matrix of the estimated parameters  $(\mathbf{A}^T \mathbf{P} \mathbf{A})^{-1}$  which is where the choice of excess constraints play a huge part. There is a difference between using different weight matrices, which indicates that the primary influence on the local redundancy of the observations is the stochastic information provided through the weight matrices. The geometry of the network only exhibits a secondary effect.

The figure shows that about 1200 observations have a local redundancy number less than 0.1 when the precision of the observations is used as weights, which indicates that one third of the network had hardly undergone any improvement. However, this is not the case with the other two weighting schemes. They behave very similar to each other, and they show an improvement in the error estimates of those adjusted observations that had a local redundancy number of 0 with the precision of observations as weights. The possible reason could be that the stochastic information provided by the precision of observations was true and the adjustment could not improve it. The reason could not be the network geometry, because if it was the primary influence then no matter what stochastic information is used the local redundancy numbers do not change. However, for the little less than 500 observations that show 0 local redundancy, no matter what stochastic information is provided. The primary influence for such a behaviour is the geometry of the network, and these observations will be adjusted without consideration of the network. The spatial plots (Figures 5.15, 5.16, and 5.17) also prove this point as some of the levelling lines can be seen in all the spatial plots.

The spatial distribution of these observations are shown in Figures 5.15, 5.16, and 5.17 along with the points having a degree of vertex value of 2 without the relevellings taken into consideration. The spatial distribution shows that the observations with 0 local redundancy are scattered all over the network and most of these observations originate in a point with degree of vertex 2. Thus, this proves the point that the degree of vertices of the underlying simple graph of a kinematic levelling network play a vital role in predicting how well conditioned the network is to provide reliable estimates of the parameters as mentioned in pre-adjustment analysis. Further, on a closer look at these observations in the spatial plots

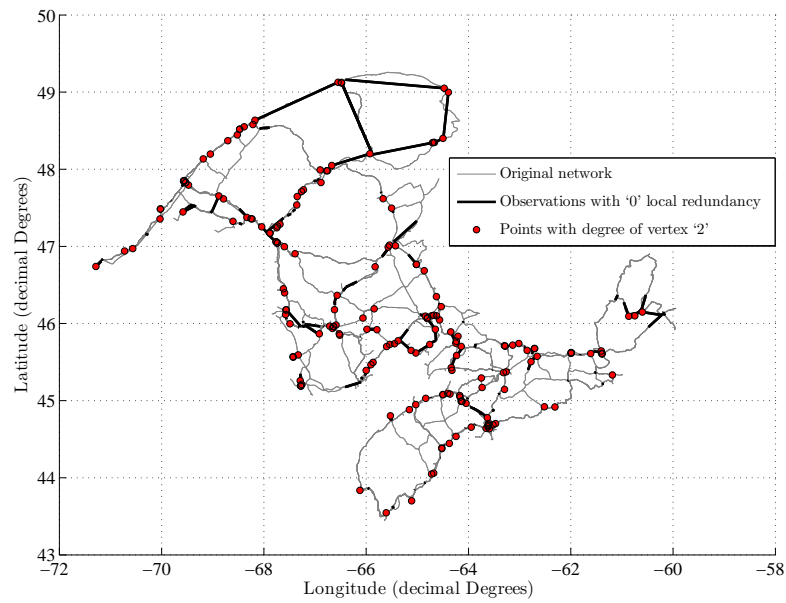


(1) Excess constraints fixed with velocities

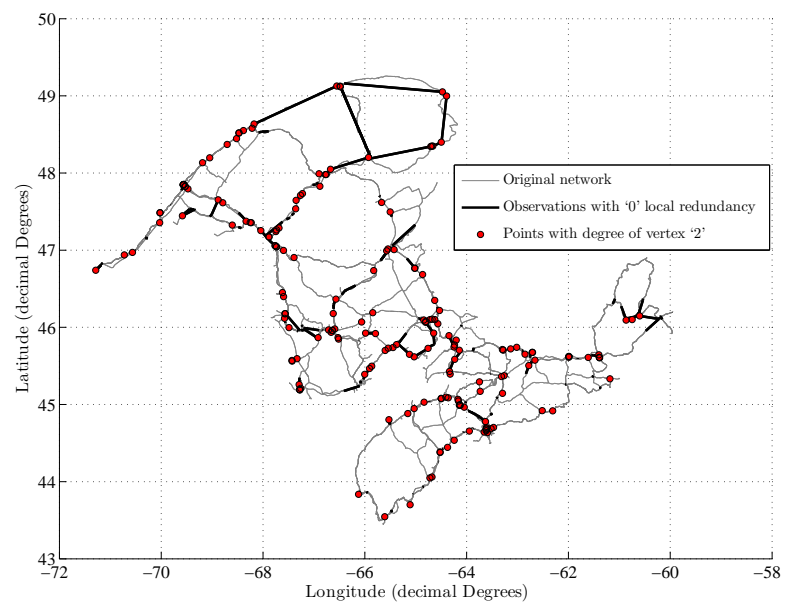


(2) Excess constraints fixed with heights

Figure 5.15: Spatial plot showing observations with a local redundancy value of '0', estimated with the precision of the observations as the weights, and network points with a degree of vertex of '2'

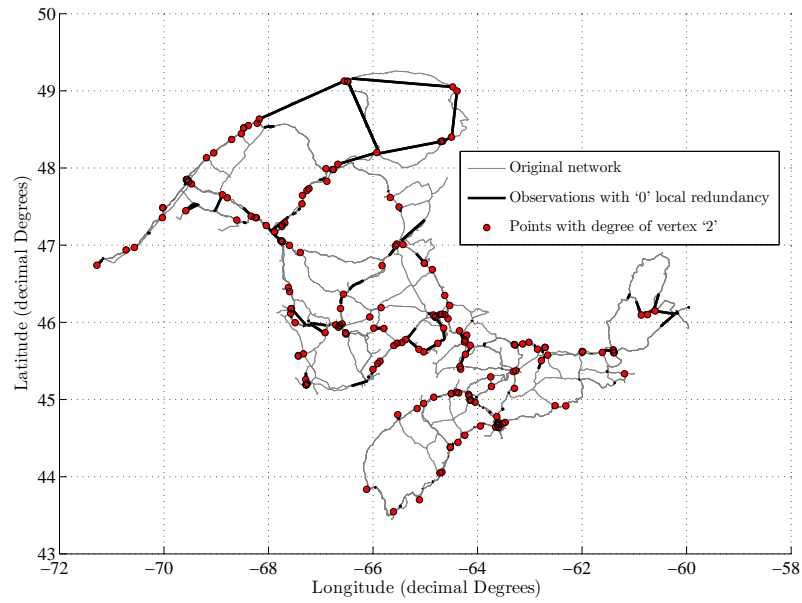


(1) Excess constraints fixed with velocities

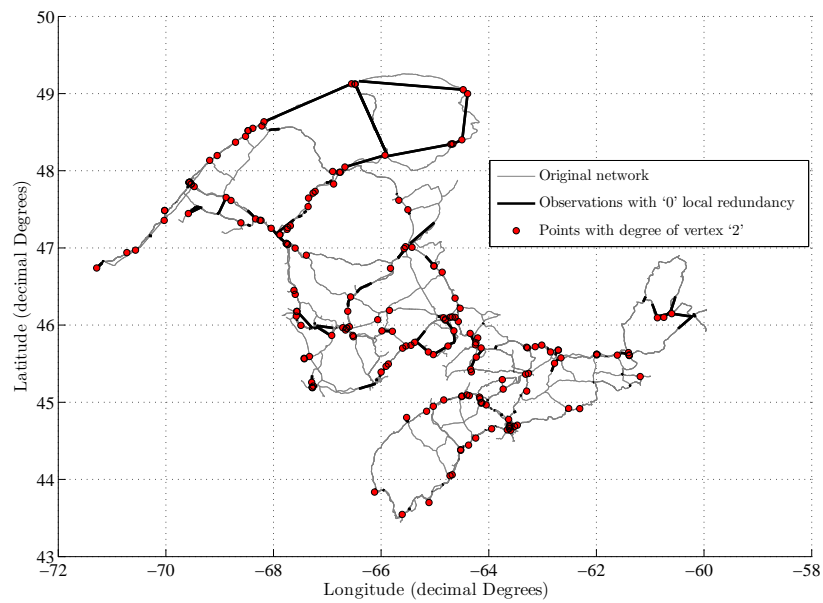


(2) Excess constraints fixed with heights

Figure 5.16: Spatial plot showing observations with a local redundancy value of '0', estimated with unit weights for all observations, and network points with a degree of vertex of '2'



(1) Excess constraints fixed with velocities



(2) Excess constraints fixed with heights

Figure 5.17: Spatial plot showing observations with a local redundancy value of '0', estimated with the time interval between observations as the weights, and network points with a degree of vertex of '2'

of velocities suggests that the points involved with these observations often have an outlier as their estimate. This strongly emphasizes that the constancy in pattern is mainly due to the behaviour of the network similar to a minimum constraint network.

## 5.5 Statistical testing of the observations

According to Baarda & Alberda (1962), the geodetic adjustment theory based on least squares extends in itself into statistical tests. A geodetic adjustment procedure based on least squares can be considered complete only after proper statistical testing of the observations is carried out because of the fact that the least squares method is very sensitive to large random errors in observations. If these large errors are not identified and a proper action is not taken then the parameter estimates can be unrealistic. The action that is usually taken on erroneous observations is to remove them from the network and perform a readjustment. However, in the present case statistical testing is performed for the sake of the completeness of the adjustment rather than detection of outliers. The reason is that it is felt that the network is fragile and any further removal of observations would mean degradation of the fragile network, which is not favoured. So, the observations that were found to be erroneous were down-weighted; however, an effective down-weighting of the observations made the weight matrices singular. Hence, the detected outliers are only listed rather than removed and readjusted. Here, two basic statistical tests were applied, viz., Baarda's *data snooping*, and Pope's *tau test*.

### 5.5.1 Baarda's data snooping

Baarda's data snooping test can be applied only when the *a priori* variance-covariance information is close to the truth, because according to Baarda & Alberda (1962), realistic numerical weight values are essential for the purposes of mathematical statistical tests they have proposed. According to this statement, data snooping can be performed only on the adjustment that used the precision of observations supplied by Geodetic Survey Division, Natural Resources Canada, as weights because of the fact that these weights were prepared based on the stochastics of levelling observations. The time weights do not represent any stochastic, but they are logical weight values. Figure 5.18 shows the ratio between the test static of the residual of every observation and the critical value for the test. The observations

outside the black lines are the erroneous observations. Here, there are close to 500 erroneous observations in the case with velocity excess constraints. This number reduces to half when the excess constraints are fixed with heights.

$$T_i = \frac{\hat{\epsilon}_i}{\sqrt{Q_{\hat{\epsilon}_{ii}}}} , \quad (5.19)$$

where

$T_i$  is the test statistic,

$\hat{\epsilon}_i$  is the estimated residual of the observation  $i$ , and

$Q_{\hat{\epsilon}_{ii}}$  is the estimated variance of the residual.

The test statistic is tested against a critical value  $N_q$  taken from a normal distribution table with a level of significance of 1%.

$$N_q = N_{1-\frac{\alpha}{2}} , \quad (5.20)$$

where

$N_{1-\frac{\alpha}{2}}$  follows the standard *normal distribution curve*  $N(0, 1)$ , and

$\alpha$  is the level of significance (Rizos, 1999).

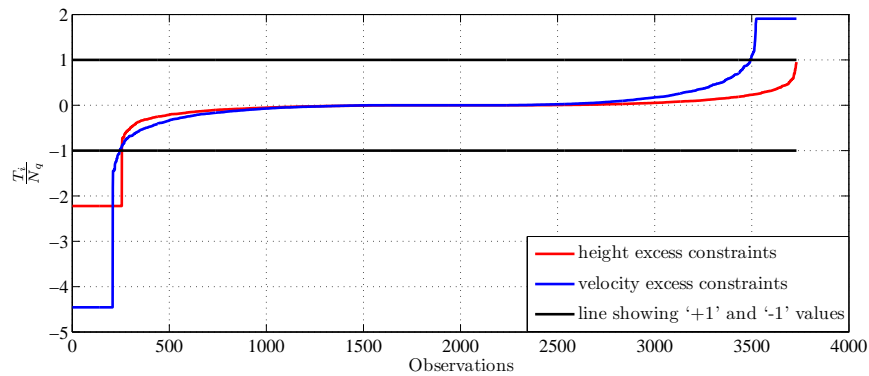


Figure 5.18: Baarda's data snooping performed on the adjusted residuals that used the precision of observations as the weight values. Figure shows the ratio between the test static of every individual residual and the critical value. Values ' $> 1$ ' and ' $< -1$ ' are the erroneous observations

The values of estimated residuals depend heavily on the constraints used. This is far more critical in the case of excess constraint adjustments than in minimum constraint adjustment

because, if incorrect set of excess constraint values are used then they will produce distortions. Hence, this results in big residuals even for error-free observations, which then will be detected by the statistical tests as errors. Also, incorrect excess constraints can hide the erroneous observations. Since the Baarda test also heavily depends on the *a priori* variance-covariance matrix, incorrect or unrealistic variance-covariance matrix entries can lead to unreliable results.

In the case under consideration, the weight matrix is the same for both adjustments performed, but the excess constraint values differed. Also, height excess constraints are clearly closer to reality than the velocity excess constraints, eventhough the height excess constraints contain unaccounted vertical crustal motion and other systematic errors. Thus, the reduction in the number of erroneous observations can be attributed to the better fit of the height excess constraints than the velocity excess constraints.

### 5.5.2 Pope's $\tau$ -test

Pope's  $\tau$ -test comes into play when the sample variance-covariance information is used, or if the *a priori* variance factor ( $\sigma_0^2$ ) is not known. Thus, in the case with precisions as observation weights, the true variance factor is not known, and in the unit weights and time interval as weights cases, the weights themselves are not true weights. So, the  $\tau$ -test can be applied to all the three weight matrices to identify erroneous observations. Figure 5.19 shows the  $\tau$ -test values for all the different adjusted residuals estimated. The figure clearly shows that there are less erroneous observations when unit weights and time intervals are used as weights.

$$T_i = \frac{\hat{\epsilon}_i}{\sqrt{\hat{\sigma}_0^2 Q_{\hat{\epsilon}_{ii}}}} \quad (5.21)$$

$$\hat{\sigma}_0^2 = \frac{\hat{\epsilon}^T \mathbf{P} \hat{\epsilon}}{m - n + d} \quad , \quad (5.22)$$

where

$\sigma_0^2$  is the estimated variance factor.

The test statistic is tested against a critical value  $q$  taken from a  $\tau$  distribution table with a

level of significance of 1%.

$$\begin{aligned}\tau_q &= \tau_{1-\frac{\alpha}{2}, m-n+d} \\ &= \sqrt{\frac{(m-n+d) \times t_{1-\frac{\alpha}{2}, m-n+d-1}^2}{(m-n+d-1) + t_{1-\frac{\alpha}{2}, m-n+d-1}^2}},\end{aligned}\quad (5.23)$$

where

$t$  is the  $t$ -distribution table values for the given degrees of freedom and the level of significance (Gökap & Boz, 2005).

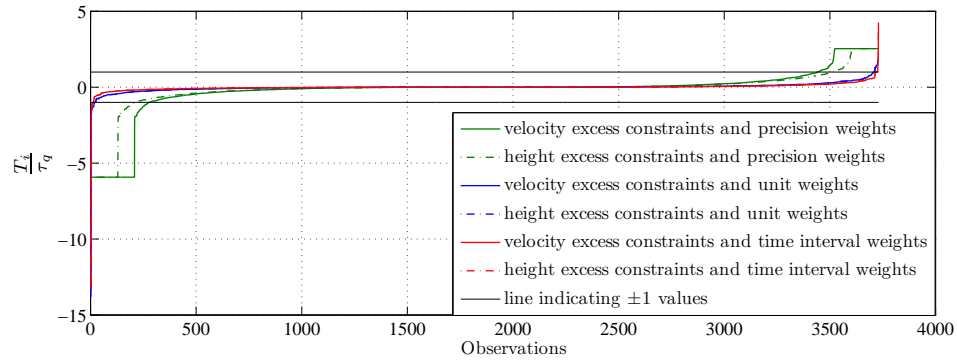


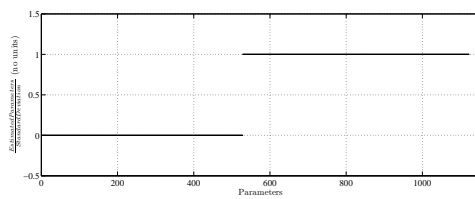
Figure 5.19:  $\tau$ -test performed on all adjusted residuals estimated using different weight matrices. Figure shows the ratio between the test static of every individual residual and the critical value. Values ' $> 1$ ' and ' $< -1$ ' are the erroneous observations.

The  $\tau$ -test completely relies on the residuals because of the fact that the variance factor used for the scaling of the *a priori* variance-covariance matrix is computed from the residuals (equation (5.22)). So, the results are purely an indication of the fit or misfit of the excess constraints used here. In that sense the results show that if using velocity excess constraints and precision weights, there are more outliers, and hence a larger misfit. However, Figure 5.19 also indicates that when the unit weight matrix and the time interval based weight matrices are used, a difference in the use of constraints is hardly visible in the detection of erroneous observations.

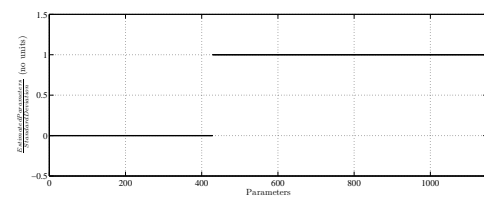
## 5.6 Statistical significance of the estimated parameters

The statistical significance of the parameters is calculated by taking the ratio of the estimated parameters and the corresponding estimated errors of the parameters. This is equivalent to

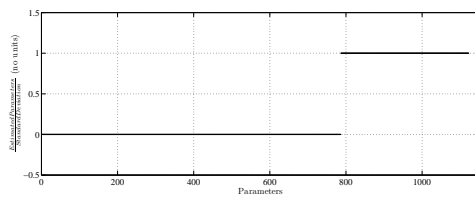
calculating the  $1\sigma$  significance test of the estimated parameters as the errors are normally distributed. In Figure 5.20, the plots indicate values of 0 and 1 for the estimated parameters. The 0 values indicate that the parameters are insignificant with respect to their estimated error values, and the 1 values indicate that the estimated parameters are significant. This is a very simple test, but clearly shows the statistical significance of the estimated parameters. This test has been performed on all the combinations of excess constraints and different weight matrices.



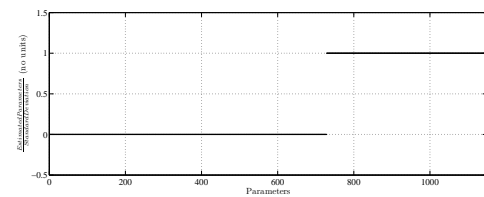
(1) Velocity excess constraints; Precision of observations as weights



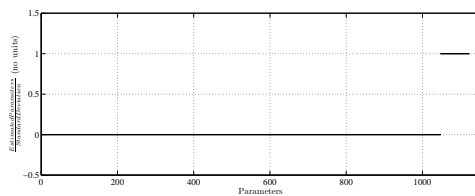
(2) Height excess constraints; Precision of observations as weights



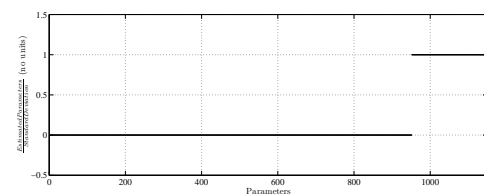
(3) Velocity excess constraints; Unit weights



(4) Height excess constraints; Unit weights



(5) Velocity excess constraints; Time interval as weights



(6) Height excess constraints; Time interval as weights

Figure 5.20: The plots indicate the ratio between the parameter estimates and their error estimates, which is being used as an indicator for statistical significance of the estimated parameters. Statistically significant parameter estimates are plotted as value 1 in the plot and the other statistically insignificant parameter estimates are plotted as value 0.

In the Figures 5.20(1)–5.20(6), it can be seen that the number of significant estimated parameters increase substantially when the precision of the observations are used as weights.

Also, the difference between the use of height and velocity constraints is seen conspicuously. Based on these plots it can be said that the best results are obtained with the use of height excess constraints and precision of the observations as weights. In other words, it can be said that the number of significant parameters are more than 50% when the precision of observations is used as weights, and the number of significant parameters are significantly less than 50% when unit weights or time interval weights are used. Table 5.4 shows the percentage of significant values in the different cases of estimation and validates the above statements. The table elucidates that the time interval between observations as weights deteriorates the significance of the parameter estimates.

| Excess constraints | Weights                            | % of significant parameters |
|--------------------|------------------------------------|-----------------------------|
| Velocity           | Precision of observations          | 52.9                        |
| Height             | Precision of observations          | 62.6                        |
| Velocity           | Unity                              | 30.0                        |
| Height             | Unity                              | 36.4                        |
| Velocity           | Time interval between observations | 6.7                         |
| Height             | Time interval between observations | 16.9                        |

Table 5.4: Percentage of the significant parameters for the different cases of estimation. The table clearly indicates that the combination of height excess constraints and precision of the observations as weights provide the best results. It also indicates that the precision of the observations as weights provide more statistically significant parameters than any other type of weights.

A point has to be noted here: the estimation based on unit weights purely indicates the quality of the network (cf. section 4.2), which means that the network provides at the most only 36.4% of significant values. It can be inferred that the network geometry contributes considerably to the outcome of the results. However, this has been rectified to an extent with the use of precision of observations as weights. In spite of this rectification there are about 37.4–47.1% of parameters are insignificant. In estimating errors of the velocities the only

influence other than network geometry is the time difference between observations at each point in the network (cf. section 4.2).

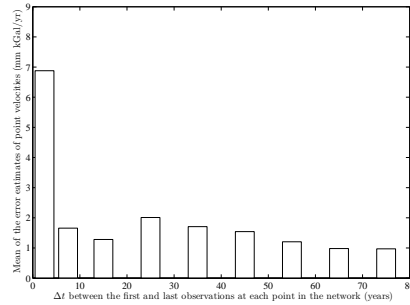
In Figure 5.21, the mean of the parameter error estimates are taken based on the time interval between the first and last observations at each point in the network (cf. Figure 4.11). All the figures indicate that when the time difference between observations is short then the mean of the errors are higher and *vice-versa*. However, there are some abnormalities in this pattern in both the velocity and height excess constraint situations. In the former there is a jump at the 20–30 year interval, while in the latter there is a jump at the 60–70 year interval. The reason for this being there are large outliers in these time intervals, and they correspond with points that have degrees of vertex of 2 without taking the relevelings into account. Thus, these simple tests elucidate the point that a good network for crustal motion determination requires a strong network – in the sense of degree of vertices, and sufficient time interval between observations at different epochs.

## 5.7 Chapter summary

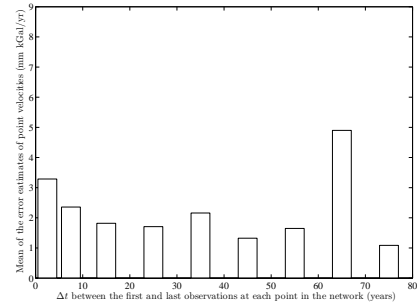
In this chapter, various methods of implementing a kinematic vertical datum adjustment in excess constraint situations were discussed in detail. Three different types of implementations were identified:

1. excess constraints fixed with velocities,
2. excess constraints fixed with heights, and
3. excess constraints with a mix of heights and velocities.

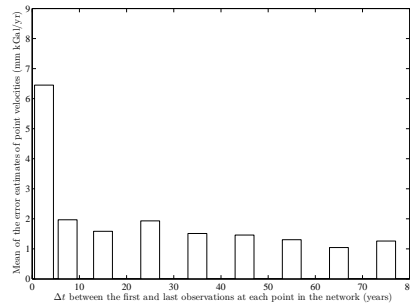
Of the three methods identified, only the first two were implemented as the third was felt to be unreasonable for the situation in hand. For fixing the excess constraints with velocities, five different *a priori* post-glacial rebound models were used, and for fixing the excess constraints with heights, heights computed by Geodetic Survey Division, Natural Resources Canada, with the levelling data were used. The adjustment was carried out based on least squares, where the weight matrix was formed from the inverse of diagonal variance-covariance matrix of the observations. The diagonal variance-covariance matrix of the observations was in turn formed from the precision of the observations given with the data.



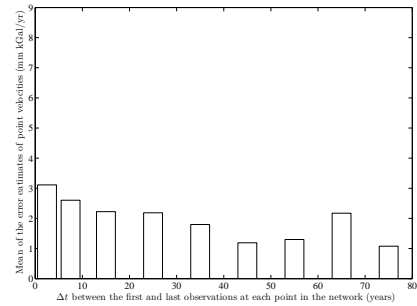
(1) Velocity excess constraints; Precision of observations as weights



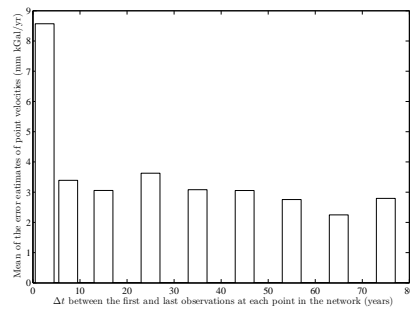
(2) Height excess constraints; Precision of observations as weights



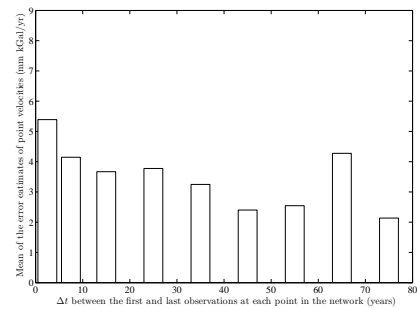
(3) Velocity excess constraints; Unit weights



(4) Height excess constraints; Unit weights



(5) Velocity excess constraints; Time interval as weights



(6) Height excess constraints; Time interval as weights

Figure 5.21: The bar graphs show the means values of the error estimates for the points based on the statistic shown in Fig. 4.11. The figures indicate that the time interval between the first and last observations have an impact on the estimated errors of the parameters.

The results from the adjustment showed that there was a constancy in the pattern of occurrence of the vertical crustal motion rates, and in addition, there were also some conspicuous local patterns in the occurrence of vertical crustal motion rates. In order to figure out the constancy in pattern of the vertical crustal motion occurrence, in spite of the fact that different excess constraints were applied, it was decided to change the weight matrices to study their influence. Two other weight matrices were applied, viz., unit weights, and time interval between the observations as weights. Again for both the weight matrices height and velocity excess constraints were applied. The results showed that local patterns in vertical crustal motion rates were exaggerated patterns heavily influenced by the weight matrix formed based on the precision of observations. However, the general pattern of vertical crustal motion rates in the network remained the same.

Least square error analysis was carried out to ascertain the cause of the constancy in vertical crustal motion pattern. To this effect the resolution and the redundancy matrices were computed. While the resolution matrices provide insight into the contribution of the data and the excess constraints in the estimates of heights and their velocities; the redundancy matrices shows if there is any improvement in the estimated errors of observations. This analysis showed that the network behaved like a minimum constraint network due to the presence of groups in a multiple rank deficient kinematic levelling network.

Then, statistical testing of the observations was carried out, although not in complete detail. The statistical testing of observations demonstrated that excess constraints fixed with height are a better choice to overcome the multiple rank deficiency situation in the adjustment of kinematic levelling networks. The error spatial plots from height excess constraint adjustments also provided sufficient evidence that such adjustments give out a minimum constraint adjustment for velocities, which is essential to interpret the velocities without any influence from *a priori* geophysical and geodynamical models.

Finally, statistical significance of the estimates was also analysed. The analysis showed that only if the precision of observations are used as weights, a little more than 50% of the estimates are significant at  $1\sigma$  level. The significance test of the estimates from adjustment using unit weights gave a direct indication of the quality of the network available in terms of both degree of vertices and time interval between observations. Also, analysis of the mean of the estimated errors based on time interval between first and last observations at a point,

---

provided insight into the essentials of a good network for estimating vertical crustal motion: strong network of points with good degree of vertices (preferably  $> 3$  for each point), and sufficient time interval between observations made at different epochs (preferably  $> 10$  years in this study).

## Chapter 6

# Geological and Geophysical Interpretation

Least squares adjustment of the kinematic levelling networks only provides numerical quantities based on the parameterization in the observation equation. In order to evaluate the validity of the estimated numerical quantities, especially vertical crustal motion rates, a geological and geophysical interpretation is essential. In this chapter, the structural geology with respect to the faults in the region will be explained briefly; the earthquake history in the region will be discussed; some postglacial rebound models will be shown to elucidate the nature of the postglacial rebound phenomenon in the region; and finally, the velocities obtained from the adjustments will be discussed and interpreted with geology and geophysics of the region.

### 6.1 Geological fault lines in the study area

Before delving deep into the geological faults in the study area, a review of the different fault types is essential. There are three major types of faults: *strike-slip faults*, *normal faults*, and *thrust faults*. In a strike-slip fault, the two fault planes slide along the fault line parallel to the horizontal plane, and hence, there is no vertical movement in a strike-slip fault. In a normal fault, one of the two fault planes moves downward along the fault line and this fault plane is called the upper fault plane. In the thrust fault as the name suggests one of the fault planes is thrust upon the other. Since one of the fault plane is resistant to the one that is being thrust upon, the thrust fault plane topples over the stable fault plane. Thrust faults are also referred to as *reverse faults*, because the upper plane moves in the upward direction. These thrust faults are very common in the regions of converging plate boundaries; however, these three types of faults are the only types of tectonic faults (Lowrie, 1997). These three different types of faults are illustrated in Figure 6.1

Figure 6.3 shows the fault lines over the study area, which suggests that there is significant faulting in most parts of the network. All the fault lines in the northern part of the network are thrust faults, which means that the faulted plane moves in upward-downward direction and hence, causing vertical crustal motion (cf. Figure 6.2). Wu (1998) indicates the reason

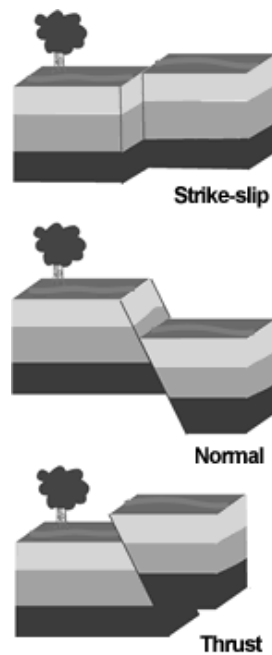


Figure 6.1: Different types of faults

for these thrust faults can be a result of the postglacial rebound phenomenon experienced in that region. The rest of the fault lines have not been classified by the Geological Survey of Canada (Wheeler et al., 1996), which will hamper to an extent the geological interpretation of the velocities in those regions. However, the presence of thrust faults in the northern part of the network suggests that the vertical crustal motion estimates will show some sudden changes between the adjacent velocity values across the fault lines. The cause for concern over kinematic levelling networks in such heavy faulted regions is that if there were occurrences of episodic movements due to earthquakes then a linear model for the vertical crustal motion will smooth out the episodic movement and display it as linear motion. However, the geological and geophysical interpretation that will be done will help identify such smoothing effects.

## 6.2 Earthquake history in the study area

Figure 6.4 shows that the region has been seismically active given the large number of earthquakes recorded. The figure shows that the region is prone to earthquakes predominantly in the magnitudes between  $>3$  and 5. Also, there is a heavy concentration of the earthquakes at



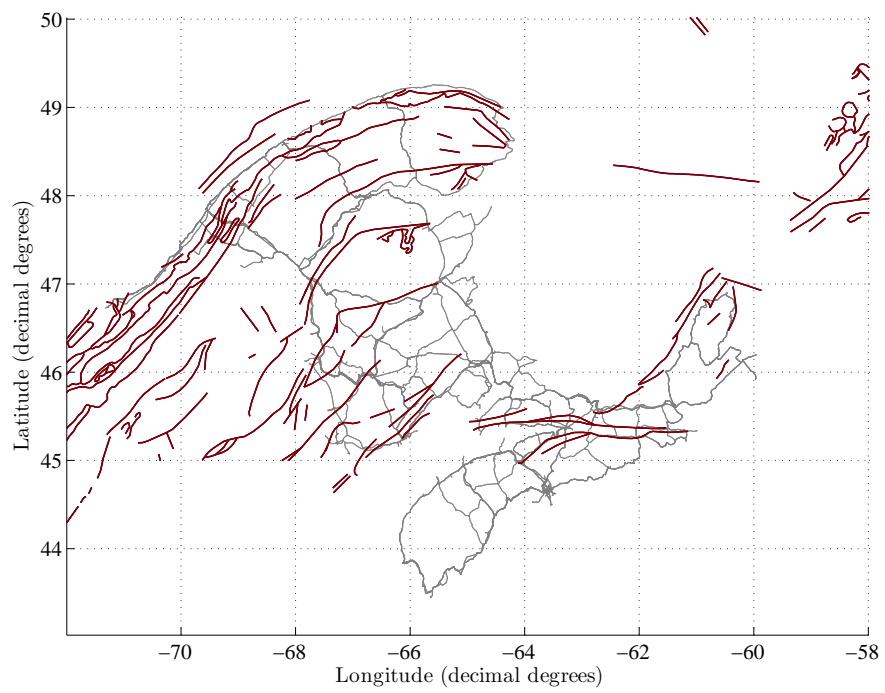


Figure 6.3: Geological fault lines in the study area

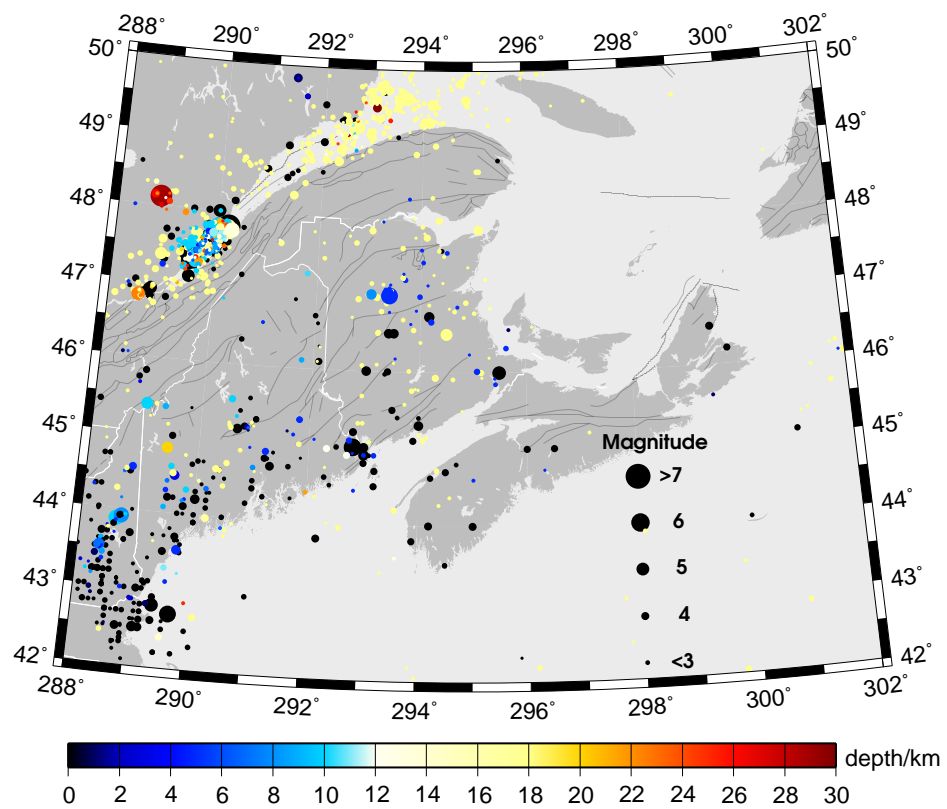


Figure 6.4: Occurrences of earthquakes in the study region with their magnitude and depth.  
Data courtesy: Dr. John Adams, Geological Survey of Canada, Ottawa.

shallow depths in the north-northwestern part of the network, i.e., closer to the St. Lawrence river. In addition, the region just above the northern part of the network, in the mouth of St. Lawrence river, again shows heavy concentration of earthquakes of substantial magnitude and substantial depth. However, although there have been many earthquakes of a substantial magnitude in the middle of the network, the depth suggests that most of them have occurred at a shallow depth. This indicates that these earthquakes would not have caused any major episodic movements but, insignificant displacements. Also, a thorough look into the data reveals that there have been no major earthquakes during the measurement period (1904–1999) of the levelling network in the region. Thus, the nature of earthquake data suggests that the vertical crustal motion information that is extracted from the levelling network is primarily contributed by the other phenomenon of consideration – *postglacial rebound*.

### 6.3 Postglacial rebound phenomenon in the study area

Postglacial rebound, also known as *glacial isostatic adjustment*, is a phenomenon that refers to the rebound of the crust after melting of the Laurentide ice sheet since the last glacial maximum  $\approx 21,000$  years ago. Due to glaciation, ice formed on land and the ice-load depressed the crust causing it to subside. After this, the ice melted, and at the end of the ice age the load was removed from the crust and then the crust rebounded due to the viscous nature of the Earth at time-scales  $>1000$  years. The ice-sheets covered the whole of Canada and hence, Canada experiences postglacial rebound resulting in a uplift rebound of upto  $1.2 \text{ cm/yr}$  in areas around Hudson Bay and gradually decreasing to  $0 \text{ cm/yr}$  around the Great Lakes region.

Figure 6.5 shows vertical crustal motion rates from the five different postglacial rebound models used as *a priori* information for fixing the velocity excess constraints. The model simulations are carried out by considering the Earth as a radially symmetric entity and made up of 6 layers, which represent the major discontinuities in the Earth's viscosity structure. Details of the simulations can be found in Rangelova et al. (2005). Here, all the models follow a six-layer mantle model with the same type of crust and core. The model values are given in Table 6.1.

The purpose of showing these models is to provide an overview of the nature of the vertical crustal motion due to postglacial rebound. There are ongoing studies using GPS

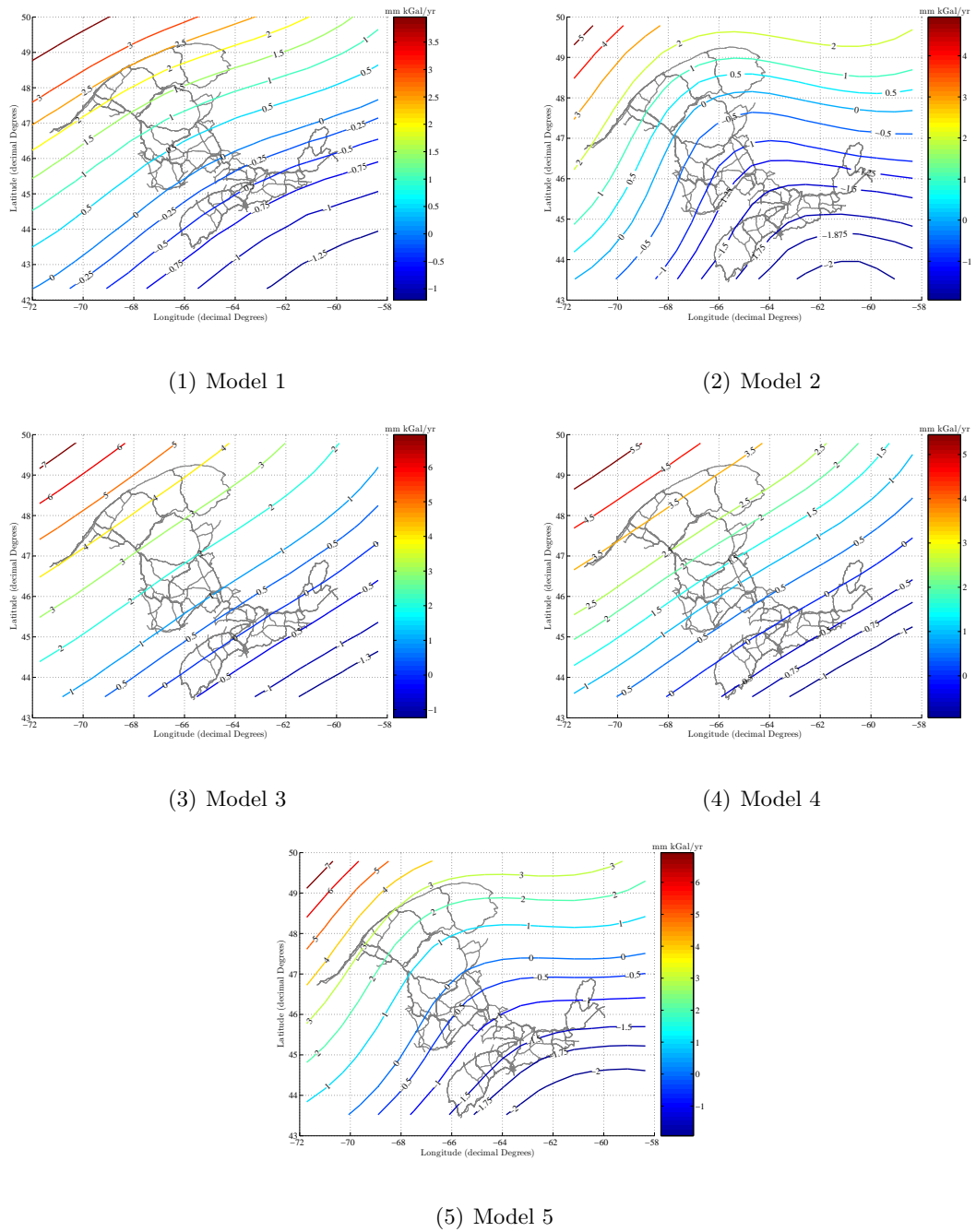


Figure 6.5: Vertical crustal motion rates from postglacial rebound models that were used as *a priori* information for fixing the velocity excess constraints

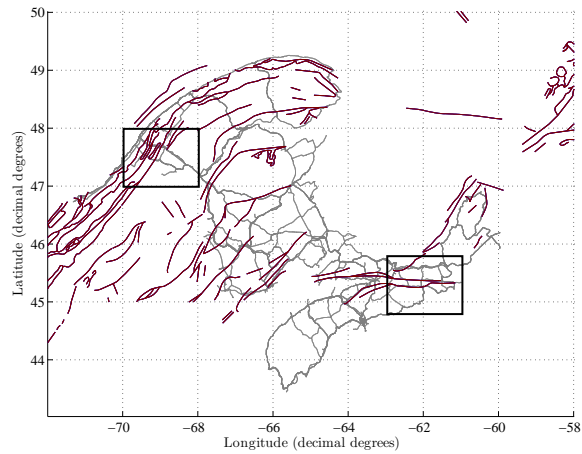
| Layer | $R$<br>(km) | $\rho$<br>(kg/m <sup>3</sup> ) | $\mu$<br>(GPa) | $\eta$ (Pas) |         |         |         |         |
|-------|-------------|--------------------------------|----------------|--------------|---------|---------|---------|---------|
|       |             |                                |                | Model 1      | Model 2 | Model 3 | Model 4 | Model 5 |
| Crust | 6371        | 3191.7                         | 60.2           | 1.0e43       | 1.0e43  | 1.0e43  | 1.0e43  | 1.0e43  |
| UM1   | 6256        | 3442.1                         | 73.1           | 0.4e21       | 1.0e21  | 0.4e21  | 0.4e21  | 1.0e21  |
| UM2   | 5971        | 3882.4                         | 109.5          | 0.4e21       | 1.0e21  | 0.4e21  | 0.4e21  | 1.0e21  |
| LM1   | 5701        | 4527.3                         | 180.6          | 2.0e21       | 2.0e21  | 10.0e21 | 6.0e21  | 6.0e21  |
| LM2   | 5200        | 5084.2                         | 240.9          | 4.0e21       | 4.0e21  | 10.0e21 | 6.0e21  | 6.0e21  |
| Core  | 3480        | 10925.0                        | 0              | 0            | 0       | 0       | 0       | 0       |

Table 6.1: Layers and their parameters of the 5 postglacial rebound models used for *a priori* velocity excess constraints.  $R$  – radius from the centre of Earth,  $\rho$  – density,  $\mu$  – rigidity,  $\eta$  – viscosity, UM – upper mantle, LM – lower mantle

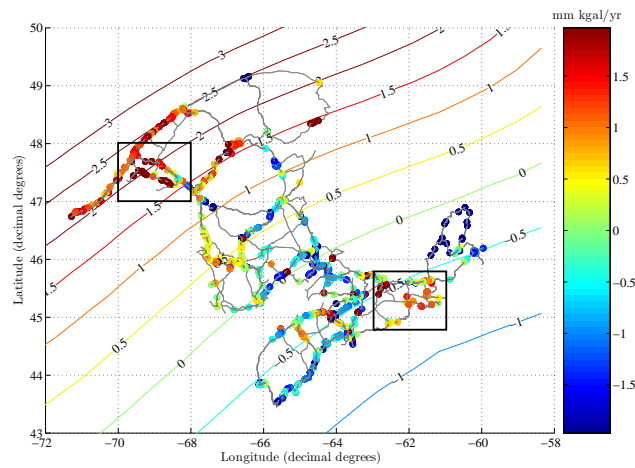
and absolute gravimetry to constrain and validate these models. The models show that the study area is a region of transition from uplift to subsidence, which implies that there will be no vertical motion coming from postglacial rebound at some points in the network. Also, the models indicate that it is a region of minimal vertical motion, which further implies that the detection of vertical crustal motion will be difficult given the time interval between the repeated levelling observations (cf. Figure 4.5).

#### 6.4 Interpretation of results from kinematic vertical datum adjustment

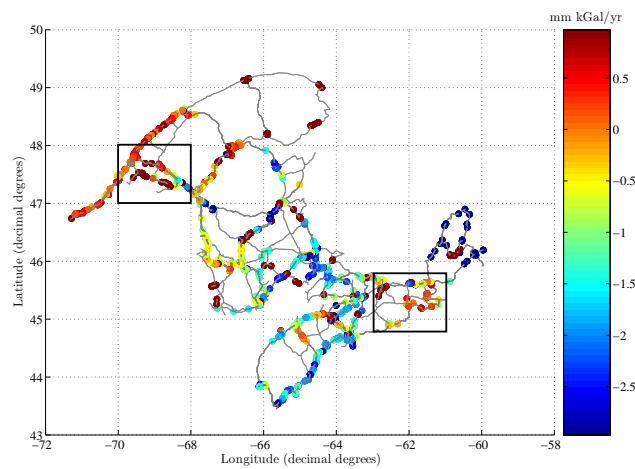
For the geological and geophysical interpretation of the kinematic adjustment results, only the results from adjustments using unit weights are used as it was shown previously (section 5.3.4) that the weights based on the precision of the observations exaggerate some of the local patterns and have a heavy influence on the results. Also, it was shown that there is not much difference between time interval between observations as weights and unit weights. Results from the adjustments with both the velocity excess constraints and the height excess



(1) Fault lines over the network



(2) Velocities from adjustment using velocity excess constraints



(3) Velocities from adjustment using height excess constraints

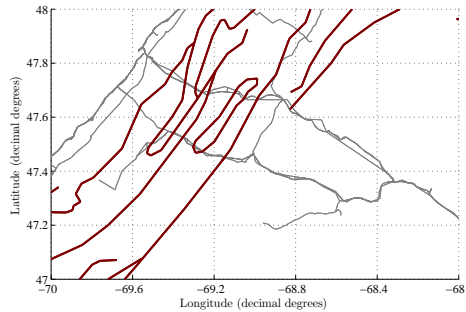
Figure 6.6: Illustration of the two regions of focus within the entire network

constraints are presented in the interpretation.

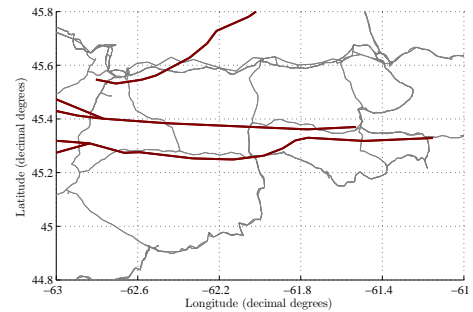
In Figures 6.6(2) and 6.6(3), it can be clearly seen that there is a significant trend of velocities from positive values in the northwest to the negative values in the southeast. In other words, there is trend in the vertical crustal motion in the direction from northwest to southeast. The trend was initially thought to come from the *a priori* postglacial rebound model used but, the doubts were clarified by the velocity estimates from the height overconstraint adjustment. Since, it was shown that height overconstraint adjustment is the best possible way of estimating biasless velocities. Thus, it can be clearly seen that this trend of positive to negative is infact the postglacial rebound signal in the region. It can also be seen that in Figure 6.6(2) the trend is seen as a strong signal whereas in Figure 6.6(3) the signal is a little bit under-toned. However, there are some deviations to this trend in the network.

In Figure 6.6 two boxes are shown, one in the northern part of the network close to the St. Lawrence river, and the other in the southern part of the network in Nova Scotia. The reason for showing these particular regions is that there is a strong correlation between the estimated velocities and the geological faults in the area. Taking a closer look into the box in the northern part of the network in Figure 6.6 (Figures 6.7(3) and 6.7(5)) it can be seen that the velocities suddenly change from brownish-red to red and then again moves back to brownish red. This transition coincides with a fault line of a thrust fault, which, as is known, contributes to vertical crustal motion. Similarly, the velocity values of the points in the box in the southern part of the network all show high positive values in a region of subsidence (Figure 6.6). A glance at the fault lines suggest that this anomaly coincides with fault lines; however, these fault lines have not been classified. Nevertheless, this anomaly is ample indication that the velocities may have a contribution from the tectonics in the region as well.

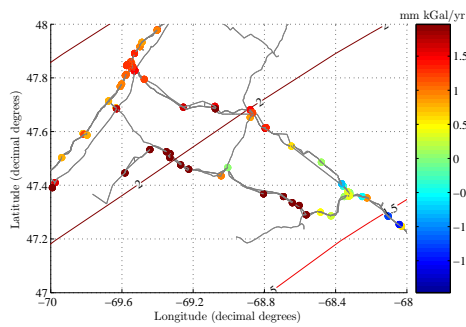
Apart from the correlation with the faults and earthquake zones, the velocity estimates also correlated with the rock types. In Figure 6.8 two areas are highlighted with boxes. The areas show a marked change in the velocity values, which when compared with the geology map of the region (Figure 6.2) shows that these two areas are areas of change in rock types. In the upper rectangle the rock types change from Silurian and Silurian & Devonian stratified sequences to Carboniferous stratified sequence. In the lower rectangle the rock types change from Devonian intrusive rock to Cambrian & Ordovician rock types.



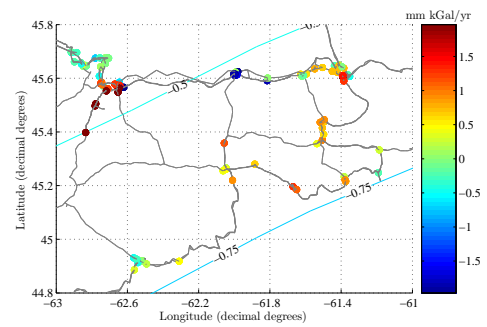
(1) Fault lines over the network



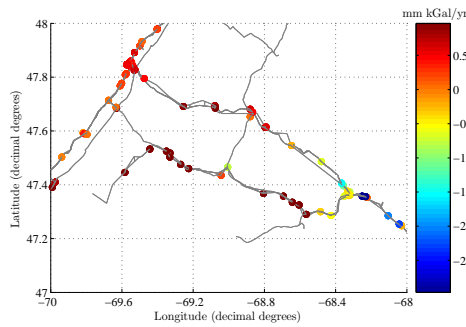
(2) Fault lines over the network



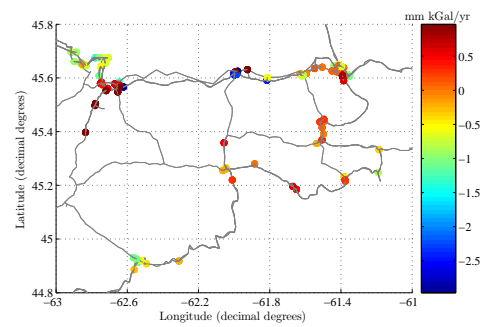
(3) Velocities from adjustment using velocity excess constraints



(4) Velocities from adjustment using velocity excess constraints

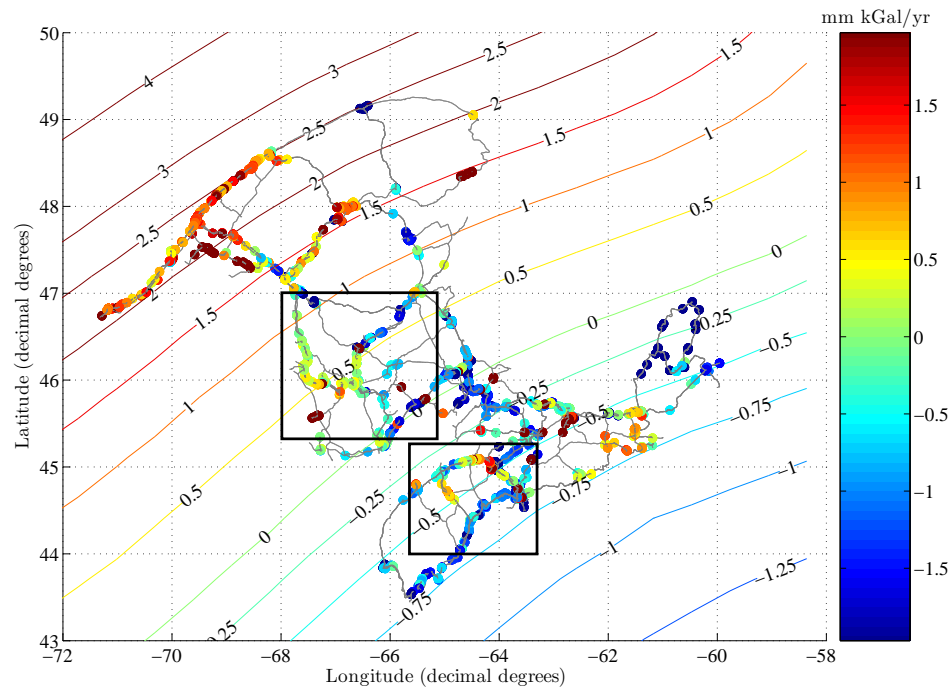


(5) Velocities from adjustment using height excess constraints

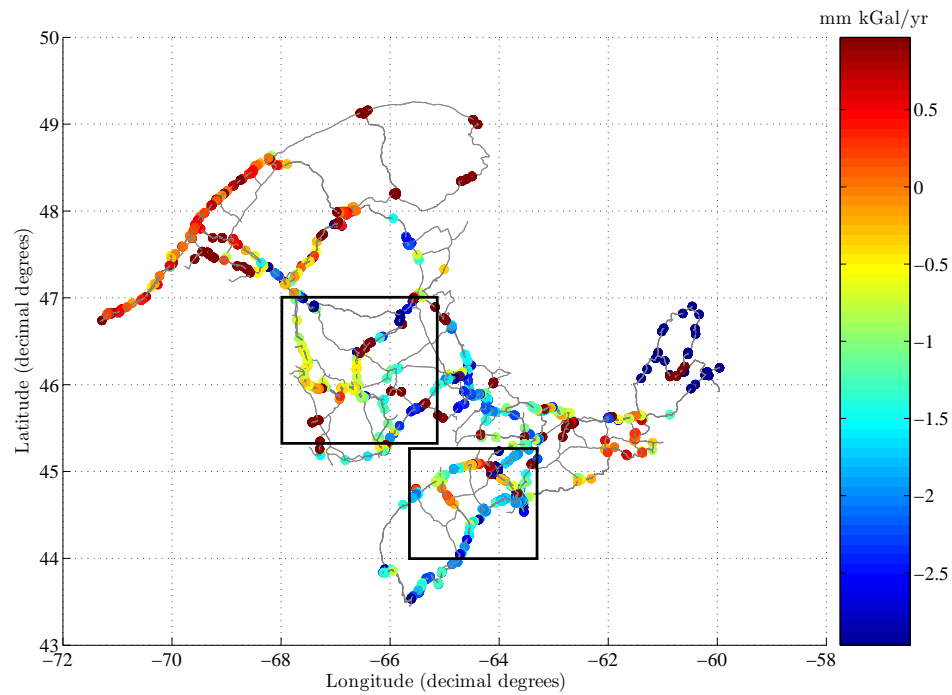


(6) Velocities from adjustment using height excess constraints

Figure 6.7: A closer look at the two areas of the network highlighted in Figure 6.6, whose velocity values correlate with the faults



(1) Velocity estimates from adjustment using velocity excess constraints



(2) Velocity estimates from adjustment using velocity excess constraints

Figure 6.8: Illustration of the areas in the network, whose velocity estimates correlate with the geological rock types of the region

## 6.5 Chapter summary

In summary, the region shows complex geology and a combination of different geophysical activities, viz., seismic activity, tectonics, and postglacial rebound. The geological and geophysical interpretation indicates that the vertical crustal motion signal is being seen in the estimated results. Further, postglacial rebound has a strong signal and a trend can be seen in the Figures 6.6(2) and 6.6(3) apart from a few anomalies. A closer look at these anomalies in juxtaposition with the fault lines over the network suggests contribution from tectonics and seismicity. This is an indication that the vertical motion due to postglacial rebound acts as a background signal upon which the vertical crustal motion due to seismicity and tectonics are superposed. Although, the density and quality of the levelling network does not allow for a closer look into individual faults. In addition to them, the velocities also correlate with the rock types, especially at the rock type boundaries; however, this correlation requires further analysis.

## Chapter 7

# Concluding Remarks

### 7.1 Summary

In this research, a part of the Canadian Precise Levelling Network was analysed to study the feasibility of defining a kinematic vertical datum. Initially, the concept of kinematic vertical datum was reviewed and then the kinematic vertical datum was identified as a vertical datum incorporating a mathematical model for the vertical crustal motion. In that sense, a linear model for the vertical crustal motion was chosen in view of the geophysical activities going on in Canada, and a linear model was assumed given the quantity and quality of the data. Then, in the linear model, a reference time epoch was identified as an estimable datum parameter and hence, the equation of the linear model became non-linear in the sense of adjustment theory. The linearisation of the corresponding equation was shown.

After completing a theoretical review, the data was analysed to prepare it for the kinematic vertical datum realisation. First, a glance at the history of the Canadian Precise Levelling Network was taken to get an overview about the data quality. Then, the data format was explained and its implications towards the data processing were brought out. In the data format, for the storage of levelling network observations, information on repeated observations were also given. This made the process of finding the relevellings easier in an otherwise tedious task. Then, it was found that the network in its original topological form was not suitable for a kinematic vertical datum definition as the adjustment problem was underdetermined. Hence, data processing was required and the data was processed in three different steps: finding intersection points, reduction of the levelling observations observed in the same year, and removal of open lines and loops. These data processing methods were based on the solvability analysis of the kinematic levelling network.

When the observations were in ready-to-adjust format, a pre-adjustment analysis was carried out, where the network was characterized by the statistics calculated from the processed observations. These statistics provided a very good intuitive insight into the quality of the estimated parameters and adjusted observations that can be expected from the network. For

example, the correlation between the degree of vertex of the underlying simple graph of the network and the local redundancy numbers was illustrated. Also, trend analysis of the relative velocities of relevelings that were observed more than twice was performed to get an insight into the influence of errors in the observations. Finally, a parametric adjustment of the observations was carried out to determine the vertical crustal motion.

The processed observations provided a multiple rank deficient design matrix, which had to be supplied with *a priori* information to suffice the multiple rank deficiency. The *a priori* information was taken from postglacial rebound models and heights from static height adjustment by the Geodetic Survey Division, Natural Resources Canada. All the adjustments with different *a priori* information provided the same pattern of vertical crustal motion, which cannot be true given the differences in the *a priori* information. So, the weighting scheme was changed and it was found out that the weighting scheme had influence on some of the patterns in the estimated vertical crustal motion rates. However, there were other patterns in the vertical crustal motion that remained even after changing the weighting scheme.

In order to clarify this situation, least squares error analysis was carried out, which gave insight into the contributions of the *a priori* information and the observations towards the estimated parameters. It was found that the estimated parameters were all a consequence of the observations. Also, during the course of the adjustment, it was seen that sufficing the multiple rank deficiency with height constraints provided reliable results in that the heights did not come from the assumed modelling. Then, statistical tests were applied to illustrate the good observations and outliers. It revealed that the weighting scheme had influence on the outcome of the statistical testing. Also, statistical significance of the velocities were computed, which brought to the fore the essentials of a good network for crustal motion determination: strong network with good degree of verices for each point, and sufficient time interval between observations at different epochs. In that sense, the network of concern was a weak network.

In the end, the results from the parametric adjustment were interpreted with the geology and geophysics of the area, viz., tectonics, seismicity, and post glacial rebound. The results showed an overall pattern in the network that corresponded to the effects of the postglacial rebound phenomenon in the region. Also, the results correlated well with the geological faults in the region and also the geological rock types as far as this interpretation could be achieved here.

## 7.2 Conclusions

Recalling the objectives of this study here,

1. *to determine the feasibility of defining a kinematic vertical datum based only on the levelling network of Canada*

From the results of data processing of the network it can be confirmed that an ideal minimum constraint kinematic vertical datum, i.e., only 2 datum constraints one for velocity and one for height, cannot be established at this point as the network has some data gaps. However, this situation is overcome by fixing the excess constraints with heights, which provide a *workable* minimum constraint datum. Here, the term *workable* is used to make a distinction between minimum constraint & overconstraint datums, and a datum realized with excess constraints. This *workable* datum provides estimates of the vertical crustal motion with minor or no distortions. The reason being that the height values all come from a minimum constraint adjustment, which gives undistorted estimates of the height values. Thus, any vertical crustal motion estimates from this *workable* datum is free of any assumptions other than linear motion.

2. *to create the levelling dataset as an independent dataset for geophysical studies*

It was explained in section 1.4 that the two objectives are inter-twined and hence, it can be concluded that the levelling dataset provides independent vertical crustal motion dataset for geophysical studies. The method of applying excess constraints ensures that levelling network observations are independent and do not have to depend on any external source, like postglacial rebound models, for the *a priori* information.

Thus, it can be concluded from the study that the objectives of the study have been achieved.

## 7.3 Contributions

Various aspects of the kinematic vertical datum were dealt with in this work. Following are the contributions of this work towards the framework of kinematic vertical datum definition and realization:

- the biggest contribution of this research is that the levelling dataset has been created as an independent dataset for geophysical studies;

- reference time epoch was established as a datum parameter, and also, it was proven that the reference time epoch was estimable from the data;
- S-transformation of a kinematic vertical datum based on a linear model for vertical crustal motion was derived and also, time-shift in the datum transformation was elucidated;
- excess constraints (or multiple rank deficiency) situation in a kinematic vertical datum realization was dealt with and it was shown that the situation can be easily overcome by applying the constraints on the height part of the parameters;
- a number of statistics were derived from the ready-to adjust network, which proved to provide very good insight into the expected quality of the results and also in the interpretation of the results; and
- trend analysis of relative velocities was established as an valuable but intuitive tool to discriminate between the levellings that have velocity information and those that are smudged by errors.

## 7.4 Outlook

This research was carried out as a pilot study for the definition of a kinematic vertical datum for the Canadian Precise Levelling Network. The size of the network used for the study is small compared to the entire Canadian levelling network. Also, the study area was one of the regions that was frequently re-observed (personal communication with Mr. Véronneau). So, extrapolating the outcome of this research to the entire Canadian network, it is fair to say that an ideal minimum constraint kinematic vertical datum with a linear model cannot be realized. However, the methods described for the data processing can be applied and all the resulting excess constraints can be fixed with the heights from the static adjustment carried out by Geodetic Survey Division, Natural Resources Canada. This will ensure that the levelling data are independent of any external information for the determination of vertical crustal motion.

Apart from the above, the other areas where the study can be extended are as follows:

- In the solvability analysis, it was shown that single levellings also contribute to the vertical crustal motion estimation and that they cannot be neglected in such studies.

Keeping with that, geodetic network design methods can be developed such that they provide reliable results, and at the same time, reduce the number of repeated observations. This will be a more suitable method for larger levelling networks also in other countries.

- For the excess constraints, height values from GPS/levelling can be used, and the differences in the estimated results can be evaluated. This is an important area given that the height system of Canada will soon be modernized with GPS/levelling methods (Véronneau & Huang, 2004).
- In the geological interpretation of the results, it was seen that the network region is tectonically active, and also includes an area of seismic activity. This suggests instances of episodic motion in the region, which cannot necessarily be modelled by the linear motion model. This will be the case in national levelling networks of large countries, where the phenomenon responsible for crustal motion keeps changing with space and time. Hence, when defining and realizing a kinematic vertical datum, these things need to be taken into consideration.
- The methods that have been developed in this research have only been applied to the Canadian levelling network. These methods need to be applied to other national networks, for example, the networks of Nordic countries, and the Netherlands. This will provide another evaluation of the algorithms and methods employed for data processing in this research, and will benefit studies of vertical crustal motion in these countries.
- This research has created levelling as an independent dataset for geophysical studies and so, a surface can be fit to the estimated vertical crustal motion rates and can be used for validation of the vertical crustal motion rates estimated from tide gauges, because tide gauge measurements are very similar to levelling measurements in that they just measure the height differences between instantaneous sea level and the reference.

## References

- Altamimi Z, Sillard P, Boucher C (2002) ITRF2000: A new release of the International Terrestrial Reference Frame for earth science applications. *Journal of Geophysical Research* **107**(B10):2214, doi:10.1029/2001JB000 561.
- Arias EF, Cionco RG, Orellana RB, Vucetich H (2000) A comparison of the SAO–Hipparcos reference frames. *Astronomy and Astrophysics* **359**:1195–1200.
- Baarda W (1981) *S-transformations and Criterion Matrices*. Tech. Rep. 1, Netherlands Geodetic Commission.
- Baarda W, Alberda J (1962) The connection of geodetic adjustment procedures with methods of mathematical statistics. *Bull Géod* (66):325–345.
- Blewitt G (2000) Geodetic network optimization for geophysical parameters. *Geophysical Research Letters* **27**(22):3615–3618.
- Blick G (2003) Implementation and development of NZGD2000. *New Zealand Surveyor* (293):15–19.
- Borre K (2001) *Plane Networks and their Applications*. Birkhäuser.
- Bürgmann R, Rosen PA, Fielding EJ (2000) Synthetic Aperture RADAR Interferometry to measure Earth’s surface topography and its deformation. *Ann Rev Earth Planet Sci* **28**:169–209.
- Campbell J (2000) Very Long Baseline Interferometry – a high precision tool for geodesy and astrometry. *C R Acad Sci Paris, Série IV – Physics* **1**(10):1255–1265.
- Casparly W (1988) *Concepts of network and deformation analysis*. Tech. Rep. Monograph 11, School of Surveying, The University of New South Wales.
- Davis JL, Mitrovica JX (1996) Glacial isostatic adjustment and the anomalous tide gauge record of eastern north america. *Nature* **379**:331–333.

- Ding X, Coleman R (1996) Multiple outlier detection by evaluating redundancy contributions of observations. *J Geodesy* **70**:489–498.
- Dragert H, Hyndman RD (1995) Continuous GPS monitoring of elastic crustal strain in the northern Cascadia subduction zone. *Geophysical Research Letters* **22**(7):755–758.
- Dzurisin D (1999) Results of repeated leveling surveys at Newberry Volcano, Oregon, and near Lassen Peak Volcano, California. *Bulletin of Volcanology* **61**:83–91.
- Even-Tzur G (2001) Graph theory applications to GPS networks. *GPS Solutions* **5**:31–38.
- Fotopoulos G (2003) *An analysis on the optimal combination of geoid, orthometric and ellipsoidal height data*. Ph.D. thesis, Department of Geomatics Engineering, University of Calgary.
- Gareau RM (1986) *History of levelling in Canada and NAVD*. Master's thesis, University of Calgary.
- Gökap E, Boz Y (2005) Outlier detection in GPS networks with fuzzy logic and conventional methods. In: *From Pharaohs to Geoinformatics. FIG Working Week 2005 and GSDI-8*, Cairo, Egypt.
- Golub GH, van Loan CF (1996) *Matrix Computations*. 3 edn., The Johns Hopkins University Press. Baltimore, Maryland.
- Grafarend EW, Mader A (1989) A graph-theoretical algorithm for detecting configuration defects in triangular geodetic networks. *Bull Géod* **63**:387–394.
- Grant DB, Blick GH (2001) A national vertical datum independent of local mean sea level? In: MG Sideris (ed.), *Gravity Geoid and Geodynamics 2000*, vol. 123, International Association of Geodesy, Springer - Verlag Berlin Heidelberg.
- Hazay I (1977) Adjustment of levelling for the determination of the vertical movements of the earth's surface. In: F Halmos, J Somogyi (eds.), *Optimization of design and computation of control networks*, pp. 237–249, Geodetic and Geophysical Research Institute of the Hungarian Academy of Sciences / International Association of Geodesy.

- Hearn EH (2003) What can GPS data tell us about the dynamics of post-seismic deformation? *Geophys J Int* **155**:753–777.
- Heck B (2002) Problems in the definition of vertical reference frames. In: F Sansò (ed.), *V Hotine-Marussi Symposium on Mathematical Geodesy*, International Association of Geodesy - Italian Space Agency, Springer-Verlag.
- Heiskanen WA, Moritz H (2000) *Physical Geodesy*. Reprint edn., Institute of Physical Geodesy, Technical University of Graz, Austria.
- Jekeli C (2000) *Heights, the Geopotential, and Vertical Datums*. Tech. Rep. 459, Department of Civil and Environmental, and Geodetic Engineering, Ohio State University.
- Kenselaar F, Quadvlieg R (2001) Trend-signal modelling of land subsidence. In: *The 10<sup>th</sup> FIG International Symposium on Deformation Measurements*, FIG, Orange, California.
- Kleijer F, Kenselaar F, de Bruijne A, Molendijk R (2001) Employing the strict kinematic model for the maintenance of a height reference frame based on conventional leveling. In: H Drewes, AH Dodson, LPS Fortes, L Sánchez, P Sandoval (eds.), *Vertical Reference Systems*, vol. 123, pp. 119–124, International Association of Geodesy, Springer.
- Koohzare A, Vaníček P, Santos M (2005) Compilation of a map of vertical crustal movements in eastern Canada using smooth piecewise algebraic approximation. In: C Rizos (ed.), *Monitoring and Understanding a Dynamic Planet with Geodetic and Oceanographic Tools*, IAG, IAPSO, IABO, Springer, Cairns, Australia.
- Kuang S (1996) *Geodetic Network Analysis and Optimal Design: Concepts and Applications*. Ann Arbor Press, Inc. Michigan, USA.
- Lambert A, James TS, Thorleifson LH (1998) Combining geomorphological and geodetic data to determine postglacial tilting in Manitoba. *Journal of Paleolimnology* **19**(3):365–376.
- Lanczos C (1997) *Linear Differential Operators*. Republication edn., Dover Publications, Mineola, New York.
- Linkwitz K (1999) Quo vadis geodesia...? *Festschrift for Erik W. Grafarend on the occasion of his 60th birthday*, vol. I of *Technical Reports, Department of Geodesy and Geoinformatics*,

- Universität Stuttgart*, chap. About the generalized analysis of network-type entities, pp. 279–293. Universität Stuttgart.
- URL [http://www.uni-stuttgart.de/gi/research/schriftenreihe/quo\\_vadis/](http://www.uni-stuttgart.de/gi/research/schriftenreihe/quo_vadis/)
- Lowrie W (1997) *Fundamentals of Geophysics*. Cambridge University Press.
- Mainville A, Craymer MR (2005) Present-day tilting of the Great Lakes region based on water level gauges. *Geological Society of America Bulletin* **117**(7/8):1070–1080.
- Mäkinen J, Lidberg M, Schmidt K, et al. (2003) Future height systems in the nordic countries, their relation to the evrs2000 and to inspire gis standards. Position paper presented to the meeting of the Technical Working Group of the IAG subcommission for the European Reference Frame (EUREF).
- Mäkinen J, Saaranen V (1998) Determination of post-glacial land uplift from the three precise levellings in finland. *Journal of Geodesy* **72**:516–529.
- Marti U, Schlatter A (2001) The new height system in switzerland. In: H Drewes, AH Dodson, LPS Fortes, L Sánchez, P Sandoval (eds.), *Vertical Reference Systems*, vol. 123, pp. 50–55, International Association of Geodesy, Springer.
- Mather RS (1973) Four dimensional studies in earth space. *Bulletin Géodésique* (108):187–209.
- Mather RS (1978) On the realization of a system of reference in four dimensions for ocean dynamics. *Boundary-layer Meteorology* **13**(1–4):231–244.
- Matsumura S, Murakami M, Imakiire T (2004) Concept of the new Japanese Geodetic System. *Bulletin of the Geographical Survey Institute* **51**:1–9.
- Mazzotti S, Dragert H, Henton J, et al. (2003) Current tectonics of northern Cascadia from a decade of GPS measurements. *Journal of Geophysical Research* **108**(B12).
- Meyer TH, Roman DR, Zilkoski DB (2004) What does *height* really mean? Part I: Introduction. *Surveying and Land Information Science* **64**(4):223–233.
- Meyer TH, Roman DR, Zilkoski DB (2005) What does *height* really mean? Part II: Physics and Gravity. *Surveying and Land Information Science* **65**(1):5–15.

- Mitrovica JX (1997) Going halves over Hudson Bay. *Nature* **390**:444–445.
- Nassar MM (1977) *Gravity field and levelling heights in Canada*. Tech. Rep. 41, Department of Surveying Engineering, University of New Brunswick.
- Peltier WR (2002) Global glacial isostatic adjustment: palaeogeodetic and space-geodetic tests of the ICE-4G (VM2) model. *Journal of Quaternary Science* **17**(5-6):491–510.
- Rangelova E, van der Wal W, Wu P, Sideris MG (2005) Numerical models of the rates of change of the geoid and orthometric heights over Canada. In: C Rizos (ed.), *Monitoring and Understanding a Dynamic Planet with Geodetic and Oceanographic Tools*, IAG, IAPSO, IABO, Springer, Cairns, Australia.
- Rizos C (1999) *Principles and Practice of GPS Surveying*, chap. 9.1.5. Outlier testing and residuals. The University of New South Wales.  
URL [http://www.gmat.unsw.edu.au/snap/gps/gps\\_survey/principles\\_gps.htm](http://www.gmat.unsw.edu.au/snap/gps/gps_survey/principles_gps.htm)
- Sjöberg L, Vaníček P, Kwimbere M (1990) Estimates of present rates of land and geoid uplift in eastern North America. *Manuscripta Geodaetica* **15**:261–272.
- Snay RA (1978) Solvability analysis of geodetic networks using logical geometry. *Manuscripta Geodaetica* **3**:321–346.
- Sneeuw N (2000) *A semi-analytical approach to gravity field analysis from satellite observations*. Dissertationen Heft Nr. 527, Deutsche Geodätische Kommission, bei der Bayerischen Akademie der Wissenschaften.
- Strang G (1986) *Introduction to Applied Mathematics*. Wellesley-Cambridge.
- Strang van Hees GL (1982) Variance-covariance transformations of geodetic networks. *Manuscripta Geodaetica* **7**:1–20.
- Tapley B, Schutz B, Eanes R (1985) Satellite LASER Ranging and its applications. *Celestial Mechanics* **37**:247–261.
- Teunissen P (1985) Zero order design: Generalized inverses, adjustment, the datum problem and S-transformations. In: E Grafarend, F Sansò (eds.), *Optimization and Design of Geodetic Networks*, pp. 11–55.

- Torge W (2001) *Geodesy*. 3 edn., Walter de Gruyter. Berlin. New York.
- Tushingham AM, Peltier WR (1991) Ice-3G: A new global model of late pleistocene deglaciation based upon geophysical predictions of post-glacial relative sea level change. *Journal of Geophysical Research* **96**(B3):4 497–4 523.
- van Loan C (1985) On the method of weighting for equality-constrained least-squares problems. *SIAM Journal on Numerical Analysis* **22**(5):851–864.
- Vaniček P, Christodulidis D (1974) A method for the estimation of vertical crustal movement from scattered geodetic relevellings. *Canadian Journal of Earth Sciences* **11**(5):605–610.
- Vaniček P, Cross PA, Hannah J, et al. (1987) Four dimensional geodetic positioning. *Manuscripta Geodaetica* **12**:147–222.
- Vaniček P, Krakiwsky E (1986) *Geodesy: The Concepts*. 2 edn., Elsevier.
- Vaniček P, Nagy D (1981) On the compilation of the map of contemporary vertical crustal movements in Canada. *Tectonophysics* **71**:75–86.
- Véronneau M, Huang J (2004) Modernization of the height system in Canada: progress and challenges. In: *Gravity, Geoid and Space Missions 2004*, International Association of Geodesy.
- Wheeler JO, Hoffman PF, Card KD, et al. (1996) *Geological Map of Canada*. Map 1860a edn., Geological Survey of Canada.
- Wright P, Stow R (1999) Detecting mining subsidence from space. *International Journal of Remote Sensing* **20**(6):1183–1188.
- Wu P (1998) Will earthquake activity in eastern Canada increase in the next few thousand years? *Canadian Journal of Earth Sciences* **35**(5):562–568.
- Wu P (2006) Sensitivity of relative sea levels and crustal velocities in Laurentide to radial and lateral viscosity variations in the mantle. *Geophys J Int* **165**:401–413.
- Xu P, Shimada S, Fujii Y, Tanaka T (2000) Geodynamical value of historical geodetic measurements: A theoretical analysis. *Earth Planets Space* **52**:993–997.

- 
- Zelt CA (1999) Modelling strategies and model assessment for wide-angle seismic traveltime data. *Geophys J Int* **139**:183–204.
- Zilkoski DB, Richards JH, Young GM (1992) Results of the general adjustment of the north american vertical datum of 1988. *Surveying and Land Information Systems* **52**(3):133–149.